A conceptual solution to instable dynamic positioning during offshore heavy lift operations

Using computer simulation techniques

F.C. Bakker

Technische Universiteit Delft

TU Delft Delft University of Technology

Challenge the future

A CONCEPTUAL SOLUTION TO INSTABLE DYNAMIC POSITIONING DURING OFFSHORE HEAVY LIFT OPERATIONS

USING COMPUTER SIMULATION TECHNIQUES

by

F.C. Bakker

in partial fulfillment of the requirements for the degree of

Master of Science
in Mechancial Engineering

at the Delft University of Technology,
to be defended publicly on Wednesday April 15th, 2015 at 14:00.

Thesis committee:	Prof. dr. ir. G. Lodewijks,	TU Delft
	MSc P. de Vos,	TU Delft
	MSc E. el Amam,	Imtech Marine
	Dr. R.R. Negenborn,	TU Delft

TU Delft Delft University of Technology

ABSTRACT

This Msc graduation study covers the installation of topsides on a jacket by an offshore heavy lift crane vessel, and its related problems. One of the problems take place after the topside is hoisted on the jacket, during the weight shift from the hoist cable onto the jacket. The topside then exerts large horizontal forces upon the crane and vessel. The problem is that the DP system is not designed to cope with the changed force characteristics. Due to the changing force characteristics the DP system may build up oscillations and even instable behavior. The ultimate consequence may inflict great (economic) damage, human injury or even loss of lives. The current industry solution to this problem is found to be unsatisfying. The goal of this thesis is to propose one final conceptual solution to this problem. This final conceptual solution is selected from four candidate solutions after simulation performance tests. All candidate solutions use the same basic idea of estimating the large horizontal force and feed this into the DP controller.

The performance of the candidate solutions is tested on a simulated model of a crane vessel hoisting a topside on a jacket. This simulation model is based on the Imtech Marine DP and vessel model which is extended with a heavy lift crane. With the use of this simulation model the problem of instable behavior is reproduced in a simulation environment using realistic parameters.

One of the candidate solutions, denoted the *Feed Forward solution candidate*, translates the estimated force into compensation thrust by the vessel's own actuators. As a result, the horizontal forces are eliminated, whereby the DP controller will not be disturbed by the changed force characteristics anymore. In literature, this feed forward control law performed very well during scale model tests. In this study however, the performance proved to be very poor. It is shown that the performance is mainly poor because of the acceleration and deceleration rates of the thrusters are too low.

The second candidate solution, denoted the *Kalman solution candidate*, is a more simple candidate and only feed the estimated forces to the Kalman filter. This candidate is performing good, but DP stability is not guaranteed under all conditions. To determine the stability, with or without the Kalman solution candidate, an theoretical analysis method is explained.

It is concluded that of all candidate solutions *the Kalman solution candidate* proved the best performance. Consequently, it is recommended to develop the conceptual candidate to an industrial solution. During this development it is recommended to take extra measures to increase the robustness against differences between the heavy lift vessel model and the true heavy lift vessel.

PREFACE

Many thanks to the following persons and organizations who made this MSc graduation thesis possible. First of all my supervisor Ehab el Amam (MSc) of Imtech Marine, for taking great effort in supervising me throughout the period. Furthermore many thanks to the company Imtech Marine itself for providing the resources for doing my thesis. Secondly many thanks Peter de Vos(MSc) of the TU Delft for supervising me throughout the total period during my MSc degree, including supervising this graduation study. Also many thanks to Professor Gabriel Lodewijks(Dr. Ir.) of the TU Delft for being the graduation professor of this MSc thesis.

Also many thanks to some marine industry players. Thanks to Seaway Heavy Lifting (SHL), and in particular Matthijs Noordegraaf, for giving a broad context from the heavy lift industry by having multiple meetings. Also many thanks to Rene Wouts and Eelco Harmsen of Heerema Marine Contracting for having a clarifying conversation about the heavy lift industry challenges. Furthermore many thanks to Arjen Tjallema of Bluewater for his interest and help.

As last but perhaps most important, many thanks to friends and family for support and the desired distraction.

F.C. Bakker
Delft, March 2015

Contents

List of Figures

LIST OF TABLES

1

INTRODUCTION

1.1. INTRODUCTION TO THE PROBLEM

Due to the world's never ending hunger for energy and other natural resources, the quest for these resources shift from easy to more difficultly accessible locations. Drilling in water depths of 3[km], exploiting oil fields in Arctic locations and lifting weights of 10,000 tonnes offshore is no longer fiction. There are many structures of various kinds used in the oil, gas and lately in the renewable energy industry. Submersed structures, pipelines and wells are deployed on the ocean bed for oil field exploitation. Furthermore oil and gas processing and storage is performed on production units at sea. These units can be on fixed, floating or even submersed platforms with all kinds of different appearances.

Furthermore, wind, current and tidal power generation are upcoming sectors in the offshore industry. These different kind of structures have to be installed in some way or another. In the 1970's, large platforms were prefabricated and transported in relatively small units and installed offshore. However, offshore manual labor is very expensive compared to onshore manual labor hence the tendency was to fabricate larger pieces on shore and install them in as small number of units as possible.

The demand for larger installations – both in size and weight - and the increase in decommissioning of installations have resulted in heavy lifting vessels becoming much larger between the 1970's to the 1990's. [HMC, n.d.]. For installation work, offshore heavy lift crane vessels can be used like the modern Oleg Strashnov which is imaged on the front cover. Not only installation work but also decommissioning of offshore structures is a sector with long-term perspective. The owner/operator is legally bound to properly remove their platform and return the site back to its predevelopment condition. In recent years, removals have exceeded 100 platforms per year. This trend is expected to continue since one-fourth of the 3800 platforms in the Gulf of Mexico have been in place for more than 25 years. In the decade of the 1990's, the number of removals has outpaced the number of new platforms installed for three years.[Thornton, 2000]. Nowadays, Dynamic Positioning (DP) is commonly used for offshore heavy lifting. DP systems automatically control the position and heading of a ship using its own actuators, while the ship is subjected to environmental and external forces,. The first DP systems emerged from the need for deep water drilling by the offshore oil and gas industry, as conventional mooring systems, like a jack-up barge or an anchored rig, can only be used in shallow waters. Also a vessel using DP is more flexible, does not need anchor handling tugs, and has a lower set-up time in comparison to conventional stationary keeping methods.

In this MSc graduation study the installation of a topside on a jacket is the main operation analyzed. Such an operation is depicted on the front cover. During a topside installation, a topside, (e.g. a oil processing plant) is transported on the vessel or on a

barge to the installation location. The fixed structure on the seabed for the topside is already installed. This structure is called a jacket.

Next, the topside is hoisted from the barge or the heavy lift vessel itself (See Figure 1.1a). Where after the topside is positioned above the jacket and hoisted down on the jacket (See Figure 1.1b). The weight of the topside is slowly transferred from the crane to the jacket. After the topside is placed on the jacket but before the weight transfer is finished, the system resembles mooring characteristics. Horizontal hoist cable forces may increase rapidly as a function of the horizontal displacement of the vessel. The horizontal force is called Mooring stiffness force throughout this thesis (See Figure 1.1c). The rate at which the mooring stiffness increases the force as function of horizontal displacement is called mooring stiffness throughout this thesis. This mooring characteristics can be approached as if there is a large linear spring with stiffness as large as the mooring stiffness (See Figure 1.1d). The mooring stiffness can increase by up to 10 times the stiffness of the DP system, which is the force the actuators of the DP system would apply when the vessel position offset is one meter.

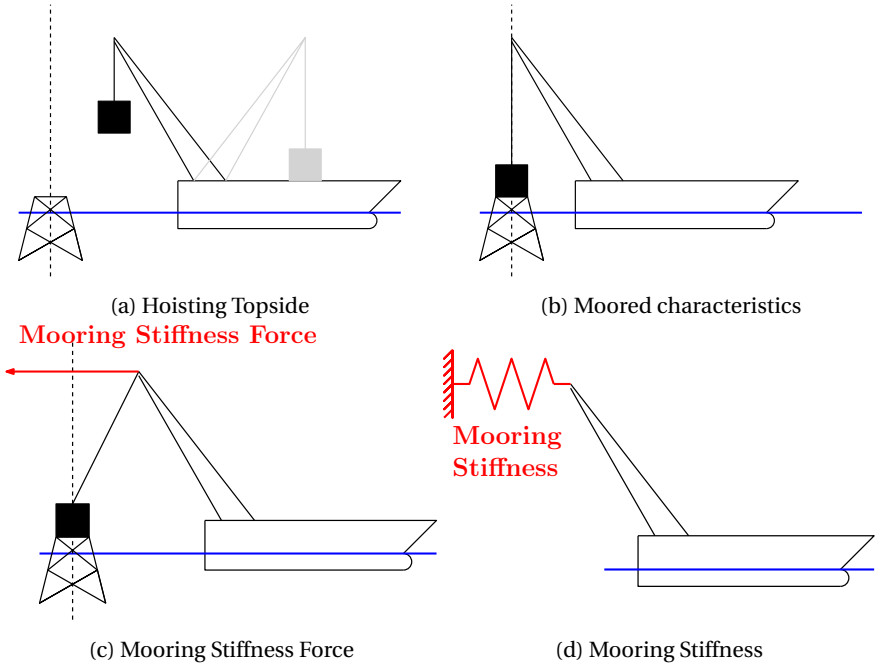

(a) Hoisting Topside (b) Moored characteristics

(c) Mooring Stiffness Force (d) Mooring Stiffness

Figure 1.1: Illustrations of topside installation operational stages and concepts.

Due to the high mooring stiffness the heavy lift vessel becomes a different dynamic system than for which the DP controller is tuned. This can result in poor and even instable behavior of the DP system. In the following paragraph a real-world example of the effect of the mooring stiffness is visualized.

The real-life example in Figure 1.2 illustrates the result of the mooring stiffness force. The progress of transferring the weight of the topside by unloading the tension in the crane is depicted in Figure 1.2. The thick black line is the hook load which is a measure for the tension in the cables and the thin black line is the horizontal (surge) position of the heavy lifting vessel. When inspecting the horizontal (surge) position of Figure 1.2 one could recognize this immediately as a case of control instability, as the oscillation in surge position of the vessel is increasing. Normally the operators don't have visualization in the time range of a few oscillation. Hence it is hard to identify this situation when it occurs. Fortunately there was no damage or injury in this case.

The ultimate consequence of loss of control may inflict great (economic) damage,

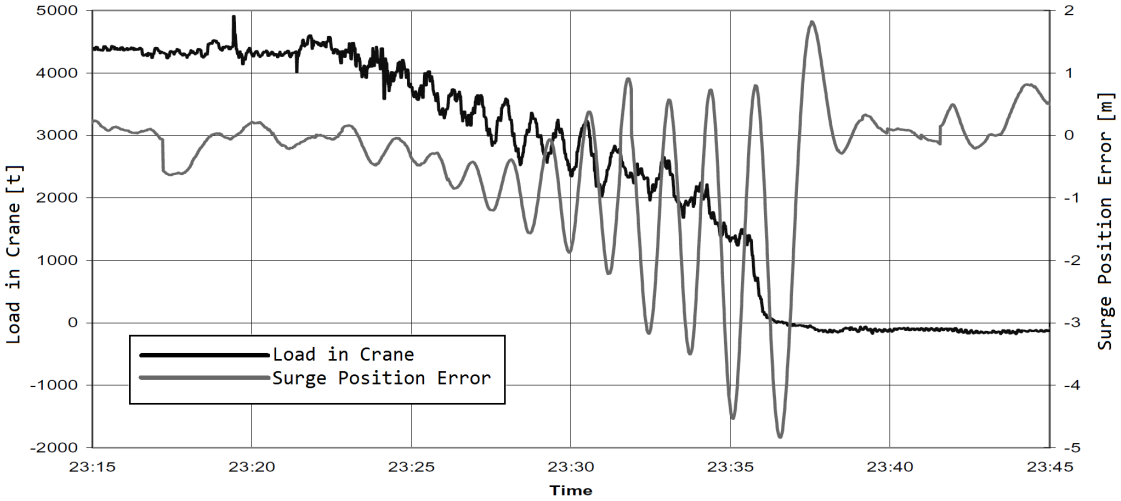

Figure 1.2: A plot of surge position and hook load during an installation of a topside on a jacket. (HMC, 2002)

human injury or even loss of lives. For this reason, the marine contracting industry is waiting for a reliable solution to this problem. This justifies this graduation study that aims to investigate the cause of the DP system's instable behavior and propose a concept solution.

1.2. PRELIMINARY GOAL

The latter example from practice is showing poor and instable behavior of the DP system caused by the large mooring stiffness forces. From now on this problem is related to as Mooring stiffness problem. In Section 3.3 a more thorough definition is given to the Mooring stiffness problem.

The goal of this thesis is to investigate the cause of the mooring stiffness problem, which is defined as instable behavior of the DP system during topside installation, and propose a conceptual solution.

The goal in this section is preliminary as the mooring stiffness problem also defined in this section is preleminary. In Section 3.5 the final goal of this thesis is given.

The following paragraph describes the scope of this thesis.

1.3. THESIS SCOPE

While there are many offshore heavy lift installation methods, this thesis will focus on topside installation operations, since the mooring stiffness problem is the most urgent during topside installations. Two main causes can be identified:

Firstly, the topside heavy lift tend to be the most heavy, which increases the mooring stiffness. In this thesis therefore the focus will be on loads of 500[t] and up.

Secondly, mooring stiffness is a typical problem when hoisting a heavy load on a fixed platform.

This thesis will focus on topside installations from the stern as shown in Figure 1.1. This will be explained later in section 3.2. The objective of this study is finding a conceptual solution to unstable dynamic positioning during offshore heavy lift operations. The results of this study is a good basis for development to a practical design. Therefore practical and realistic values and boundaries are considered, designing the concepts with a further elaboration to a real-world design in mind.

When observing heavy lift operations, many factors influence the overall performance of the operation, like weather, ballasting, crane characteristics, DP-system, crane operator experience. In this thesis the solution is searched for in the DP-system to solve the mooring stiffness problem.

Within this scope, 4 candidate solutions are designed. In literature [Waals, 2010] a model experiment with a solution to instable behavior of a heavy lift vessel on DP is described. The idea of the solution is to estimate the horizontal mooring stiffness forces and feed forward the forces by the vessel's own actuators. As a result the mooring stiffness forces are theoretically cancelled out by the actuators and the original system for which the DP system is tuned for is retrieved. If the DP controller for the original heavy lift vessel is theoretically stable, the feed forward solution is also theoretically stable. A promising conclusion of the latter referred paper is "The proposed feed forward method enhances the stability of the DP system during the installation of a large load in a model test experiment." The first solution concept is based on the feed forward solution concept from [Waals, 2010].

However the concern is that the estimated mooring stiffness forces, which are requested by the feed forward control law, can't be delivered by the thrusters because of insufficient performance. So three other solution are proposed which take this concern into account. These solutions are not theoretically stable but they ought to stabilize the vessel.

Furthermore, an addition to the 4 candidate solutions is suggested which is called DP Setpoint adaption. This additional concept can be used in combination with any of the 4 candidate solutions. The idea of the DP Setpoint adaption is to calculate the 'ideal' DP setpoint and automatically set this 'ideal' set point into the DP controller. The 'ideal' DP setpoint is the setpoint for which the mooring stiffness forces are zero.

To test the four candidate solutions and the DP set point adaption a computer simulation model of the heavy lifting vessel is created. This simulation model is based on the Imtech company Vessel DP software, which has proven itself in many real-world systems in vessels around the world, hence this DP software is well developed, realistic, validated and containing many practical details like thruster limitations, sensor noise, thrust allocation etc. Starting with Imtech company software a heavy lifting crane is modeled and added resulting in a simulation model of a heavy lifting crane vessel with DP software. A schematic diagram of the model is presented in Figure 1.3. In this figure the orange parts represent what is created for this study and the blue parts are used from other sources. The obtained heavy lifting vessel model will be used to simulate the topside installation on a jacket with and without the solution concepts.

As already mentioned, the idea of the proposed solution to the mooring stiffness problem is to estimate the mooring stiffness forces and feed the forces into the DP controller. In the computer simulation environment with Heavy lift vessel model the estimation of the forces by the solution is effortless. The estimation of the forces can be done by a copy of the same crane model as is used in the heavy lift vessel model. On one hand this is unrealistic because now the proposed conceptual solution is using a model which is perfectly matching with the model of reality. But on the other hand this is powerful as the proposed solution concepts will be tested in an environment where differences in model and reality are excluded. In other words the true conceptual working can be tested.

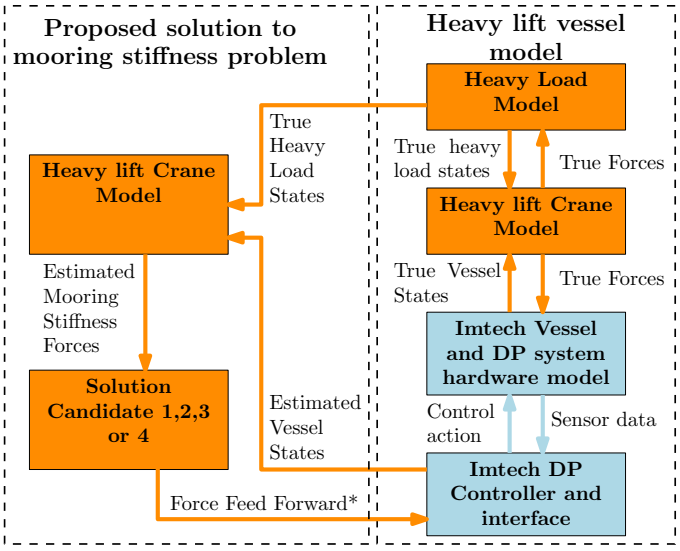

Figure 1.3: Simulation environment depicted in model blocks.
* Force Feed Forward depending on Solution Concept

With the use of this computer simulation model the solution concepts are tested and the performance is analyzed and compared with the performance without any solution concept. Results are remarkable as they differ from literature [Waals, 2010].

1.4. SCIENTIFIC CONTRIBUTION

The scientific contribution of this MSc graduation study is ought to be the following.

- The modeling of a heavy lift crane including internal cable damping.
- A concept found in existing literature is implemented in a model with a realistic DP system. This study tests whether the results found in [Waals, 2010] can be reproduced using a realistic DP system model.
- The design of 3 new conceptual candidate solutions.
- The practical implementation in computer simulation software of:
  - The heavy lift crane model
  - The candidate solutions into the simulation environment
  - DP setpoint adaption
- The analysis of the performance of the candidate solutions and the DP setpoint adaption.
- Obtaining recommendations for future research and practical design of a solution to the mooring stiffness problem.

1.5. THESIS OUTLINE

In Chapter 2 the reader is presented a thorough background of offshore heavy lifting in combination with Dynamic Positioning (DP). The subjects form basic knowledge needed to comprehend the rest of this thesis. Further in the thesis there is discussion about why the topside installation in particular is the most challenging heavy lift operation while using Dynamic Positioning.

In Chapter 3 the problem of mooring stiffness during topside installation is further discussed. First the topside installation on a jacket is investigated in detail. Then the

mooring stiffness problem is analyzed theoretically. Furthermore the current industry solution to the mooring stiffness problem is discussed, which seem to be a work-a-round instead of a thorough solution. Finally, the thesis goal is defined which is to find a conceptual solution to the mooring stiffness.

In Chapter 4 first the requirements of the conceptual solution are defined in Section 4.1. Then the solution space is investigated and from this solution space a solution direction is chosen in Section 4.2 and Section 4.3. In Section 4.4 4 candidate solutions are proposed. Also a practical concept for estimating the mooring stiffness forces is proposed. Furthermore an addition to the 4 candidate solutions is proposed which is named "DP Setpoint adaption". This is a possible addition to the other 4 candidates and is also incorporated in the study to find a conceptual solution. Now the performance of the candidates to solve the mooring stiffness problem have to be determined.

In Chapter 5 the methods of determining the performance is discussed. First a strategy of 3 phases to score the candidate solutions is proposed in Section 5.1. Scoring was done using the following strategy:

- Creating a simulation model of the heavy lifting vessel with DP system, this is discussed in Section 5.2.
- Implementing the 4 candidate solutions and the DP Setpoint adaption, which is discussed in Section 5.3.
- Defining a general simulation environment for testing the candidate solutions, this is done in Section 5.4.
- Defining the measures for scoring the candidate solutions, which is done in Section 5.5

After studying this chapter the reader will have a detailed understanding of the implemented methods. Next, the scoring strategy can be applied, of which the results shown in the next chapter.

In Chapter 6 the results of the scoring strategy are shown. A part of the direct discussion of the results is already done in this chapter. For example the non linear behavior of the oscillating motion of the vessel theoretically explained. Furthermore the performance of various solutions is discussed and explained theoretically why the concepts are performing as they do. This chapter concludes with one winning solution concept, however, not the one which was found to be promising in [Waals, 2010].

In Chapter 7 questions which arise from the results are further discussed thoroughly. First limitations and side notes on the study are given. Next, the instability is theoretically investigated. Finally recommendations for further studies are given and the main conclusions of this study are described.

2

BACKGROUND OF OFFSHORE HEAVY LIFTING ON DP

This chapter contains a detailed overview of the offshore heavy lifting industry and heavy lifting vessels, which allows the reader to obtain a theoretical basis to understand the rest of the report to the fullest. First, the subject of offshore heavy lifting is described in general in Section 2.1. Subsequently, Dynamic Positioning and the DP system with its components are described in Sections 2.2 and 2.3. Then a combination of the two subjects, heavy lifting of a vessel during dynamic positioning is described in Section 2.4. The last Section of this chapter describes why the topside installation is the most challenging heavy lift operation with respect to the mooring stiffness problem.

2.1. OFFSHORE HEAVY LIFTING

As mentioned before in Section 1.1, for oil field exploiting often submersed structures, pipelines and wells have to be deployed on the ocean bed. Furthermore oil and gas processing and storage is often performed directly in production units at sea. These units can be on a fixed or floating and even submersed platforms in all kind of different manners as is shown in Figure 2.1. Furthermore, offshore wind, current and tidal power generation is an upcoming sector in the industry. Windmills can be placed on bottom supported and floating structures, the latter is shown in Figure 2.2. According to [Rock and Parsons, 2010] Europe is the leader in offshore wind energy, with the first offshore wind farm being installed in Denmark in 1991. In 2010, there were 39 offshore wind farms in waters of Belgium, Denmark, Finland, Germany, Ireland, the Netherlands, Norway, Sweden and the United Kingdom, with a combined operating capacity of 2,396[MW]. Furthermore all structures which have been installed have to be decommissioned at some

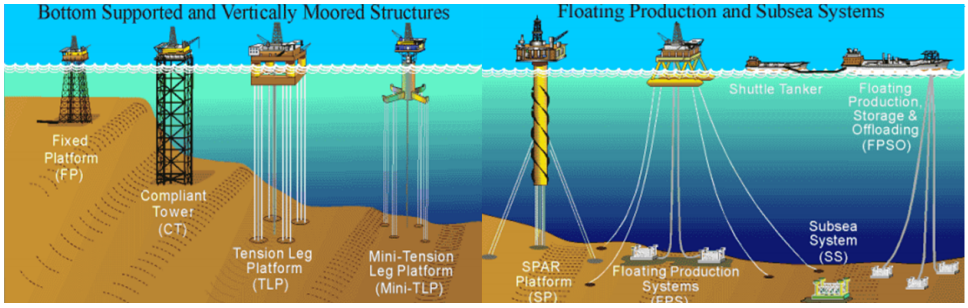

Figure 2.1: Examples of offshore supports structures(Kaminski, 2012a)

Figure 2.2: Example of an offshore wind park and a windmill floating support structure (Unknown, 2014)

Figure 2.3: Heavy lifting crane vessel Thialf(Kaminski, 2012b)

Figure 2.4: Image of heavy lifting vessel Dockwise Vanguard (Dockwise, 2014)

point in time. According to [Deloitte, 2011] with over 470 platforms to be wholly or partially removed from the North Sea, industry and governments face decommissioning costs which may approach USD 80 billion over the next three decades.

This growth of installation and decommissioning work has resulted in a tremendous increase of size of lifting vessels. In 1949, the Derrick Barge Four was built, a barge that was outfitted with a 150[t] revolving crane. In 1963, Heerema converted a Norwegian tanker, the Sunnaas, into a crane vessel with a capacity of 300[t]. In the year 2000 the Heerema Thialf has the largest offshore lifting capabililties in the world and is able to lift 14200[t]. [HMC, n.d.] In Figure 2.3 the Thialf is depicted.

In this thesis the most important of the definition of a heavy lift operation is that the dynamics of ship and the heavy load are noticeably coupled in normal operating conditions. I.e. the ship influences the dynamics of the heavy load but the heavy load also influences the dynamics of the ship. By definition, if the load has only minor influence on the dynamics of the ship, we do not consider it heavy load. More specifically, the weight of the heavy load must weigh at least 1% of the displacement of the vessel. Furthermore the focus of this thesis is on the heaviest loads in the industry at the time of writing. The lower weight boundary of heavy lift definition is taken as 500[t]. To give an idea of the displacement (mass of ship) and lifting capacity ratio the largest heavy lift vessel Thialf has an own displacement of approximately 150.000[t] in lifting conditions and can lift 14.000[t] [HMC, 2014]. The Oleg Strashnov has an own displacement of 77.210[t] and can lift 5.000[t] [SHL, 2014]. Based on these two examples the maximum heavy lift capacity is around 8[%] of the mass of the displacement of the vessel.

There is another heavy lifting method, where a semi-submersable vessel is used to lift a heavy load. This method can be used for transporting heavy loads or to install heavy loads. An example is the semisubmersible ship Dockwise Vanguard which is depicted in Figure 2.4. In this Thesis this kind of operation is not considered because this is out of the scope of this thesis.

In the next paragraph dynamic positioning of the heavy lifting vessel is discussed.

2.2. DYNAMIC POSITIONING (DP)

The next three paragraphs is an edited copy from [Wit, 2009, p. 2].

> Offshore drilling dates back to the mid 1920's when the first subsea wells were drilled. Starting at tidal zones and piers, the first drilling activities soon occurred from concrete platforms near the shore. In the 1940's fixed drilling/production platforms allowed drilling at a water depth of 6 meters, tens of kilometers off the coast. Keeping a fixed position in these shallow waters obviously never was a problem, but when the demand for deep water drilling increased in the 1950's station keeping became a large obstacle. This resulted in different positioning solutions.
>
> A jack-up barge can be used in water depths up to approximately 120[m]. When it is on location, it can raise itself clear of the sea with its three or more, massive legs. A jack-up barge has the benefits of a fixed platform combined with the ease of mobility. A large advantage of this system is that the station keeping is not vulnerable to blackouts or power shortages and there is no need for a position reference system, once on location. The maximum water depth at which it can operate, however, is very limiting compared to the other mooring solutions.
>
> Spread mooring and anchor pattern like systems can be used for many different structure types in water depths exceeding 1000[m]. The position is controlled by fixing the vessel to the seabed using mooring lines and anchors. Positioning therefore takes up a lot of time and can be quite expensive due to the required anchor-handling tugs. When a large position shift

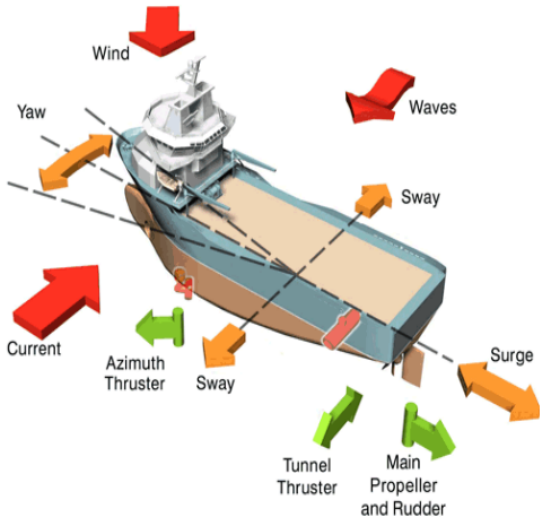

Figure 2.5: Sketch of basic nomenclature with respect to DP[Fossen, 2011]

is required, all or some of the anchors will need to be lifted and relaid. Then there is also the possibility of underwater hazards represented by any existing underwater installation, such as pipelines.

The rest of this Section is based on [Wit, 2009, p. 2]. Dynamic positioning (DP) is more than a mooring system. Dynamic Positioning is a method to automatically maintain a vessel at position and/or heading or maintaining a predefined track by use of its thrusters and/or rudders. In general the DP system should counteract wave, wind and current forces. Figure 2.5 gives these environmental loads in red, the possible horizontal movements in yellow and the possible actuator working directions in green. DP systems are not limited to a maximal water depth as they automatically control the position and heading of a vessel by using its own propulsion system. Although this gives a lot of freedom, it also makes DP systems relatively complex. This complexity comes with a price hence DP systems are typically high capital expenditures. The propulsion system needs to react to environmental/external changes continuously, which brings more reliability problems. This online approach is more vulnerable to failures regarding the power supply, thrusters, electronics or the reference system than offline approaches as jack-ups and spread anchor moorings. On the other hand, DP systems provide a solution that can be used at any water depth (only excluding some shallow waters), DP systems can be very precise because they can response relative rapidly on environmental/external changes and DP is commenced very quickly and easily. The position footprint of a professional DP system used in offshore operations is typically smaller than 2[m][El Amam, 2013] during low seastate. No assisting tugs are required whatsoever and a DP ship can easily change to another location without a lot of extra costs. Also underwater equipment like submersed structures on the seabed, pipelines and wells form no obstacle, as DP only relies on its own propulsion of the vessel instead of mooring by using the seabed.

Having discussed the usage of DP, now we can focus on the DP system itself in the following section.

2.3. THE DP SYSTEM

In this section, which is based on [Fossen, 2011], the DP system with all its building blocks is reviewed thoroughly. As already mentioned the DP system enables to auto-

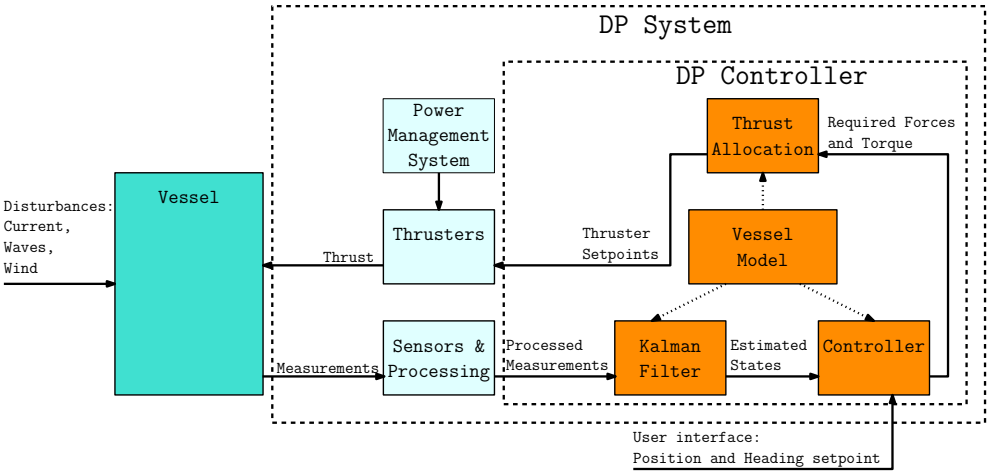

Figure 2.6: Overview of building blocks of DP System

matically maintain a vessel at position and/or heading or maintaining a predefined track by use of its thrusters and/or rudders. To do this, a number of hardware and software building blocks are required. These blocks are depicted in a schematic overview of a DP system in Figure 2.6. For automatically positioning the vessel, sensors are required. After obtaining sensor data, it is to be processed. The vessels true states(i.e. position, velocity, orientation, etc.) are estimated by a state estimator. A state observer technique widely used in the industry is the Kalman Filter. Next the position and heading controller will send out a required control action based on the estimated states of the vessel and the setpoints defined by the operator. This control action is an amount of force in surge and sway direction and an amount of torque in the yaw direction. The thrust allocation block will calculate the optimal individual thruster settings corresponding to the control action. The power management system delivers the required power. In several building blocks a model of the vessel is used. In the DP Controller the vessel model is used for estimating the right states by the Kalman filter, calculating the right control action in the controller and calculating the right thruster settings by the thrust allocation.

Now all building blocks will be discussed separately.

SENSORS & PROCESSING

The sensors & processing block of the DP system consists of several types of sensors. A typical sensor equipment for a heavy lift vessel consists of 3 GPS sensors, 3 motion reference units containing acceleration and gyroscopic sensors, wind sensors and draft sensors. Furthermore some special sensor systems which can be selected during certain operations. For example hydro acoustic sensor systems to measure distance from reference beacons in the water, or laser/radar distance measurement systems which are measuring distances to certain reference beacons.

Also an important part of the sensor system is the sensor measurement processing. All signals from external sensors should be thoroughly analyzed and checked in a separate signal processing module. This comprises testing of the individual signals and sensor signal voting and weighting when redundant measurements are available. The individual signal quality verification should include tests for signal range and variance, frozen signals and signal wild points. If an erroneous signal is detected, the measurement should be rejected and not used by the positioning system. The weighted signals from each sensor group should not contain any steps or discontinuities when utilized further in the system ensuring a safe operation.

KALMAN FILTER

A state observer is a very important component in the DP Controller. A state observer technique widely used in the industry is the Kalman Filter.

In most cases today, accurate measurements of the vessel velocities are not available. Hence, estimates of the velocities must be computed from noisy position and heading measurements by a Kalman filter. The position and heading measurements are corrupted with colored noise, mainly caused by wind, waves and ocean currents. Furthermore, the Kalman filter can also be used when the position or heading measurements temporarily are unavailable. This situation is *called dead reckoning*, and in this case the predicted estimates from the observer are used in the control loop. Another feature of the Kalman Filter is that it estimates the unmodeled and unmeasured slowly-varying forces and torques, mainly due to second-order wave loads and ocean current. Normally ocean current is not measured but estimated as follows: First the Kalman filter estimates the vessels velocity through the water by using the vessel model and the thruster settings. This velocity is compared to the measured ground speed which is measured by the GPS system. The current velocity is calculated by subtracting the true vessel speed from the estimated velocity. This principle is called *the current model buildup*. The consequence is that if the true vessel is wrongly modeled in the DP controller, other forces are also included into the current model.

Next, the working principle of the Kalman filter is discussed. To do this an example of a linear Kalman filter in state space is depicted in Figure 2.7. In pink the plant is depicted in state space description, with its corresponding **A B** and **C** matrices. In reality the plant matrices are unknown. In blue the model of the plant is depicted in statespace with its corresponding matrices $\hat{\mathbf{A}}$, $\hat{\mathbf{B}}$ and $\hat{\mathbf{C}}$. **u** is the known input of the plant and the model. **y** is the output vector of the plant which can be measured. $\hat{\mathbf{y}}$ is the estimated output vector by the Kalman filter. **K** is the Kalman gain which can be chosen free to give more emphasis on the measurements **(y)** or on the estimated output values $\hat{\mathbf{y}}$. For example if the measurements are very noisy but the model is very precise, one can give more emphasis on the estimated output values $\hat{\mathbf{y}}$. Furthermore, **x** is the state vector of the plant which can not be measured and $\hat{\mathbf{x}}$ is the estimated state vector. Next, to clarify the working of the Kalman filter some examples of use cases are given.

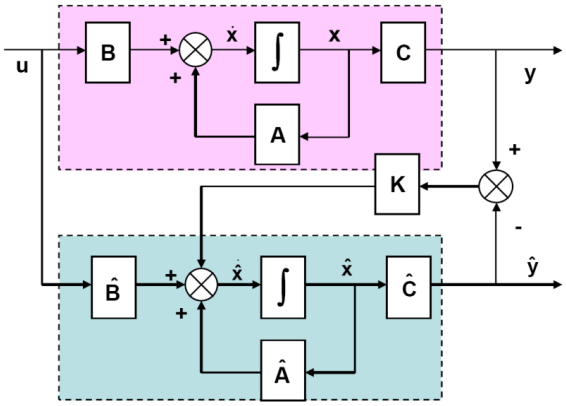

Figure 2.7: Concept of Kalman Filtering in State space[El Amam, 2013]

Suppose this Kalman filter is used for estimating the state 'surge position' of the vessel. In reality the plant is unknown and only the output of the plant **y** can be measured. In this case the position can be measured by GPS measurements, but the GPS measurements are noisy. Now the state 'surge position' (**y**) is compared with the estimated 'surge position' $\hat{\mathbf{y}}$. The Kalman filter updates the model state $\hat{\mathbf{x}}$ towards the real plant according to the Kalman gain **K** such that the estimated states converge to the real plant. The result

is a smoother (filtered) signal by mediating between the sensors and the model.

Now suppose one wants to know the velocity of the vessel. This is not directly measured by a sensor, but this state is available in the state vector $\hat{x}$ of the Kalman filter. Now the Kalman filter is a state estimator.

Now suppose all sensors fail and no measurements of y are available anymore (dead reckoning). Because the control action u is known, an educated guess can be done by using only the model plant (in blue) to estimate the states $\hat{x}$ of the real plant. With these estimated states better control actions can be calculated than if no estimator was used.

Depending on the Kalman filter algorithms one can do smoothing, filtering and prediction. This can be seen in 2.8.

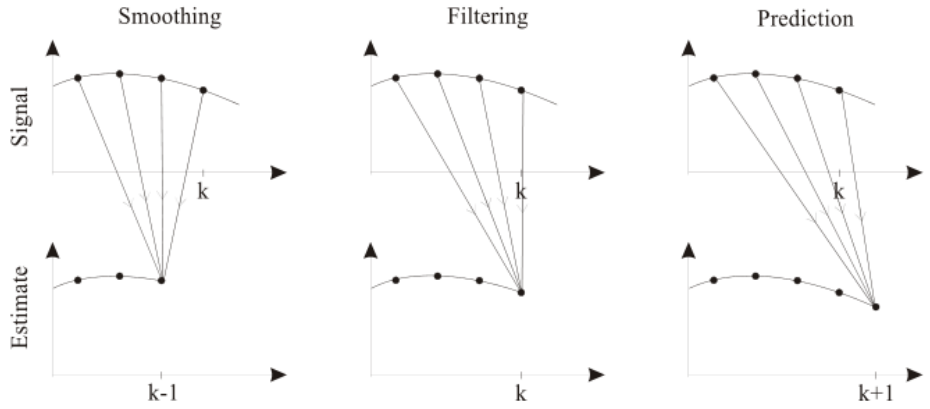

Figure 2.8: Operational modes of Kalman Filter

POSITION/HEADING CONTROLLER

The positioning controllers are often of the PD type (multivariable or decoupled in surge, sway and yaw), where feedback is produced from estimated position and heading deviations and estimated velocities. In addition to the PD part, integral action is needed to compensate for the static (or slowly-varying) part of the environmental loads. The controller should be optimized with respect to positioning accuracy, fuel consumption, and wear and tear of the propulsion system. The positioning controller calculates the desired force in surge and sway direction. Furthermore it calculates the torque to achieve a desired yaw motion.

THRUST ALLOCATION

The high-level feedback and feedforward controllers requests desired forces and torques. The thrust allocation module computes the corresponding force and direction commands to each thrust device. The low-level thruster controllers will then control the propeller pitch, speed, torque, and power satisfying the desired thrust demands. The thrust allocation algorithm should be optimized for fuel consumption, wear and tear of the thruster devices and for obtaining the commanded thrust in surge, sway and yaw. In addition, the function should take into account saturation of the rpm and pitch inputs and forbidden directional sectors. The thrust allocation module is also the main link between the positioning system and the power management system.

POWER MANAGEMENT SYSTEM

In this thesis the power management system is assumed to be ideal and is not further part of the study.

THRUSTER SYSTEM

As already mentioned, the thrusters are controlled by the low-level thruster controllers.

Heavy lift operations are often operated during DP. Hence the heavy lift operation on DP is discussed.

2.4. HEAVY LIFT OPERATION ON DP

The accuracy of the DP system is high enough to use DP during heavy lift operations. The clearance between vessel and heavy load is usually in the order of 5[m] to 10[m]. Apparently the advantages of using DP during heavy lifting operations are greater than the disadvantages, because in general marine contractors only use alternatives in very shallow waters. The advantages of using DP during heavy lift operations are:

- In comparison to other offshore operations, heavy lift operations take a small period of time. For example installation of a transition piece of a offshore wind turbine takes 12 hours of work. Hence DP is a favorable choice because DP station keeping is initiated and deactivated very quick.
- By using DP the vessel is maneuvered by one operator, contrary to tug support where more separate tugs are maneuvering the heavy lift vessel. Hence it is more easy to maneuver the vessel, also when a heavy lift is to be positioned.
- Because of the complex operation involving other vessels and (submersed) structures the usage of anchor lines by the heavy lift vessel doesn't have the preference.

Disadvantages are obviously the higher fuel usage than station keeping with anchors. To give an impression the Oleg Strashnov has six thrusters of 4,3MW installed [SHL, 2014]. On the other hand no anchor handling and positioning tugs are needed. Furthermore a certain probability of running off position by system failures or blackouts is present. Due to redundancy this probability is minimized.

Heavy lift operations are never limited by the capability of the DP system to withstand higher waves and stronger wind, as the heavy lift operations are in this case already limited by the safety of personnel during these stronger weather conditions.

As already mentioned, the advantages are larger than the disadvantages so DP is used often during heavy lift operations.

In the next section is described what the general challenges of heavy lifting on DP are and in why the topside installation is the most challenging with respect to the mooring stiffness problem.

2.5. WHY THE TOPSIDE INSTALLATION IS CHALLENGING

As mentioned in Section 2.3, the DP controller uses a mathematical model of the system for maintaining the correct position and heading of the vessel. This mathematical model (see Fig. 2.6) contains the characteristics of the vessel among other information about winds and tidal currents. The mathematical model is fed with information through parameters, setpoints and realtime sensor information. It is paramount that the model should meet the 'real world' as close as possible, since mismatching may lead to poor performance or even to an unstable system. The ultimate consequence of loss of control may inflict great (economic) damage, human injury or even loss of lives.

During a heavy lift operation the heavy load and vessel experiences four fundamental different operational states that imposes very different forces on the heavy lift crane and the vessel.

1. the heavy load rests on the vessel.
2. the heavy load is lifted and free hanging or submersed.
3. the heavy load is on a fixed platform like a jacket.

4. the heavy load is on a floating platform like a barge.

During all states is assumed that the hoist cable is taut and almost all weight of the heavy load is on the crane.

States 2 and 3 have very different load characteristics: When free hanging, the load can sway and impose limited forces. When resting on the jacket the system resembles a mooring characteristic. Horizontal hoist cable forces may increase rapidly as a function of the displacement and may even increase even 10 times as fast as the thruster forces. The difference in load characteristics between states 2 and 3 is larger than states 2 and 4, as the movement of the barge decreases the stiffness of the mooring characteristics. Now consider a transition between state 2 and 3 like installing a topside on a jacket. During touch down of the topside the load characteristics of state 2 are followed up by the load characteristics of 3 in a few seconds. Due to this large change in load characteristics the heavy lift vessel becomes a totally different dynamic system as the DP controller is tuned for. This may result in poor, or even unstable performance of the DP positioning system.

The described challenges of large mooring stiffness and rapid change of load characteristics apply especially to topside installations with massive loads. As the horizontal hoist cable forces increase when the load is more heavy. Now it is clear why the topside installation is the operation which is in the focus of this study.

In Section 3.1 the topside installation on a jacket is described thoroughly.

3

PROBLEM OF MOORING STIFFNESS DURING TOPSIDE INSTALLATION

In this chapter the mooring stiffness problem during a topside installation is studied thoroughly. For doing so, first the topside installation is described thoroughly in Section 3.1. Afterwards the problem of the mooring stiffness is explained in Section 3.2. Next the formal definition of the mooring stiffness problem is given in Section 3.3. In Section 3.4 is described why the industry solution to the mooring stiffness is not satisfying. Subsequently, in Section 3.5 the goal of this MSc graduation thesis is stated.

3.1. TOPSIDE INSTALLATION ON JACKET

In this section the topside installation on a jacket is described thoroughly. Furthermore, formal definitions are given to operational stages. This section is an introduction to the Section 3.2 which analyzes the mooring stiffness problem during the topside installation on a jacket.

Consider an installation of a topside on a jacket on DP which is depicted in Figure 3.1. From now on the operation is divided in three operational stages which are described below and sketched in figure 3.2.

1. Hoisting DP operation stage (Figure 3.2a)
   In the operation a topside is lifted from a barge or the heavy lifting vessel itself. In the case of a barge it is moored to the heavy lifting vessel with fenders in between. The barge and heavy lift vessel are approximately 1 free floating body now. The heavy load is hooked to the hoisting cables and other manual preparations are done by deck personnel. Next the heavy load is hoisted from the barge or vessel while, if necessary, the ballast levels are rearranged. Then, the barge is removed from the heavy lifting vessel and the heavy lift vessel maneuvers to the jacket. The heavy load is positioned above the jacket and hoisted down towards touch down to the jacket. After touchdown the next stage is commenced.

2. Moored DP operation stage (Figure 3.2b)
   In the beginning of the moored DP operation stage the tension in the hoisting cables is as large as the hoisting DP operation stage. During the current stage the tension is released to zero. During this operation the ballast levels are changed manually to keep the roll and pitch of the vessel acceptable. During this stage the heavy lifting vessel is practically moored via the crane. The transition of the weight to the jacket is taking approximately 30 minutes. When the tension in the cables is released the next operational stage is commenced.

Figure 3.1: Offshore wind power converter station installation on a jacket by the HMC Thialf (HMC, 2015)

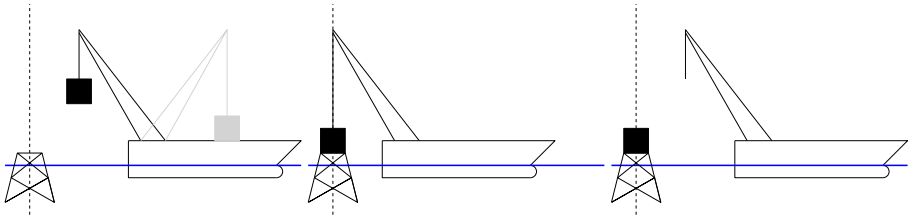

(a) Hoisting DP (b) Moored DP (c) Free floating DP

Figure 3.2: Sketches of operational stages of a topside installation on a jacket heavy lift operation

3. Free Floating DP operation stage (Figure 3.2c)
   To finalize the operation typically some manual installation work has to be done and the hoisting cables are detached by deck personnel. Now the heavy lift vessel maneuvers away from the jacket increase clearance.

During the operation a clearance between the crane and the platform is typically 5 meters. A minimum clearance have to be maintained in any case. Furthermore a maximum motion of the platforms is not to be exceeded, as this is dangerous for deck personnel.

In Figure 2.1 was shown that there are besides a jacket also SPAR and TLP structures to install a topside on. There are close resemblances between the latter and the topside installation on a jacket, but this MSc graduation study will be focused on topside installations on jacket.

According to the industry during the moored DP operation stage and during changeover to the Free floating DP operation stage the most difficulties arise. In the next section the reason to this is explained thoroughly.

3.2. MOORING STIFFNESS AND ITS PROBLEMS

As already explained in Chapter 1 and Section 2.5, the most crucial part of this heavy lift operation is when the heavy load is placed on the jacket but there is still tension on the hoisting cables. Due to the mooring characteristics of the load, the heavy lift vessel becomes a totally different dynamic system as the system the DP controller is tuned for. In this section this effect and the consequences is described. This section is based on the paper [Waals, 2010]. During this explanation a heavy lift vessel with the following realistic specifications is used as an example:

Example parameters	
Mass vessel	100000 [t]
Mass heavy load	1000 [t] (1% of Mass vessel)
Hoist cable length	50 [m]

Now the topside installation is analyzed in the sequence as is described in section 3.1. For the explanation a simple linear model of a vessel with PID controller and viscous hydrodynamic damping is used. Furthermore in this section the hoist cable is assumed to be inelastic. For this analysis only the surge of the vessel is studied of which the reason becomes clear at the end of this section. First let's consider a vessel during the Hoisting DP operation stage.

HOISTING DP OPERATION STAGE

This vessel carries a heavy load on deck. The vessel is equipped with a DP system which can deliver thrust. A simple linear equation of motion of this vessel in surge direction is:

$$M\ddot{x} + B\dot{x} = F_{environment} + F_{DP} \tag{3.1}$$

Where M is the rigid body vessel mass including the added mass. The mass of the heavy load is neglected in this equation. B is the hydrodynamic damping which can be estimated using linear potential theory. F_{DP} is the thrust by the DP system and $F_{environment}$ forces on the vessel by environmental loads like wind, waves, current.

As already mentioned, heavy lift operations are often conducted on DP. Proportional, Integral, Derivative (PID) control is a common and robust control method that is often used to keep the DP vessel on its target location. The size of this total thrust vector depends on the proportional gain of the PID controller and the value of the position error (Δx). The DP control action (F_{DP}) due to proportional(F_P), integral(F_I) and

derivative(F_D) are defined respectively as follow:

$$F_P = P\Delta x \tag{3.2}$$

$$F_I = I\int_{t=T-n}^{T} \Delta x dt \tag{3.3}$$

$$F_D = D\frac{d\Delta x}{dt} \tag{3.4}$$

$$F_{DP} = F_P + F_I + F_D \tag{3.5}$$

In which T is the present time and T-n is the time interval over which the mean position error is integrated. Δx is a certain position offset. The P term has the same effect of a spring which would be attached to the vessel with stiffness P. Hence the P term partially determines the 'stiffness' of the DP controller. The I-term is there to correct the mean offset. D term has the same effect as damping on the horizontal motions of the vessel. The total force that is requested by the PID controller is F_{DP}. Now substituting equation 3.2, 3.3, 3.4 in 3.5. Where after substituting this equation in 3.1 and rearrange the equation will lead to the following equation of motion for the vessel:

$$M\ddot{x} + (B+D)\dot{x} + Px = F_{environment} - I\int_{t=T-n}^{T} \Delta x dt \tag{3.6}$$

Now a damped mass spring system equation is achieved, with spring stiffness P and damping (B+D). The stability of the vessel with DP system mainly depends on the ratio between the P and D action. The damping factor is calculated as:

$$\zeta = \frac{B+D}{2\sqrt{M*P}} \tag{3.7}$$

P is chosen for a certain required aggressiveness to position errors/stiffness. Typically the D term is chosen such that the overall system behavior has 30% to 70% of the critical damping (ζ = 0.3 to 0.7). Typically the natural period of the DP system for surge and sway is in the order of 100[s] to 200[s]. These periods occur at a term P of the DP system between 50[kN] and 150[kN] thruster force each meter offset.

Now the free floating heavy lifting vessel lifts the heavy load from deck and places the heavy load on the jacket. The Moored DP operational stage commences.

MOORED DP OPERATIONAL STAGE

Now the heavy load is rigidly placed on the jacket, but the load is not yet transferred from the vessel to the jacket. So the load in the hoist cable is still approximately 1000[t]. This mean load in the hoisting wire will lead to a contribution to the horizontal stiffness. Now the equation of motion is derived for the vessel in the Moored DP operational stage.

Suppose the vessel drifts from position in such a way that the crane tip is not above the jacket anymore. A restoring force F_x, which is called *mooring stiffness force* throughout this thesis, is exciting on the vessel via the crane. See Figure 3.3.

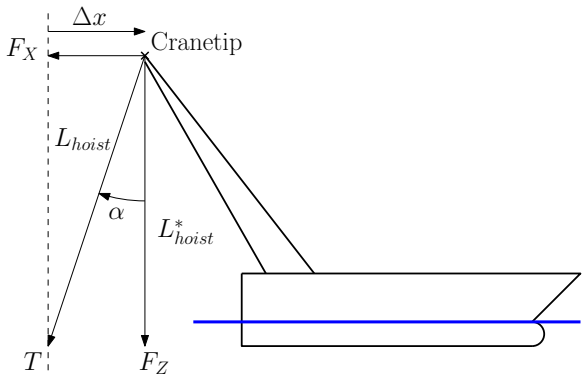

Figure 3.3: A schematic image of geometrics and forces in the crane tip of the heavy lifting vessel in Moored DP operational stage.

F_X is the mooring stiffness force in horizontal plane. T is the tension in the cable and F_Z is the force downwards on the cranetip. F_Z is approximately the gravitational force of the heavy load. Assume that α is small, now $L_{hoist} \approx L^*_{hoist}$ and $T \approx F_Z$. Because α is small the following equations hold:

$$\alpha \approx \frac{F_X}{T} \tag{3.8}$$

$$\alpha \approx \frac{-\Delta x}{L} \tag{3.9}$$

$$F_X \approx -\frac{T\Delta x}{L} \tag{3.10}$$

The equations state that the mooring forces are linear dependent on Δx. Due to the mooring stiffness forces there is practically a linear spring attached to the vessel with stiffness (T/L) which is sketched in Figure 3.4.

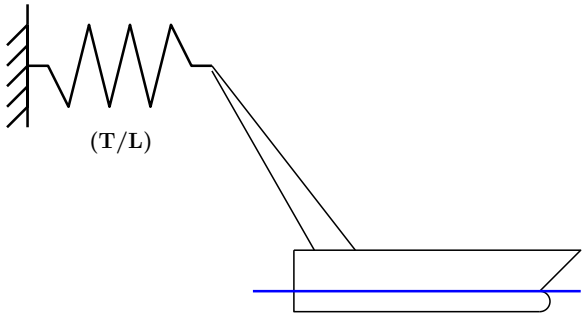

Figure 3.4: A schematic image of a heavy lifting vessel with linear spring stiffness (T/L).

The equation of motion of the vessel moored via the crane is now obtained by adding F_X from equation 3.10 to equation 3.6:

$$M\ddot{x} + (B+D)\dot{x} + (P + \frac{T}{L})x = F_{environment} - I\int_{t=T-n}^{T} \Delta x dt \tag{3.11}$$

The additional spring term (T/L) can be larger than the P term of the DP system itself. The original DP system obtains with 70[%] of critical damping a P term of 100[kN/m]. With a load in the hoist cables of 10.000[kN] and a hoisting length of 50[m] the additional spring stiffness is 200[kN/m]. For heavy lifts with 5.000[t] this additional spring may increase up to 1000[kN/m]. This concludes that the effective stiffness term $P + T/L$ in the equation of motion 3.11 can exceeds the original DP stiffness term P by a factor 10.

This sudden increase is achieved in a few seconds after touch down of the topside on the jacket.

So due to the mooring stiffness a considerably higher effective spring stiffness is obtained. Now is focused on the effect of the effective spring stiffness to the damping ratio ζ of the system. Lets take the critical damping $(B+D)_{crit}$ which is the damping of the system which is needed to let the system be critically damped. Critical damping is obtained when $\zeta = 1[-]$ is filled in equation 3.7. Doing so, equation 3.7 becomes 3.12.

$$(B+D)_{crit} = 2\sqrt{M * (P + \frac{T}{L})} \tag{3.12}$$

Furthermore, the damping ratio ζ is:

$$\zeta = \frac{(B+D)}{(B+D)_{crit}} \tag{3.13}$$

Now to visualize the effect of an increase of effective spring stiffness Table 3.1 is added to this section. In this table the effective spring stiffness $(P+T/L)$ is increased which can be the effect of lifting higher loads. This table compares the true damping $(B+D)$ with the critical damping $(B+D)_{crit}$. The true damping is constant, and the critical damping is a function of $(P+T/L)$ as is given in Equation 3.12. In Table 3.1 one can see that the damping ratio is decreasing almost with a factor 3.5 to 22[%].

Effective spring stiffness $(P+T/L)$ [kN/m]	Critical damping $(B+D)_{crit}$ [kNs/m]	Damping $(B+D)$ [kNs/m]	Damping relative to critical damping (damping ratio) $\zeta = (B+D)/(B+D)_{crit}$ [%]
100	6325	4427	70 %
200	8944	4427	49 %
500	14142	4427	31 %
1000	20000	4427	22 %

Table 3.1: Increasing critical damping for increasing effective spring stiffness

The results of this relatively large increase in the effective spring are:

- As already mentioned and visualized in Table 3.1, the effective damping of the system decreases.
- Shorter natural period of the vessel. Due to the shorter natural period thrusters will change more often in magnitude and direction so the difference between required and actual delivered thrust increases. The actual delivered thrust can differ in amplitude and lag in time. In the first case the thrusters had too little time to buildup their revs and in the second case the delivered thrust lags from requested thrust.
- Due to a deviation between required and actual delivered thrust, of which it is likely that the required thrust is more than the actual thrust, the hydrodynamic damping B due to operating thrusters may also be smaller.
- The mooring stiffness forces are unknown to the Kalman filter of the DP controller. Now the estimation of the states of the system by the Kalman filter (e.g. acceleration, velocity, position) is less good than in the case that no mooring stiffness forces are present. A larger difference between the true states and estimated states by the Kalman filter is the consequence. Also in this case a difference in amplitude and in time can be the consequence. For example in periodic movement the estimated velocities are lower which can lead to a larger deviation between required and actual delivered thrust.

The consequences to the results mentioned above, are that the system is more sensitive to instable behavior because of 3 aspects:

1. Lower effective damping, due to:
   (a) Higher effective spring stiffness
   (b) Less hydrodynamic damping
2. Control action are worse, due to
   (a) the fact that the controller is tuned for a different dynamical system.
   (b) Difference in amplitude and lag between the true and estimated states.
3. Thrusters are likely to lag more, due to:
   (a) Lag in state estimation
   (b) More lag in thrust build up because the oscillation period decreases(i.e. oscillation frequency increases) and the thrust buildup rate is equal.

Due to aspect 3a the problem is that the thrusters are within the Feedback system and introduce lag, lag in feedback system means instability.

Now it becomes clear why only the surge direction is studied. As the low damping is one of the key aspects of the problem, vessels have the lowest damping in surge direction. This is also the reason why just heavy lift operations over the stern of the vessels are considered. Otherwise, if operated over starboard side or port side the vessel will yaw and motion will be damped more with respect to only stern operated operations.

One more effect is to be discussed, which is the *current model buildup*. Normally tidal current is not measured but estimated by the DP system. The DP controller contains a model of the vessel so it can estimate the vessel's velocity through the water given certain thruster setting. The ground speed is measured by GPS and using these two values the tidal current velocity and direction is estimated. This principle is called *the current model buildup*. Because of the nature of this technique all unmodeled long lasting forces are included into this 'current'. The result is that because the mooring stiffness forces are unknown to the Kalman filter in the DP controller, the current model is also including mooring stiffness forces to the current. The result is a large error in the built current model.

If everything went well, in spite of the potential problems described above, the load is transferred to the jacket. Now the next operational stage commences.

FREE FLOATING DP OPERATIONAL STAGE

In this stage the tension in the cables is zero hence the mooring stiffness is zero. Hence the original equation of motion (Equation 3.1) is retrieved. But as mentioned above, the current model is estimated with a large error. The result is that after the stage transition the DP controller will compensate for environmental forces which are not present. The end result is that the vessel will drift of position just after commencing the Free floating DP operational stage.

As already mentioned, incidents have already been reported of the mooring stiffness problem. A real life example to illustrate the consequences of the problem is already given in the introduction of this thesis(Section 1.1). Now knowing the exact problems and being the operational stages defined, the definition of the Mooring stiffness problem can be described in its final form the next section.

3.3. DEFINITION MOORING STIFFNESS PROBLEM

The mooring stiffness problem is defined as follow:

> "Instable behavior of the DP system during a heavy lift topside installation on a jacket and non-smooth behavior during the stage change from moored DP operation stage to free floating DP operation stage"

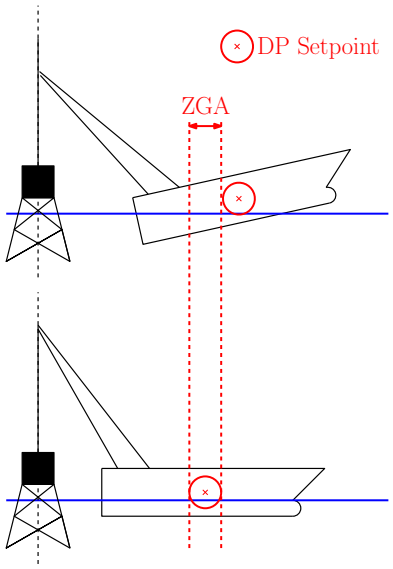

Figure 3.5: Example of working principle due to pitching the vessel is pushed outside of the ZGA

The next section will focus on the current industry solution and why the solution is not satisfying.

3.4. INDUSTRY SOLUTION TO THE MOORING STIFFNESS PROBLEM

The mooring stiffness problem is already recognized by one of the leading DP controller suppliers and a solution which is a specialized heavy lift function is already developed. One way to look at the moored DP stage is the following. If the heavy load is placed on the intended platform, the platform will determine the position of the heavy lifting vessel instead of the DP system of the heavy lifting vessel itself. The difference in order of magnitude between the mooring stiffness and the 'DP stiffness' enforces this idea.

The heavy lift function is based on this idea. So the jacket will determine the position instead of the DP system and the thruster usage can be minimal when position deviations are small. This is applied by defining a *Zero Gain Area*(ZGA) around the DP setpoint. In this area the DP controller settings are changed as follow:

1. The proportional gain of the DP controller is zero
2. The damping by the controller can be increased.
3. current model and I-action of DP controller is frozen

The operator guidelines with respect to using the heavy lift mode are as follow:

- The heavy load should be positioned in normal (free floating) DP mode
- When the heavy load is engaged on the jacket the ZGA function should be activated
- If the hoist cable tension is almost zero the mooring stiffness will not overrule the DP forces anymore and normal DP mode should be initiated again.

The working principle is as follow. Due to point 1 of the changed DP controller settings the effective spring stiffness will decrease and the thruster usage is less. This combination lead to less difference between required and delivered thrust. Due to less usage of the thrusters the average mooring stiffness are probably also lower so the state estimation by the Kalman filter is also better. Due to point 2 and due to the decrease of

effective spring stiffness the effective damping is increased. Due to point 3 the value of the current is saved and not wrongly adjusted anymore during moored stage of operation. So the poor performance after stage transition from moored stage to free floating stage is reduced.

In general the *Zero Gain Area* will improve stability. But the industry solution has its disadvantages.

The first disadvantage is that instability can still occur by oscillating from one side to another of the ZGA. Hence with the idea that the jacket will define the position in mind, DP operators are advised to increase the ZGA range or change the center of the ZGA to the current position if the vessel is tending to the ZGA border.

Furthermore some operators don't use this function during a heavy lifting operation because they think the mode is unpredictable. Because inside the ZGA the DP system doesn't react to position deviation but if the vessel drifts outside the ZGA the DP system suddenly act aggressively with respect to inside the ZGA. Some industry players stated that their operators instead of using this ZGA mode they lower manually gains and/or increase the damping term of the controller. This approach can also be very effective but an operator have to really understand the possible consequences.

Another disadvantage of the industry solution is that the *Zero Gain Area* is defined for the position of the heavy lifting vessel and not for the heavy load. Hence if the vessel is ballasted in a way the vessel pitches or rolls, an extra force can be induced by the change of the crane tip position which is not taken into account by the system. So due to pitch or roll the vessel can be pushed out of the zero gain area. See 3.5 for a sketch of this principle.

When the operation is almost finished, the ZGA is switched off if the hoist cable tension is almost zero. During the heavy lift operation the environmental forces can be changed because of for example a change in current and wind direction and velocity. But the current model is still the same as in the beginning of the operation, therefore this can induce a sudden reaction of the DP system of the vessel. This is dangerous because the vessel is still close to the platform.

To conclude this section, the ZGA mode will help preventing the mooring stiffness problem. But generally speaking the current industry solution is not solving the essential problem, but working around it.

3.5. THESIS GOAL

This section is concluded with the goal of this thesis. But first the findings in this chapter are shortly summarized.

The problem is that the DP system can behave instable during a topside installation. This instability is induced by forces in the horizontal plane which are acting on the vessel via the crane, so called mooring stiffness forces. These forces are changing from amplitude and direction and are not modeled by the DP controller. The mooring stiffness can grow up to an order of 10 times the original stiffness term from of the DP system. The combined effective stiffness result in:

- Lower effective damping
- Poor control action
- Lagging thrusters
- Erroneous current buildup

Furthermore the current industry solution, the *Zero Gain Area* (ZGA), will help preventing the mooring stiffness problem. But generally the ZGA is not solving the essential problem, it is just a workaround. Within an area the proportional gains are set to zero and extra damping is added in order to reduce the chance on instable behavior. But instability is still possible due to oscillating from one to another side of the ZGA area. And with the ZGA mode activated there is still chance for no smooth stage transition from

moored to free floating stage.

With the problem properly analyzed, the goal for this thesis can be set up. The goal is defined as:

> ***Investigate and propose a conceptual solution to the mooring stiffness problem, which is instable behavior of the DP system during a heavy lift topside installation on a jacket and non-smooth behavior during the stage change from the moored DP operation stage to the free floating DP operation stage***

With the goal defined, a solution is to be found in the next chapter.

4

CANDIDATE SOLUTIONS

Chapter 3 concluded with the goal of this thesis. In this chapter conceptual candidate solutions are proposed, which can be basis for a final design. The requirements for the conceptual solution are set up in Section 4.1. As already mentioned in the introduction in Chapter 1 the choice for all the candidate solutions is to estimate the mooring stiffness forces and include them in the DP controller. In Section 4.2 the solution space of the problem is explored. Where after in Section 4.3 the solution space is narrowed and the main concept solution is chosen. Then in section 4.4 the final 4 different conceptual solution candidates are discussed plus another supplementary possibility.

4.1. REQUIREMENTS

In this section the requirements for a conceptual solution are discussed. The requirements will make the goal more concrete for the design of the solution. Also the requirements are the basis for measures for scoring the solution concepts later in this thesis. The measures for scoring the solution are given in Section 5.5. The requirements for more detailed design, which are out of the scope right now, are discussed during the recommendations in Section 7.2.

The goal is to propose a conceptual solution to the mooring stiffness problem. To recapitulate, the mooring stiffness problem is instable behavior of the DP system during moored stage and poor performance of the DP system during transition from moored and free floating stage.

As already mentioned during the topside heavy lift operation a narrow clearance between the vessel and heavy load should be maintained. A minimal physical clearance of 5[m] between heavy load and vessel is common in the industry, which leads in to a maximal DP setpoint offset of 3[m]. Exceeding the 3[m] offset is accounted as a serious incident. Hence the main requirement of the solution is to make the vessel not pass the clearance between vessel and load of 3[m]. It is important that the heavy lift vessel maintains stability in any situation or combination of parameters, because instability can lead to exceeding the maximal DP setpoint offset of 3[m].

Another requirement of the solution is reducing the mooring stiffness forces. First of all, mooring stiffness forces on the jacket via the crane induce extra load on equipment. Furthermore the horizontal mooring stiffness forces influence the position of the vessel. When using a state estimator (e.g. Kalman filter) the effect of these horizontal forces have to be estimated and estimations always have errors. Hence it is good to keep the horizontal forces as low as possible.

Closely related to the previous requirement is a requirement to keep the thrust as low as possible. During the moored stage the position is more or less kept due to the mooring stiffness forces, so the DP system should only give thrust for minor adjustments.

Furthermore by reducing thrust the fuel cost can probably be reduced.

Furthermore, the conceptual solution should maintain the current heavy lift vessel equipment and lay-out as much as possible. In this way the solution can be implemented in existing heavy lifting vessels without high investments.

As last requirement, the conceptual solution should be as generic as possible, such that this solution can be translated as easily as possible to other kind of vessels or operations.

4.2. SOLUTION SPACE

For tuning the DP controller certain dynamic behavior is assumed. Chapter 3 shows that due to the mooring stiffness the dynamic behavior of the vessel is changes significantly. The result is the mooring stiffness problem. Now to solve this problem there are 2 approaches possible.

1. Make the controller suitable to cope with the mooring stiffness forces.
2. Diminish the mooring stiffness forces such that the original dynamic system is retrieved where the DP controller is originally tuned for.

The solution can be found in the following solution space:

OPERATION AND OPERATIONAL CONDITIONS

Operating in good weather can reduce the mooring stiffness problem, because less disturbances from the environment leads to less motion of the vessel. In turn, this leads to less DP system activity and less mooring stiffness forces. In a perfectly calm sea the DP system can practically be switched off. Another option is to change the operation itself. For example the heavy load weight can be reduced to reduce the mooring stiffness. But obviously the industry doesn't want to let their position keeping be dependent on weather and operation specifications. So the operation and operational conditions are not part of the solution.

OPERATION OF BALLAST SYSTEM

Consider a heavy lift vessel during moored stage. The DP setpoint is placed in such a way that the crane tip is precisely above the heavy load. This DP setpoint can be considered as the perfect setpoint. If the vessel does not have an offset from the 'perfect' setpoint the mooring stiffness forces are zero. However, when the vessel rearranges its ballast tank levels, the vessel pitches and consequently the previous perfect DP setpoint is not the perfect anymore as the cranetip moved due to the pitching. This principle was shown before in Figure 3.5. Mooring stiffness forces will be induced due to a non perfect setpoint.

Ballasting the vessel in such a way the DP setpoint is the perfect DP setpoint can reduce the mooring stiffness forces. The ballasting installation, howevever, is not useful as an actuator to position the crane tip above the load, because the ballasting system is too slow. So ballasting the vessel is not part of the solution as diminishing the mooring stiffness forces by ballasting is impossible.

OPERATION OF DP SYSTEM

The DP system is obviously a major subject of interest. If the DP system of the heavy lift vessel in moored DP stage is turned off, the vessel can't get instable. In this sense the DP system is the source of the instable behavior.

OPERATION OF CRANE SYSTEM

A crane can theoretically react fast enough to be able to reduce the mooring stiffness forces. For example it should be possible to boom in and out in such a way that the tip of the crane is always precisely above the heavy load, so there is no horizontal force whatsoever. As a result the operation of the crane is also a subject of interest.

4.3. NARROW DOWN SOLUTION SPACE

Now there are still two options available in the solution space to reach the goal of solving the mooring stiffness problem. The numbering of the two available options stated next are in line with the numbering of the two different approaches discussed in the beginning of Section 4.2.

1. Change the operation of the DP system to let the controller cope with the mooring stiffness forces.
2. Change the operation of the crane in a way the mooring stiffness forces are diminished.

This study focuses on the first option due to the following reasons:

- As already discussed, a disabled DP system results in stable behavior. So the DP System can be considered the source of the problems. As the mooring stiffness forces will never be perfectly diminished by approach 2 (i.e. there will be always some forces left) the DP system should cope with this remaining forces regardless. This is why the first focus is on the DP controller, but if this does not satisfy the requirements the second option should be studied. Now the approaches 1 and 2 are discussed from a more practical point of view.

- In heavy lifting vessels the crane controls are situated in the control house of the crane in the crane, in contrary to the controls of the DP system which are situated in the general control room of the vessel. Therefore rearrangement of the cabling is necessary. Furthermore the winches which control the crane are not built to be used as frequent as in a dynamically controlled crane. Hence to implement this solution in existing vessels major adjustments have to be done in for example cabling and winches. This is does not match with the requirement of a low cost solution for current heavy lift vessels.

- Furthermore to dynamically control the tip of the crane very precisely a very good performing control system must be designed. This is not yet accomplished for this size of cranes on floating platforms. Designing this control system would be a major technical challenge.

Nonetheless both options are theoretically feasible. Therefore if after conducting this study no reasonable performance is achieved with option 1 alone the second option should be considered.

Now the controller should be modified to be able to cope with the mooring stiffness forces. On one hand a new control method can be implemented, such as fuzzy control, sliding mode control, model predictive control, robust control etc. On the other hand, it is also possible to maintain the basic PID based controller and add a solution particular for the mooring stiffness problem to this controller. The two latter options, respectively named *new control method solution* and *addition solution*, shall be explored.

In general the current PID based controllers are performing very well. Even without the solution proposed in this thesis, the marine contractors manage to do successful topside installations. The industry is using the PID based controller for years without many problems. Note that the offshore industry is conservative. When considering the *addition solution* the industry knows that the basis of the controller(i.e. PID based controller) have proven to work very well in practice, in contrary to the *new control method solution* which has yet to prove itself. Furthermore if the *addition solution* is chosen this will lead to faster implementation and faster results than if the *new control method solution* is chosen. The *addition solution* meets the requirement to maintain the current heavy lift vessel equipment as much as possible.

Finding a new control method which can better cope with the mooring stiffness problem is scientifically a very interesting option. Many studies can be done on new

control methods for Dynamic Positioning during heavy lift operations. It is therefore recommended to examine other control methods in the recommendations. But this study continues using the existing PID based DP controller and add a *feed forward solution*. In other words the *addition solution* is chosen and the addition is a feed forward solution.

FEED FORWARD OF MOORING STIFFNESS FORCES

With this feed forward solution the estimated horizontal mooring stiffness forces on the vessel are estimated and fed forward. In other words the estimated horizontal mooring stiffness forces are directly counteracted by the thrusters. This idea is discussed in the following section.

The linear equation of motion of the vessel in surge direction was discussed in Section 3.2. Now the mooring stiffness force F_X is added. The equation becomes:

$$M\ddot{x} + B\dot{x} = F_{environment} + F_X + F_{DP} \tag{4.1}$$

Now with the mooring stiffness force feed forward (F_{ff}) by the DP system, the thrust by the DP system becomes:

$$F_{DP} = F_{DP(original)} + F_{ff} \tag{4.2}$$

The mooring stiffness force feed forward counteracts the mooring stiffness forces ($F_{ff} = -F_X$), the equation becomes:

$$M\ddot{x} + B\dot{x} = F_{environment} + F_X + F_{DP(original)} + F_{ff} \tag{4.3}$$

$$M\ddot{x} + B\dot{x} = F_{environment} + F_{DP(original)} \tag{4.4}$$

As already mentioned, the current PID based controllers are performing very well in general. But the DP controller is tuned for a different dynamic system than during the moored stage due to the mooring stiffness forces. The equations 4.1 to 4.4 allow for the conclusion that with the mooring stiffness force feed forward the original system is retrieved for which the DP system is tuned for (i.e. the vessel without mooring stiffness forces). So in theory all problems discussed in Section 3.2 will be solved. The feed forward solution is chosen due to the following reasons:

- The variables and parameters of the dynamic system are well-known. These variables include for example crane length, crane height and elasticity of the cables. This allows a first principle model to be made to estimate the mooring stiffness forces precisely.
- Combining feedforward with feedback control can significantly improve performance over simple feedback control whenever there is a major disturbance that can be measured before it affects the process output. In the most ideal situation, feedforward control can entirely eliminate the effect of the measured disturbance on the process output. Even when there are modeling errors, feedforward control can often reduce the effect of the measured disturbance on the output better than that achievable by feedback control alone[Brosilow and Joseph, 2002].
- If the PID controller without mooring stiffness forces is theoretically stable the PID controller with feed forward is also theoretically stable.
- The paper "On the use of main hoist tension measurement for feed forward in DP systems during offshore installations" [Waals, 2010] also suggested to feed forward the horizontal mooring stiffness forces into the original PID based DP controller. In this paper the proposed method is studied by doing a series of model tests where after the results are presented. A conclusion is "The proposed hoist tension feed forward enhances the stability of the DP system during the installation

of a large load in a model test experiment." So the results of this paper regarding feed forward of the mooring stiffness forces are very positive.

Control accuracy can often be improved if the mathematical model is of sufficient quality and implementation of the feedforward control law is well thought out. But if the feed forward is measured or estimated with errors the feed forward can also frustrate the controller leading to possibly dangerous situations during the topside installation. Hence the feed forward has to be implemented safely. Furthermore, the drawback of the feed forward solution is that the solution is not a solution for all kind of heavy lift operations. This does not meet the last requirement in Section 4.1, the solution being a generic solution.

The feed forward addition is named *Feed Forward Solution*, in short the *FF Solution*, in the rest of this report. In Section 4.4 this concept and some other variants of the FF solution solution candidate are discussed.

RECAPITULATION

To conclude this section a quick recapitulation is given of this section. First of all, to find a solution this study focuses on letting the DP controller cope with the mooring stiffness forces instead of diminishing the mooring stiffness forces by the crane. This because the DP system is the source of the problem and a solution for the controller is more feasible to implement. Secondly the choice is to keep the existing control strategy instead of designing a total new controller. This is because the offshore industry is a conservative industry so when adding a solution for the mooring stiffness problem the industry already is convinced the PID based controller is performing well. Furthermore the solution is more feasible to be practically implemented. Thirdly, a feed forward solution concept is chosen because in general, a combined feedforward plus feedback can significantly improve performance. Furthermore the solution is theoretically stable if the DP system itself is stable tuned. Furthermore the paper [Waals, 2010] has promising conclusions about using feed forward of mooring stiffness forces with respect to stability during offshore crane installations.

For these reasons, the feed forward conceptual solution is the most feasible and therefore chosen as the main solution direction of this thesis. This does not discard the other solution directions. They are also worth looking into scientifically. Therefore it is recommended recommends also investigating the other solutions directions.

4.4. SOLUTION CANDIDATES

The idea of the FF Solution is to feed forward all the mooring stiffness forces by the thrusters. But as already mentioned, the implementation of the feedforward control law must be well thought out. This means that different concepts of using the mooring stiffness forces to enhance the controllers performance can be applied. In this section the four final candidate solutions, including the FF solution, are proposed in Section 4.4.2. Firstly, however, the forces which are to be fed forward have to be determined. The method of determining the mooring stiffness forces is discussed first in 4.4.1. In 4.4.3 a supplementary addition to the conceptual solution is discussed which is named *DP Setpoint adaption*.

4.4.1. ESTIMATION OF FORCES

As mentioned in the previous section, the mooring stiffness forces have to estimated correctly otherwise the feed forward law can frustrate the controller. In [Waals, 2010] is proposed to estimate the horizontal mooring stiffness forces by using the angle of the hoist cable and the tension in the hoist cable. In theory these values can be measured and used directly for force feed forward.

However, this is assumed to be "unsafe" because in this way a value obtained from sensors is directly fed forward into the controller. In the case the sensors are failing or

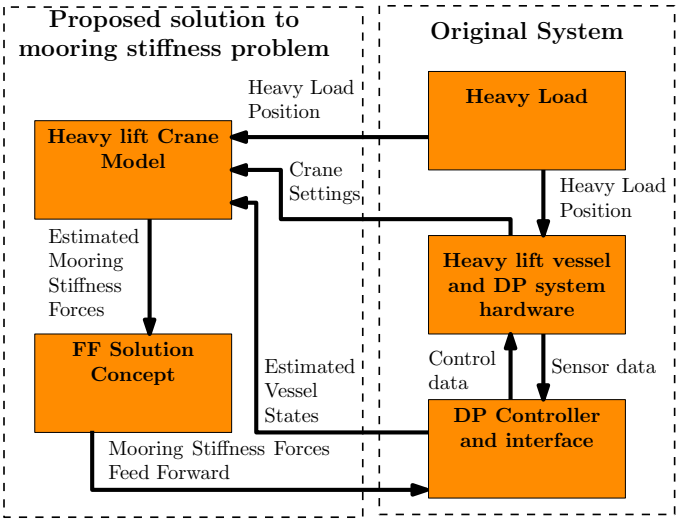

Figure 4.1: Schematic representation of proposed Feed Forward Solution (FF Solution)

are polluted with noise the force estimation also fails immediately. Furthermore current heavy lift vessels do measure the tension in the cable, but the obtained value is not very precise. Angle measurement is currently not done in practice consequently new equipment should be installed.

Consequently, now a different way of estimating the mooring stiffness forces is proposed. Many parameters and variables like dimensions of the vessel and settings of the crane are known quite precisely. Furthermore the dimensions and weight of the heavy load are known and the position and velocity of the heavy load are known when the load is in moored stage. It is proposed to use a first principle crane model to calculate the mooring stiffness forces on the vessel. It is proposed that the inputs of this first principle model are the estimated states by the Kalman filter of the DP controller. In this case a 'safe' estimation of the mooring stiffness forces is achieved due to the safe state estimation characteristics of the Kalman filter (see Section 2.3).

In Figure 4.1 a schematic representation of the feed forward solution (FF Solution) including the estimation of the mooring stiffness forces is shown.

4.4.2. FOUR CANDIDATE SOLUTIONS

The concept of the Feed Forward Solution (FF Solution) is already discussed in Section 4.3. As the mooring stiffness can be 10 times the DP stiffness, the magnitude of the forces by feed forward control law can be large and also fluctuating quickly. The concern is that the thrusters are not able to achieve the demand of thrust due to the new feed forwarding control law of *Feed Forward Solution*. This concern is basis for the candidate solutions 2, 3 and 4.

1. FEED FORWARD SOLUTION (FF SOLUTION)

This concept is already discussed in Section 4.3. The concept is to estimate the mooring stiffness forces feed forward the forces directly by the thrusters such that the original vessel for which the DP system is tuned for is retrieved. Apart from this, the estimated forces are also fed to the Kalman filter.

2. MOORING STIFFNESS FORCE FEED IN KALMAN FILTER SOLUTION (KALMAN SOLUTION)

As already mentioned, a major concern is that the thrusters are not able to achieve the demanded thrust by the controller due to the new feed forwarding control law of the *Feed Forward Solution*. In the paper [Waals, 2010] nothing of this subject is mentioned

so tests have to show the consequences of this to the performance. With this potential problem in mind, another variant of the Feed Forward candidate is suggested in this section. The concept of the *Kalman Solution* candidate is to feed the estimated forces only into the Kalman filter. In other words, in this solution concept no direct feed forward control law is implemented like in the *Feed Forward Solution* concept.

The idea is that this will mostly lead to better estimated states by the Kalman filter because the model used by the Kalman filter is now extended with the mooring stiffness forces. Consequently, the lag between the true states and estimated states by the Kalman filter is reduced. The *Kalman Solution* candidate is not theoretically stable but it should help to reduce or prevent the mooring stiffness problem. The idea is that this candidate solution improves the following with respect to the no solution case:

- Less difference in amplitude between the true and estimated states by the Kalman filter. This lead to:
  - A smaller deviation between required and actual delivered thrust amplitude where after the hydrodynamic damping due to operating thrusters may be larger.
  - Better chosen control actions by the controller
- Less lag of state estimation
- The current model buildup is performed better because the mooring stiffness forces are known. Hence no poor performance after stage transition of moored stage to free floating stage during the topside installation on a jacket operation.

The next two candidate solutions are combinations of the *FF Solution* and the *Kalman Solution* candidates.

3. THRUST CAPABILITY CORRECTED MOORING STIFFNESS FORCE FEED FORWARD SOLUTION (CORRECTED SOLUTION)

The idea of this solution candidate is that the thrusters only should be used for feed forwarding mooring stiffness forces if the feed forward control law doesn't dominate the thruster demand. When the mooring stiffness forces become larger than the thrust limits of the thrusters, the DP controller should stop with feedforwarding the mooring stiffness forces and only act according to the original controller laws.

In other words, if it is possible the mooring stiffness forces are fed forward by the thrusters, just like the FF Solution concept, such that the original dynamic system is obtained. If this can't be achieved by the thrusters the feed forward control law demand is reduced such that the original feedback control law is not dominated.

The estimated mooring stiffness forces are always 100% implemented in the Kalman filter. This means that the advantages of the *Kalman Solution* candidate also transfer over to the *Corrected Solution* candidate.

4. FILTERED MOORING STIFFNESS FORCE ESTIMATION FEED FORWARD SOLUTION (FILTERED SOLUTION)

There is still a concern that the thrusters are not able to achieve the thrust demand, but this solution candidate focuses on the fast fluctuating character of the mooring stiffness force. The idea is that the fast fluctuating behavior of the mooring stiffness force is due to rolling and pitching of the heavy lift vessel by waves. Roll and pitch will heavily affect the crane tip position and therefore also the mooring stiffness force. This means that the fast fluctuating behavior is periodic, which in turn means that is not needed to counteract the periodic force directly using the thrusters.

One could suggest to filter the mooring stiffness forces by for example a low pass filter. Unfortunately this has the disadvantage that the filtered estimated forces are obtained with a delay. To tackle this problem, the following filter approach is suggested:

- Filter the roll and pitch before using these states for determining the final force by the crane model. Consequently the periodic horizontal force is filtered.

- Use the unfiltered horizontal x and y position states of the vessel, because this will influence the steady part of the mooring stiffness forces which should be corrected by the DP system.

The idea is that this filter approach result in a more steady demand of thrust which is more likely to be achieved by the thrusters.

In Figure 4.2 all 4 solution candidates are depicted in one diagram. Each arrow with numbers represent an information flow only for the solution candidate with the corresponding number. For example the mooring stiffness forces estimated by the crane model are fed to the Kalman Filter in the DP Controller for all candidate solutions (1+2+3+4). But there is no direct feed forward to the thrusters in solution candidate 2(Kalman Solution) as can be seen by the absence of the number 2 below the Force Feedforward arrow(1+3+4). The Corrected solution candidate(3) is reducing the thruster feed forward control law demand by multiplying the mooring stiffness forces by the *Feed Forward Gain* (a number between 0 and 1).

Solution Candidates	
1	FF Solution
2	Kalman Solution
3	Corrected Solution
4	Filtered Solution

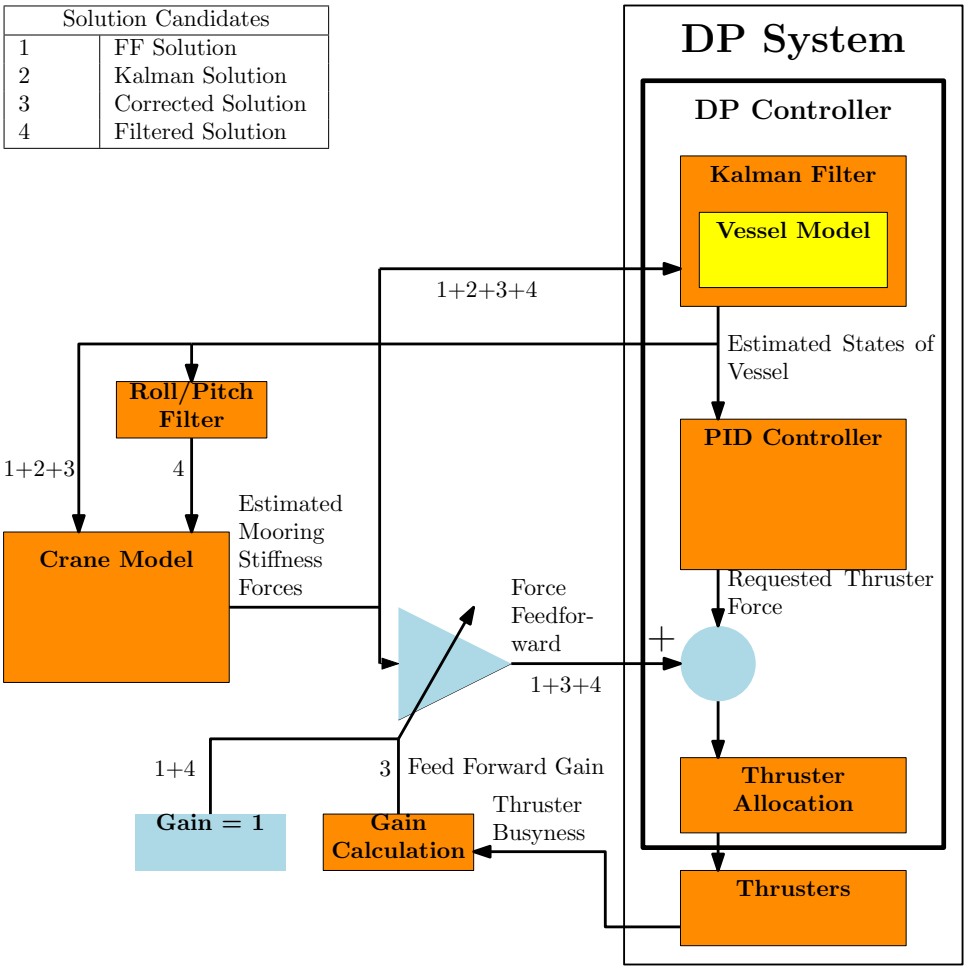

Figure 4.2: Schematic representation of all solution candidates.

4.4.3. ADDITION TO THE SOLUTION: DP SETPOINT ADAPTION

In this section an addition to the 4 solution candidates is suggested. The addition which can be part of the solution but is apart from the solution candidates is named *DP setpoint adaption*. Let's consider a vessel during a topside installation of which the DP setpoint is chosen with 5 meters offset from center position. Now no matter the solution, a certain thrust is asked from the thrusters to go to the DP setpoint position. But the mooring stiffness will pose a force on the vessel if the vessel is going towards the DP setpoint. The idea is that using thrust to compensate for a positional error which is caused by mooring stiffness forces is useless. If this is compensated by the thrusters it is useless utilization of the thruster capability. The offset of DP setpoint can be caused by a poorly chosen setpoint by the operator or by change in roll or pitch. The latter will change the vessels crane tip location while the DP reference point is not changed. The latter problem is mentioned before and depicted in Figure 3.5.

The suggested solution is to adapt the vessels DP setpoint automatically to a perfect setpoint where no mooring stiffness forces are induced. In other words the DP setpoint is chosen to the neutral position such that the heavy load is perfectly below the crane tip. The implementation is relatively simple as the estimation of the mooring stiffness force can be done using a geometric model of the crane and vessel, which already exists. The perfect DP setpoint as function of the roll and pitch can be calculated and fed to the DP system.

The advantages of the DP setpoint adaption are that there are the following:

- Less horizontal forces via the crane and less usage of the thrusters, which are both requirements according to Section 4.1.
- Less thruster usage result in less oscillation amplitude, the consequence will be a reduction in the delay between requested force by the controller and the thrust by the thrusters. This is because thrusters have an equal amount of time to build up a reduced amplitude.
- The mooring stiffness forces are never perfectly estimated. A reduction of the horizontal forces reduces the amount of erroneously estimated forces.

In the next chapter the proposed solution candidates are implemented and the testing of the solution candidates is described.

5

METHODS

In Chapter 4, the solution direction is chosen. The solution direction is to estimate the mooring stiffness forces and feed these forces into controller. For this solution direction, four different concepts of feeding the mooring stiffness forces are suggested, based on feed forwarding the mooring stiffness forces. Furthermore an addition to the solution candidates, the DP setpoint adaption, is also discussed.

Now the solution candidates have to be tested and the performance have to be scored. This is done by conducting the scoring strategy which is described in the following section (i.e. Section 5.1). All details of the conduction of this scoring strategy can be read in the rest of this chapter with the focus on reproducibility of this scoring strategy.

5.1. STRATEGY TO SCORE THE SOLUTION CANDIDATES

The basis of this scoring strategy is a computer simulation model of a heavy lifting vessel with heavy load and DP system. With the use of this simulation model it is relatively simple to run multiple simulations to test different kind of concepts. The simulation model is described in Section 5.2. After that the 4 solution candidates and the DP setpoint adaption addition are implemented in this simulation model which is described in Section 5.3. The scoring strategy consists of 3 phases of computer simulation tests which are described in this section and summarized in Table 5.1. Furthermore, the results of the scoring strategy are discussed in Chapter 6.

1. In phase 1 of the scoring strategy the mooring stiffness problem was reproduced in the simulation model. The conditions under which the simulation became instable without an implemented solution candidate is saved as the baseline conditions for further analysis.

2. In phase 2 the candidate solutions and the DP setpoint adaption were tested and scored. In phase 2, the true position and orientation states of the vessel were used for force estimation, instead of the orientation and position states estimated by the DP controller. In other words the true model states were used for estimation of the mooring stiffness forces. This is not realistic as the controller does not know the true model states in reality, but in this way the conceptual feasibility is proven without extra complications which estimating the states could possibly introduce. Each implemented solution candidate was tested by two simulation tests. The first simulation test, which is named *the baseline test*, is a simulation with the baseline conditions from phase 1. The baseline test is for showing whether the solution candidates stabilize the vessel or not. The second simulation, which is named *the Seastate test*, is a simulation with normal heavy lifting operation conditions. The

conditions are light weather conditions of Seastate 3, with some stochastic wind and wave forces. The test details of both simulation tests are further discussed in Section 5.4. The best performing solution candidate was chosen by scoring the 4 solution candidates with and without DP setpoint adaption. The candidates were scored using the measures which are described in Section 5.5.

3. In phase 3, the best performing solution from phase 2 was tested using the estimated position and orientation states of the vessel. In other words, the estimated position and orientation states by the DP controller were used for estimation of the mooring stiffness forces. Doing this the performance was tested in a more realistic setting as the controller does not know the true model states in reality. In phase 3 the same tests were done as in phase 2 but now for only the winning solution candidate of phase 2. These tests verified whether the winning solution candidate from phase 2 is still performing well using the estimated position and orientation states.

The results of the scoring strategy are discussed in Chapter 6.

Phase	Description	Scheme
1	**Without solution** Define baseline *Using model states*	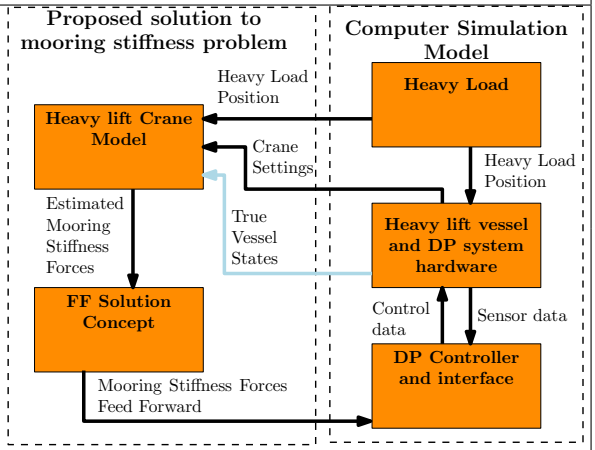
2	**With 4 candidates** Baseline test Seastate test *Using model states*	
3	**Best candidate solution With/Without DP-Setpoint Adaption** Baseline test Seastate test *Using estimated states*	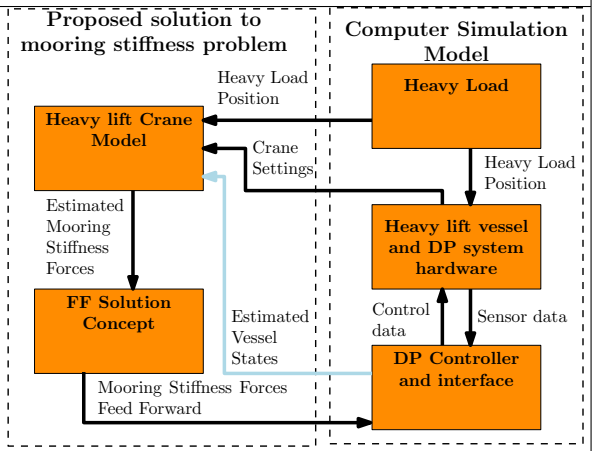

Table 5.1: Summarized schematic overview of scoring strategy.

As already mentioned, a computer simulation model is required for scoring the candidate solutions. This simulation model of a heavy lifting vessel is discussed in the next section.

5.2. SIMULATION MODEL OF HEAVY LIFTING VESSEL

This section will discuss the modeling of a heavy lifting vessel with a single heavy lifting crane which can lift a heavy load. The heavy lift vessel model is outfitted with a DP system. The purpose of making this simulation model is to use it for testing the candidate solutions to the mooring stiffness problem.

First an introduction to the model is given. After that the lay-out of how the model is implemented in Matlab Simulink is explained. Then, the further details of the model are discussed on the goal to be able to reproduce this model. Subsequently, the choice of the solver is discussed and then the visualization of the model is discussed. Finally, the verification and validation procedure is reported.

5.2.1. INTRODUCTION TO THE MODEL

The simulation model consists of a 5 dimensional vessel dynamics model block, a 6 dimensional heavy load dynamics model block and the crane mechanics model block. The vessel and crane are modeled as one rigid body together, just as the load is. Furthermore the hoist cable is modeled as a damped spring without mass.

The vessel with crane is experiencing a number of forces and moments. First of all the water surrounding the hull exerts buoyancy force upwards, and restoring moment on the hull such that the hull will stay upended. Furthermore of course both bodies experience gravity forces and the hull experiences hydrodynamic forces (e.g. potential damping, viscous damping). Wind and wave forces can also be experienced. Furthermore the load exerts a certain force on the vessel with crane via the hoist cable and crane, creating a force and a moment on the centre of gravity (COG) of the vessel. Besides this, the dynamic positioning system will order the thrusters to apply a force.

Extra explanation of any variable used in this section can be found in Table 5.2. A schematic drawing of the modeled system and their variables can be seen in Figure 5.3. The used geographic reference frame is the North-East-Down (NED). This is usually referred to as flat Earth navigation hence the curvature of the earth is not taken into account [Fossen, 2011, p. 17]. One indicates a variable in NED with {n}. Furthermore both the vessel with crane and the load have their own body-fixed reference frames as depicted in Figure C.1. One indicates a variable in body-fixed reference frame with {b}. Furthermore the notation of the forces, moments, velocities, positions and Euler angles are as described in Table C.1. The used notations and reference frames are all according to the *Handbook of Marine Craft Hydrodynamics and Motion Control* by Thor I. Fossen [Fossen, 2011, p. 17].

Even so modeling of physical systems can be done in various programming languages and environments, this model is developed in Matlab Simulink. Matlab Simulink is chosen because it is developed for modeling, accepted and well-known in the scientific world and it has a wide range of libraries and add-ons. For example in this model the MSS maritime toolbox [Fossen and Perez, 2014] which is developed by Thor I. Fossen and this toolbox is used many times.

For the sake of completeness, in this section(5.2) a model of the vessel is mathematically discussed in Section 5.2.5. Subsequently, is discussed that the Imtech vessel model is implemented instead of the mathematical model. This choice is motivated in Section 5.2.6. The Imtech vessel model and DP software is developed in C++ which have to run outside Matlab Simulink environment. It is accessed from Matlab Simulink by an Application Programming Interface (API) as is shown in Figure 5.1.

Table 5.2: Table of variables with short description

Variable	Unity and description
a_{load}, a_{crane}	[m] Distance between COG and attachment point of hoist cable in y-direction (angle w.r.t. {b})
b_{load}, b_{crane}	[m] Distance between COG and attachment point of hoist cable in x-direction (angle w.r.t. {b})
c_{load}, c_{crane}	[m] Distance between COG and attachment point of hoist cable in z-direction (angle w.r.t. {b})
A_{cable}	[m^2] Cross-sectional surface of hoist cable
COG	Centre of gravity
CO	Centre of origin
$\mathbf{C}_{RB}$	Rigid-body Coriolis and centripetal matrix.
$\mathbf{D}_{vessel}$	Linear Damping matrix
E_{cable}	[N/m^2] Linear elasticity modulus of hoist cable
F_{hoist}	[N] Force in hoist cable
$\vec{f}_g$	[N] Gravitational force vector
g	[m/s^2] Gravitational acceleration
$\mathbf{G}$	Restoring force/spring matrix of vessel
$\overline{GM}_T$	[m] Transverse metacentric height
$\overline{GM}_L$	[m] Longitudinal metacentric height
l_{hoist}	[m] Non-loaded hoist cable length
$\mathbf{M}\_RB_{vessel}$, $\mathbf{M}\_RB_{load}$	Rigid Body (inertial) mass matrix,
$\mathbf{M}\_A_{vessel}$, $\mathbf{M}\_A_{load}$	Added mass matrix
$\vec{p}_{hoist\ cable}$	Vector which represents the hoist cable length and orientation
$\vec{pos}_{crane}\{b\}$	Vector which represents the position of the crane tip with respect to the center of origin(CO) of the vessel.
$\vec{pos}_{crane\ tip}\{n\}$	Vector which represents the position of the crane tip in the NED reference frame.
$\vec{pos}_{hoist\ hook}\{b\}$	Vector which represents the position of the attachment point of the hoist cable with respect to the center of origin(CO) of the heavy load.
x_{crane}	[m] Distance between COG and base of crane in x-direction (angle w.r.t. {b})
y_{crane}	[m] Distance between COG and base of crane in y-direction (angle w.r.t. {b})
z_{crane}	[m] Distance between COG and base of crane in z-direction (angle w.r.t. {b})
α_{hoist}	[°] Crane angle w.r.t. the vertical (xz-)plane of the vessel (angle w.r.t. {b})
β_{hoist}	[°] Boom angle w.r.t. the horizontal (xy-)plane of the vessel (angle w.r.t. {b})
$\vec{\eta}_{vessel}$, $\vec{\eta}_{load}$	Position vector, see Table C.1
δ_{vessel}, δ_{load}	[°] Angle between the horizontal (xy-)direction of the hoist wire and the hoist cable (angle w.r.t. {b})
γ_{vessel}, γ_{load}	[°] Angle between the hoist wire and the z-axis (angle w.r.t. {b})
$\vec{v}_{vessel}$, $\vec{v}_{load}$	[m/s] Velocity vector, see Table C.1
ρ	Density of seawater
$\vec{\tau}_{vessel}$, $\vec{\tau}_{load}$	Force vector, see table for details of this vector
Υ_{cable}	[] Specific loss in the cable, which is the energy dissipation per cycle divided by strain energy of oscillation
∇	[m^3] Nominal displaced water volume

5.2.2. ASSUMPTIONS

In this section all assumptions which were necessary to make the model are stated and defended. A model is always made in context with a goal. The purpose of this model is to show whether the solution for the mooring stiffness problem is performing good or not. So the model is build towards the operating conditions of a vessel during heavy lift operations. To sum up the general operating profile conditions:

- Light weather conditions, maximal seastate 4.
- Stationkeeping is done on low vessel velocity, so the maximum vessel velocity is taken as 2 [m/s] vessel velocity, deviation around 0 [m/s].
- The heavy lift vessel is never rolling or pitching larger than 15 degrees, as this never done during real life operations.

The Imtech vessel model have been a gray box for the author of this thesis, as he has been aware of the general working of the model but not the exact details. The author is told that the assumptions which are made for the Imtech vessel model are the same as any standard model of this kind used for simulation. But because the model is a gray box the assumptions which are made while the implementation of the Imtech Vessel model are not described in this thesis.

1. Vessel-crane combination and load is rigid
   Compared to the relative motions of vessel-crane and load the internal motions are considered small enough to be neglected.

2. Viscous damping is assumed in the hoist cable, not in other mechanical components
   A helical wire rope strand hoist cable is known to have relatively large internal material friction, because of the cable exists of separate cable cores [Raoof and Davies, 2006]. Furthermore the mechanical components are much more stiff than the cables itself, this justifies the vessel-crane combination modeling as a rigid body and the hoist cable not.

3. Load is not affected by wind
   No damping of motions of load because of air friction, because the motions are slow and the mass is very high, this effect is considered to of a minimal interest. Furthermore the used seastates in the simulations are low.

4. Linear material stiffness is assumed in hoist cable
   The hoist cable is assumed to operate in the elastic regime.

5. Hoist cable has no inertia
   Compared to the mass of the vessel and the load the inertia of the hoist cable is neglected.

6. The NED frame {n} is inertial.
   This eliminates forces due to the Earth's motion relative to a star-fixed inertial reference system. This is a good assumption since the forces on marine craft due to the Earth's rotation are quite small compared to the hydrodynamic forces.[Fossen, 2011, p. 46-47]

7. For the hydrostatic calculations the vessel is assumed to be a box shaped structure. Hence the waterplane area is constant as function of z.
   This enables to linearize the restoring force matrix. This is a valid assumption because the vessel does not pitch or roll more than 15 degrees in the simulations.

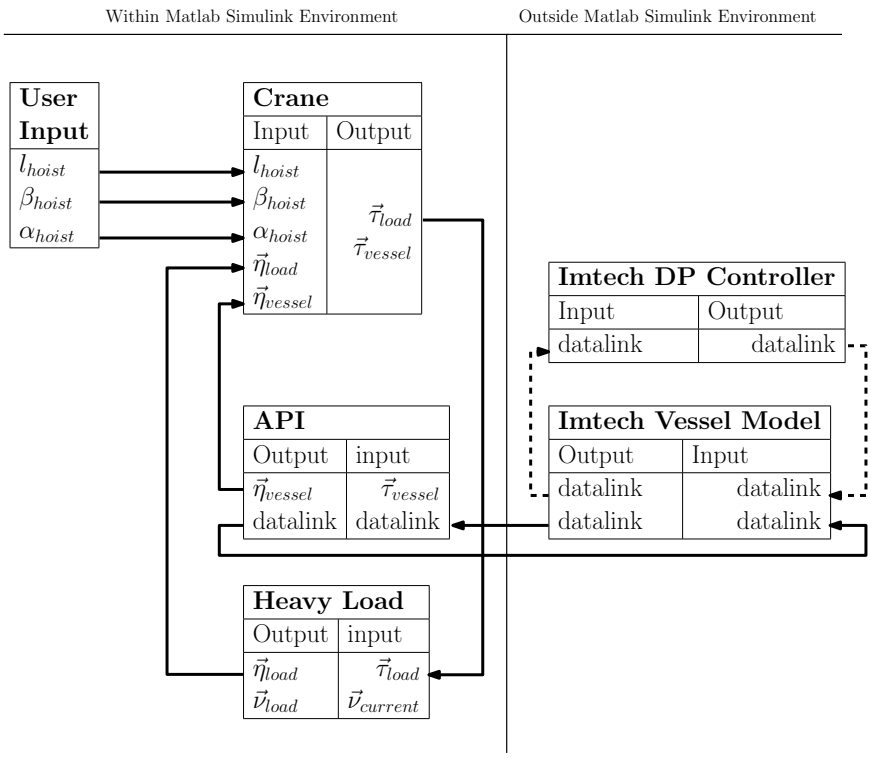

Figure 5.1: Model Layout with datastream between main model blocks. The Imtech vessel model is accessed from Matlab Simulink by the Application Programming Interface (API)

5.2.3. MODEL LAY-OUT

This simulation model consists of 3 model blocks which communicate with each other within Matlab Simulink. The API model block in Simulink is a data pass through block which sends and receives data from the Imtech vessel model which is running outside Matlab. Furthermore the Imtech DP controller and Imtech vessel model are communicating outside Simulink. In Figure 5.1 the model layout with datastream between the model blocks is depicted. The following model blocks are implemented in Simulink:

1. **Vessel:** API to the 5 DOF vessel model with vessel inertia, gravity and interaction with water, waves and wind.
2. **Load:** 6 DOF load with load inertia and gravity
3. **Crane:** Crane mechanics and kinematics
   This module will take care of the interaction between the vessel and load module which exist via the crane.

The vessel body and the load body have their own position vectors, η_{vessel} and η_{load} respectively. These vectors contain 5 and 6 states respectively, see Table C.1 for further information about this vectors. With the use of this position information of the vessel body and the load body as input, the crane model block calculates the interaction between these inertial bodies. The interaction is by means of forces and torques applying via the hoist wire on the vessel en load bodies. These forces and moments are the input to the vessel and load blocks and the new position (η) and velocity (ν) is calculated by the inertial blocks.

The crane model block acquires three states which are chosen by the crane operator in the real world (user input). These values are the non-loaded hoist wire length l_{hoist}, boom angle w.r.t. the horizontal plane β_{hoist} and crane angle w.r.t. the forward position

of the vessel α_{hoist}. The user input values are not bounded by any limits, consequently the user input have to be changed carefully to keep a realistic behavior. See Figure 5.3 for a schematic drawing of the modeled system with the used symbols indicated in the drawing.

5.2.4. HEAVY LOAD MODEL

In this section the modeling of the heavy load is discussed. The heavy load is based on a 6 degree of freedom inertial model hence this model is discussed firstly. Table 5.3 gives detailed information about inputs, constants, states and outputs of the heavy load model.

6 DOF EQUATIONS OF MOTION

The heavy load model is based on the nonlinear 6 DOF Rigid Body Equations of motion model block from the MSS toolbox [Fossen and Perez, 2014]. This model block is the implementation of the Rigid-body equations, a quick overview is depicted in this section but for full derivation [Fossen, 2011, *Chapter 3*] must be studied.
The rigid-body kinetics will be derived to the following vectorial setting:

$$\mathbf{M}_{RB}\dot{\vec{\nu}} + \mathbf{C}_{RB}(\vec{\nu})\vec{\nu} = \vec{\tau} \tag{5.1}$$

Where $\mathbf{M}_{RB}$ is the rigid-body mass matrix, $\mathbf{C}_{RB}(\vec{\nu})$ is the rigid-body coriolis and centripetal matrix due to rotation of {b} about the inertial frame {n} (remember due to assumption 6 the NED frame {n} is purely inertial). For $\vec{\nu}$ and $\vec{\tau}$ the reader is refered to Table C.1. The rigid-body equations of motion are derived using the *Newton-Euler formulation* and *vectorial mechanics*.
Time differentiation of a vector $\vec{a}$ in a moving reference frame {b} satisfies:

$$\frac{^n d}{dt}\vec{a} = \frac{^b d}{dt}\vec{a} + \vec{\omega}_{b/n} \times \vec{a} \tag{5.2}$$

where n and b above the time differentiation denotes differentiation in NED reference frame and body reference frame respectively. $\vec{\omega}_{b/n}$ is the angular velocity of {b} with respect to {n}. Now r_g is defined as the distance vector from the origin of {b} $[x_g,\ y_g,\ z_g]^T$ to the COG, hence now the origin of the body centered reference frame is different from the COG.

$$\vec{r}_{g/n} = \vec{r}_{b/n} + \vec{r}_g \tag{5.3}$$

Now after differentiation with respect to time of $\vec{r}_{g/n}$ the following equation is obtained:

$$\vec{v}_{g/n} = \vec{v}_{b/n} + \vec{\omega}_{b/n} \times \vec{r}_g \tag{5.4}$$

Now a coordinate change is done to obtain the equations of motion for an arbitrary origin CO to take advantage of the craft's geometric properties. The end result are the following equations of motion respectively for translational motion and rotational motion:

$$[X,\ Y,\ Z]^T = m[\dot{\vec{v}}_{b/n} + \dot{\vec{\omega}}_{b/n} \times \vec{r}_g + \vec{\omega}_{b/n} \times \vec{v}_{b/n} + \vec{\omega}_{b/n} \times (\vec{\omega}_{b/n} \times \vec{r}_g)] \tag{5.5}$$

$$[K, M, N]^T = I_b\dot{\vec{\omega}}_{b/n} + \vec{\omega}_{b/n} \times I_b\vec{\omega}_{b/n} + m\vec{r}_g \times (\dot{\vec{v}}_{b/n} + \vec{\omega}_{b/n} \times \vec{v}_{b/n}) \tag{5.6}$$

Table 5.3: Details of load model block

Load			
Input	Constants	States	Output
$\vec{\tau}_{load}$	$\mathbf{M}\_RB_{load}$	$\vec{\eta}_{load}$ $\vec{\nu}_{load}$	$\vec{\eta}_{load}$ $\vec{\nu}_{load}$

Equations 5.5 and 5.6 can be rewritten in the vectorial representation of equation 5.1. The rigid-body system inertia matrix M_{RB} is unique and is given by:

$$\mathbf{M}_{RB} = \begin{bmatrix} m & 0 & 0 & 0 & mz_g & -my_g \\ 0 & m & 0 & -mz_g & 0 & mx_g \\ 0 & 0 & m & my_g & -my_g & 0 \\ 0 & -mz_g & my_g & I_x & -I_xy & -I_xz \\ mz_g & 0 & -mx_g & -I_xyx & I_y & -I_yz \\ -my_g & my_g & 0 & -I_zx & -I_zy & I_z \end{bmatrix} \tag{5.7}$$

The matrix $\mathbf{C}_{RB}$ represent the Coriolis vector term $\vec{\omega}_{b/n} \times \vec{v}_{b/n}$ and the centripetal vector term $\vec{\omega}_{b/n} \times (\vec{\omega}_{b/n} \times \vec{r}_g)$. Contrary to the representation of $\mathbf{M}_{RB}$, it is possible to find a large number of representations for the matrix $\mathbf{C}_{RB}$. One of the possible representation for C_{RB} is given in equation 5.8.

$$\mathbf{C}_{RB}(\vec{v}) = \begin{bmatrix} 0 & 0 & 0 \\ 0 & 0 & 0 \\ 0 & 0 & 0 \\ -m(y_gq + z_gr) & m(y_gp + w) & m(z_gp - v) \\ m(x_gq - w) & -m(z_gr + x_gp) & m(z_gq + u) \\ m(x_gr + v) & m(y_gr - u) & -m(x_gp + y_gq) \end{bmatrix}$$
$$\begin{bmatrix} m(y_gq + z_gr) & -m(x_gq - w) & -m(x_gr + v) \\ -m(y_gp + w) & m(z_gr + x_gp) & -m(y_gr - u) \\ -m(z_gp - v) & -m(z_gq + u) & m(x_gp + y_gq) \\ 0 & -I_{yz}q - I_{xz}p + I_zr & I_{yz}r + I_xyp - I_yq \\ I_{yz}q + I_xzp - I_zr & 0 & -I_{xz}r - I_{xy}q + I_xp \\ -I_{yz}r - I_{xy}p + I_yq & I_{xz}r + I_{xy}q - I_xp & 0 \end{bmatrix} \tag{5.8}$$

LOAD MODEL

The implementation of the load model is almost the same as implementing the 6DOF inertial model, the only addition is the gravitational force. This gravitational force $f_g\{n\}$ is implemented as follows:

$$\vec{f}_g\{n\} = [0, 0, mg, 0, 0, 0]^T \tag{5.9}$$

$$\mathbf{M}_{RB}\vec{\dot{v}} + \mathbf{C}_{RB}(\vec{v})\vec{v} + R(\vec{\omega}_n)^{-1}\vec{f}_g\{n\} = \vec{\tau} \tag{5.10}$$

Where g is the gravitational acceleration, $R(\vec{\omega}_n)$ is the rotation matrix as function of $\vec{\omega}_n$ [Fossen, 2011, p. 22].

5.2.5. VESSEL MODEL

As starting point for the implementation of the vessel model, the load model equations of motion are used as is denoted by the rigid-body kinetics Equation 5.10. Now hydrostatic and hydrodynamic effects are added to this equation to retrieve the equations of motion for a vessel.

Table 5.4: Details of vessel model block

Vessel			
Input	Constants	States	Output
$\vec{\tau}_{vessel}$ $\vec{v}_{current}$	M_RB_{vessel} M_A_{vessel} C_RB_{vessel} C_A_{vessel} G_{vessel} D_{vessel}	$\vec{\eta}_{vessel}$ $\vec{v}_{vessel}$	$\vec{\eta}_{vessel}$ $\vec{v}_{vessel}$

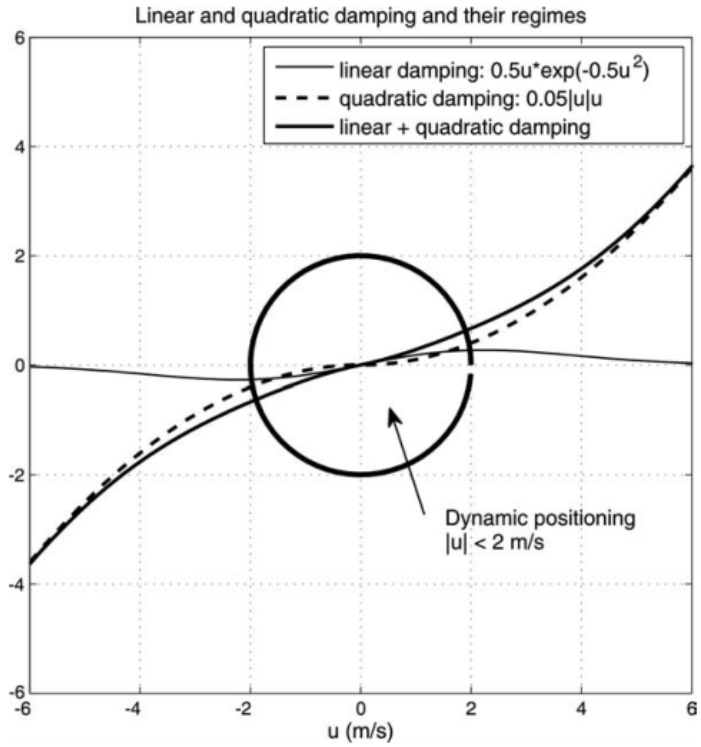

Figure 5.2: Linear and quadratic damping and their speeds regimes. Fossen, 2011, Figure 7.2, p. 138

BODY REFERENCED EQUATIONS OF MOTION

Equation 5.11 is obtained by adding the following effects to the load model:

- Hydrostatic forces
- Hydrodynamic added mass
- Hydrodynamic damping
- Irrotational ocean current, such that the relative velocity vector is $\vec{v}_r = \vec{v} - \vec{v}_c$

$$\mathbf{M}\vec{\dot{v}}_r + \mathbf{C}(\vec{v}_r)\vec{v}_r + \mathbf{D}\vec{v}_r + \mathbf{G}\vec{\eta} + R(\vec{\omega}_n)^{-1} f_g\{n\} = \vec{\tau} \tag{5.11}$$

Where $\mathbf{M} = \mathbf{M}_{RB} + \mathbf{M}_A$ - system inertia matrix (including added mass)
$\mathbf{C}(\vec{v}_r) = \mathbf{C}_{RB}(\vec{v}_r) + \mathbf{C}_A(\vec{v}_r)$ - Coriolis centripetal matrix (including added mass)
$\mathbf{D} = \mathbf{D}_p + \mathbf{D}_v$ - (linear) potential and viscous damping matrix
$\mathbf{G}$ - (linear) Restoring force matrix
$R(\vec{\omega}_n)^{-1} f_g\{n\}$ - Gravitational force in {b}

Next some simplifications are done:

- Because of the low speed station keeping operating profile it makes sense to use only linear damping [Fossen, 2011, P. 175]. See Figure 5.2 for an impression of the contributing damping in different speed regimes.
- Because the low maximum roll and pitch operating profile the static forces are implemented linearly.
- The model is reduced with one dimension, being a 5D model with surge, sway, yaw, roll and pitch. See Equation 5.12.

$$\vec{\eta} = \begin{Bmatrix} x \\ y \\ \phi \\ \theta \\ \psi \end{Bmatrix} \tag{5.12}$$

HYDROSTATIC FORCES

First the hydrostatic effects are mentioned, this is implemented according to [Fossen, 2011, section 4.2]. The concept of metacentric height is assumed to be known tot he reader. Because of the operating conditions with low angles of pitch and roll deviation a linearized hydrostatic forces calculation is justified.

A linear approximation is valid for pitch and roll angles which is a good approximation because of the operating profile. The following defines the linear restoring force:

$$g(\vec{\eta}) \approx G\vec{\eta} \tag{5.13}$$

$$G = diag \begin{Bmatrix} 0 \\ 0 \\ \rho g \nabla \overline{GM_T} \phi \\ \rho g \nabla \overline{GM_L} \theta \\ 0 \end{Bmatrix} \tag{5.14}$$

Where ∇ is the nominal displaced water volume and $\overline{GM_T}$ and $\overline{GM_L}$ are the transverse and longitudinal metacentric height ,respectively.

ADDED MASS AND LINEAR DAMPING

Secondly the hydrodynamic added mass and linear damping is discussed, this is implemented following [Fossen, 2011, section 6.2 and 6.3]. Hydrodynamic potential theory programs can be used to compute the added mass and damping matrices by integrating the pressure of the fluid over the wetted surface of the hull. These programs assume that viscous effects can be neglected. Consequently, it is necessary to add viscous forces manually. The programs are also based on the assumptions that first- and second-order wave forces can be linearly superimposed. The potential coefficients are usually represented as wave frequency-dependent matrices. Now if the natural frequencies of the decoupled motions in heavy, roll and pitch are known, the matrices $\mathbf{M}_A$, $\mathbf{D}_P$ *and* $\mathbf{D}_V$ can be approximated. This after assuming that there are no couplings between the surge, heave-roll-pitch and the sway-yaw subsystem because the natural frequencies are used as input for approximating the frequency dependent added mass, potential and viscous matrices. For station keeping models, where the velocity trough the water is low, the total damping which can be of higher order can be simplified by linear damping.

NON-LINEAR CORIOLIS FORCES DUE TO ADDED MASS

The nonlinear Coriolis and centripetal matrix $\mathbf{C}_A(\vec{v})$ due to a rotation of {b} about the inertial frame {n} can be derived using an energy formulation based on the constant matrix $\mathbf{M}_A$. This can be implemented following [Fossen, 2011, section 6.3.3]

5.2.6. IMPLEMENTATION OF IMTECH VESSEL MODEL

As already explained the in-house developed Imtech vessel model is implemented via a Simulink API instead of implementing a model directly in Simulink.

For this method is chosen because the Imtech vessel model is extensively used for testing the Imtech DP controller. When the model was developed it is validated with model scale tests, consequently this saves verification time. Also using the Imtech vessel model, the Imtech DP controller becomes available which has proven itself in many

real-world projects. Consequently, the DP controller of Imtech has more real-world features than a DP controller which is available for study purposes for example in the MSS Toolbox [Fossen and Perez, 2014]. Furthermore, excellent vessel model data is available because Imtech has model test data from existing vessels of customers of Imtech.

The use of the Imtech vessel model and DP controller is not only feasible, it is also very functional for the purpose of proving the conceptual functioning of the solution by means of simulation experiments. Now, the DP controller perfectly matches the to be controlled vessel. In this case, with these perfect conditions it should be relatively simple to prove the conceptual functioning of a solution. If the conceptual functioning is proven the solution can be designed to a more practical environment with problems like a model which is mismatching reality.

Now a short discussion of the features of the Imtech Vessel model and DP controller is discussed. Besides hydrostatics and hydrodynamics also models of thrusters and propellers are included. A various number of sensor types are also modeled. Furthermore it is possible to model environmental conditions by setting a certain seastate. Now the environmental conditions corresponding to the chosen seastate are applied to the vessel model. The wind impact is calculated by using wind impact model test data. The wave impact is calculated using basic vessel parameters.

5.2.7. CRANE MODEL

As already mentioned, the crane model block calculates the interaction between the inertial bodies. So with the use of the vessel and load position vectors ($\vec{\eta}_{vessel}$ and $\vec{\eta}_{load}$) the force and moment vectors on the inertial bodies caused by the crane ($\vec{\tau}_{vessel}$ and $\vec{\tau}_{load}$) are calculated. Firstly, an overview of the implemented calculation procedure to calculate the forces and moments on the inertial bodies is described. After that the calculation procedure is explained in a reproducible level of detail. Extra explanation of any variable used in this chapter can be found in Table 5.2. A schematic drawing of the modeled system and their variables can be seen in Figure 5.3.

OVERVIEW OF THE IMPLEMENTED CALCULATION PROCEDURE

The values for a_{crane}, b_{crane}, c_{crane} are calculated with the use of geometric constants of the vessel and the user input for the crane. After that the hoist cable length and orientation in space ($\vec{p}_{hoist\ cable}$) is calculated. This is compared with the non-loaded hoist cable length (l_{hoist}) and the force in the hoist cable (F_{hoist}) is calculated. Then the angles γ and δ for both bodies are calculated and with these angles and F_{hoist} the body referenced forces(X,Y,Z) are calculated by trigonometric relations. Having calculated the forces it is possible to calculate the body referenced moments(K,M,N) which are acting on the COG of the vessel using a_{crane}, b_{crane} and c_{crane} again. Now the calculation procedure is explained more into detail.

Table 5.5: Details of crane model block

Crane			
Input	Constants	States	Output
l_{hoist}	a_{load}	δ_{vessel}	$\vec{\tau}_{load}$
β_{hoist}	b_{load}	γ_{vessel}	$\vec{\tau}_{vessel}$
α_{hoist}	c_{load}	δ_{load}	
$\vec{\eta}_{load}$	A_{cable}	γ_{load}	
$\vec{\eta}_{vessel}$	x_{crane}	a_{crane}	
	y_{crane}	b_{crane}	
	z_{crane}	c_{crane}	
	E_{cable}	$\vec{P}_{hoist\ cable}$	
	Ψ_{cable}	F_{hoist}	

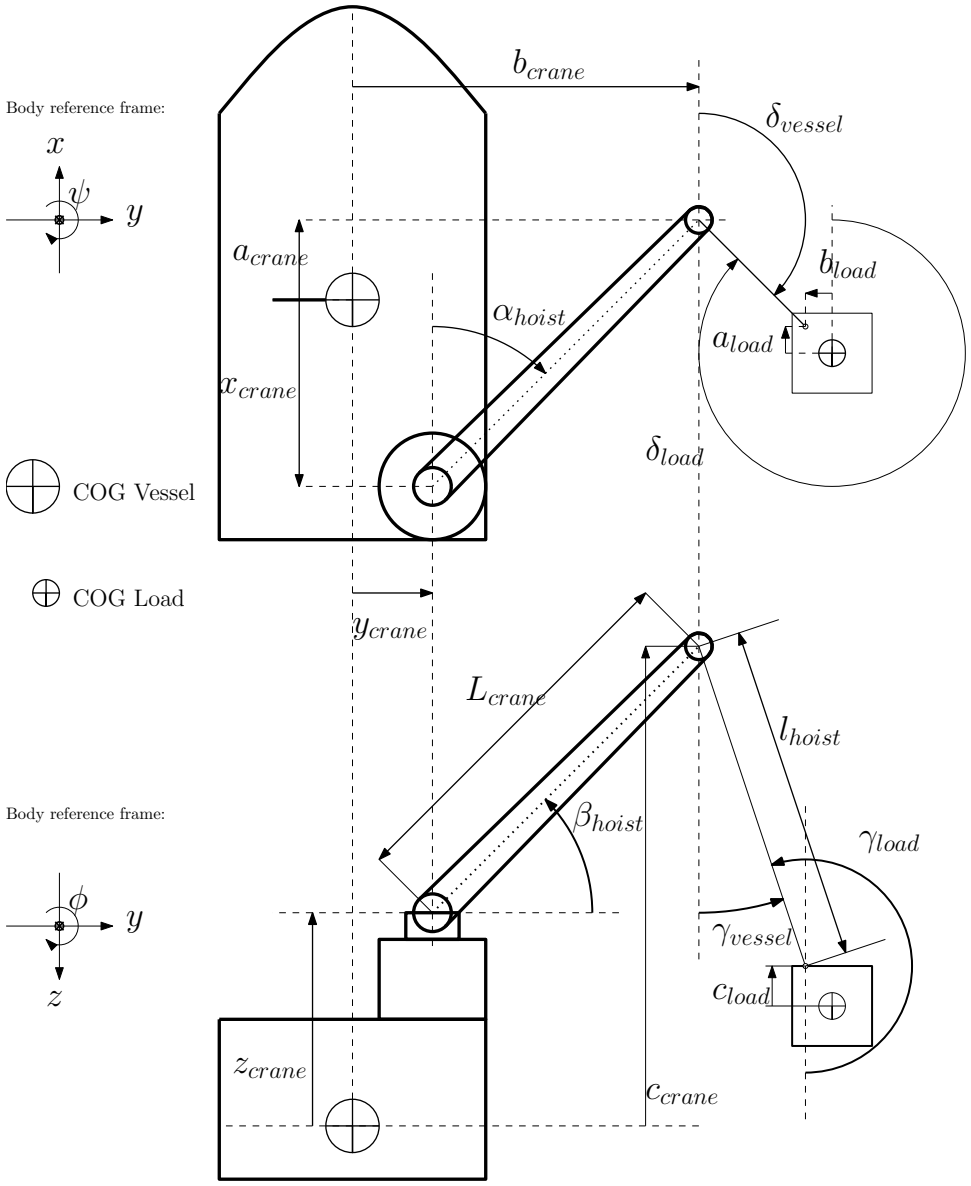

Figure 5.3: Schematic drawing of the modeled system with the used symbols indicated in the drawing

CALCULATION OF a_{crane}, b_{crane} AND c_{crane}

$$a_{crane} = x_{crane} + \cos(\alpha_{hoist}) \cdot \cos(\beta_{hoist}) \cdot L_{crane} \tag{5.15}$$

$$b_{crane} = y_{crane} + \sin(\alpha_{hoist}) \cdot \cos(\beta_{hoist}) \cdot L_{crane} \tag{5.16}$$

$$c_{crane} = z_{crane} - \sin(\beta_{hoist}) \cdot L_{crane} \tag{5.17}$$

CALCULATION OF $\vec{p}_{hoist\ cable}$

Now the length and orientation in space of the hoist cable is determined. If the cable is taut this vector ($\vec{p}_{hoist\ cable}$) represents the hoist cable in space. First the crane tip position in NED reference frame {n} ($\vec{pos}_{cranetip}\{n\}$) is derived from the $\vec{pos}_{crane}\{b\}$ which is the position of the crane tip seen from the center of origin(CO):

$$\vec{pos}_{crane}\{b\} = \begin{Bmatrix} a_{crane} \\ b_{crane} \\ c_{crane} \end{Bmatrix} \tag{5.18}$$

$$\vec{pos}_{crane}\{n\} = R(\vec{\omega}_n)\vec{pos}_{crane}\{b\} \tag{5.19}$$

$$\vec{pos}_{cranetip}\{n\} = \vec{pos}_{crane}\{n\} + \vec{p}_{vessel}\{n\} \tag{5.20}$$

Where $R(\vec{\omega}_n)$ the rotation matrix is as function of $\vec{\omega}_n$ [Fossen, 2011, p. 22], and $\vec{p}_{vessel}\{n\}$ is the position of the COG of the vessel. Exactly the same formulas can are used to calculate $\vec{p}_{load}\{n\}$.

$$\vec{p}_{hoist\ cable}\{n\} = \vec{pos}_{cranetip}\{n\} - \vec{pos}_{hoisthook}\{n\} \tag{5.21}$$

Where $\vec{pos}_{hoist\ hook}$ is the attachment point of the hoist cable on the load. Subsequently, the hoist cable from load to crane is $\vec{p}_{hoist\ cable}\{n\}$. Now the vector $\vec{p}_{hoist\ cable}\{n\}$ is to be transformed to $\{b\}$ reference frame of the vessel and load.

$$Vessel: \ \vec{p}_{hoist\ cable}\{b\} = R(\vec{\omega}_n)\vec{p}_{hoist\ cable}\{n\} \tag{5.22}$$

$$Load: \ \vec{p}_{hoist\ cable}\{b\} = -R(\vec{\omega}_n)\vec{p}_{hoist\ cable}\{n\} \tag{5.23}$$

Where $R(\vec{\omega}_n)^{-1}$ the inverse rotation matrix is as function of $\vec{\omega_n}$ [Fossen, 2011, p. 22].

CALCULATION OF γ AND δ

In this section the angles between the hoist wire and the z-axis{b} γ and the angle between the horizontal (xy-)plane{b} and the hoist wire δ is calculated.

$$\vec{p}_{hoist\ cable}\{b\} = \begin{Bmatrix} p_{hoist\ cable\ x} \\ p_{hoist\ cable\ y} \\ p_{hoist\ cable\ z} \end{Bmatrix} \tag{5.24}$$

$$\gamma = asin\left(\frac{\left\| \begin{Bmatrix} p_{hoist\ cable\ x} \\ p_{hoist\ cable\ y} \end{Bmatrix} \right\|}{\left\| \vec{p}_{hoist\ cable}\{b\} \right\|}\right) \ for\ p_{hoist\ cable\ z} \geq 0 \tag{5.25}$$

$$\gamma = \pi + asin\left(\frac{\left\| \begin{Bmatrix} p_{hoist\ cable\ x} \\ p_{hoist\ cable\ y} \end{Bmatrix} \right\|}{\left\| \vec{p}_{hoist\ cable}\{b\} \right\|}\right) \ for\ p_{hoist\ cable\ z} < 0 \tag{5.26}$$

For calculation of δ the Matlab function `atan2(y,x)` is used. `atan2(y,x)` is the four-quadrant (results are in the closed interval $[-\pi, \pi]$) inverse tangent and is able to determine the specific quadrant, in contrast with `atan(y/x)` whose results are limited to the interval $[-\pi/2, \pi/2]$. Hence:

$$\delta = atan2(p_{hoist\ cable\ y}, p_{hoist\ cable\ x}) \tag{5.27}$$

Calculations of γ and δ for the vessel and for the load are identical.

CALCULATION OF F_{hoist}

In this section F_{hoist} is calculated by calculating the difference between the length of $\vec{p}_{hoist\ cable}\{n\}$, which represent the real cable length, and the non loaded hoist length l_{hoist} which is defined by the user. Now the strain of the hoist cable Δl_{hoist} is calculated. As stated in the assumptions the hoist cable has no inertia, has linear stiffness and has constant viscous damping. Two issues are described in this subsection, which are the implementation of the cable mechanics and finding a good order of magnitude of linear viscous damping factor c. First the implementation of the cable mechanics is described.

IMPLEMENTATION OF THE CABLE MECHANICS

$$\Delta l_{hoist} = \left\| \vec{p}_{hoist\ cable} \right\| - l_{hoist} \tag{5.28}$$

$$k = \frac{E_{cable} \cdot A_{cable}}{l_{hoist}} \tag{5.29}$$

$$F_{hoist} = k \cdot \Delta l_{hoist} + c \cdot \frac{d\Delta l_{hoist}}{dt} \qquad For\ F_{hoist} \geq 0 \tag{5.30}$$

Because cables can only exert pulling force, $F_{hoist} \geq 0$ and this is implemented in the model.

ESTIMATION OF THE ORDER OF LINEAR DAMPING

Resisting forces of a complicated nature in the hoist cable is modeled in this simulation model as linear viscous damping. For the sake of a realistic vessel behavior an estimation of the right order of magnitude of the linear damping factor c must be obtained. The resisting forces are depending on the way the hoist cable is loaded. In this analysis the specific loss in the cable Υ_{cable} per load cycle plays an important roll. Υ_{cable} is defined as follows:

$$\Upsilon_{cable} = \frac{\Delta U}{U} \tag{5.31}$$

With ΔU being the frictional energy dissipation per load cycle and U being the maximum stored elastic energy. In this analysis, an value for Υ_{cable} is obtained from literature. After that the obtained Υ_{cable} is related to a linear damping factor c by calculating the energy for 1 load cycle.

$$\Upsilon_{cable} = \Upsilon_{cable\ max} \cdot \zeta \tag{5.32}$$

Now the values for $\Upsilon_{cable\ max}$ and ζ are obtained from literature:

With parameter values which are representative for values in the offshore industry (127[mm] outside diameter, 12 degree of lay angle) a maximum specific loss $\Upsilon_{cable\ max}$ of 0.32 and 0.36 is estimated [Raoof and Davies, 2006, table. 10].

ζ is a function of the value of axial load divided by mean axial load. This relation is estimated in [Raoof and Davies, 2006, Figure. 2]. The example of Figure 1.2 is used to determine a realistic factor ζ. During 23:20h and 23.35 the value of axial load divided by mean axial load is approximated between 0.05 to 0.5. Hence following [Raoof and Davies, 2006, Figure. 2] the value of ζ is between 0.25 and 1. A value of 0.5 is taken as value for ζ in further calculations as it is the right order of magnitude. To conclude this estimation the following specific loss is assumed to be in the right order of magnitude:

$$\Upsilon_{cable} = 0.5 \cdot \frac{0.32 + 0.36}{2} = 0.17[\,] \tag{5.33}$$

Now the energy dissipation during 1 load cycle is calculated. Suppose that the excitation is like a harmonic oscillating mass spring system defined by the following function:

$$t_0 = 0 \; and \; t_1 = T \tag{5.34}$$

$$\Delta l_{hoist}(t) = (\frac{v_{t0}}{\omega_0}) \cdot sin(\omega_0 \cdot t) \tag{5.35}$$

$$\frac{d\,\Delta l_{hoist}(t)}{dt} = v_{t0} \cdot cos(\omega_0 \cdot t) \tag{5.36}$$

$$\omega_0 = \frac{2\pi}{T} \tag{5.37}$$

$$T = 2\pi\sqrt{\frac{m}{k}} \tag{5.38}$$

$$F_c = c \cdot \frac{d\,\Delta l_{hoist}(t)}{dt} \tag{5.39}$$

Where v_{t0} is the velocity at t_0, ω_0 is the frequency of the excitation, t is the time, T is the period of one oscillation, k is the spring stiffness of the cable, m is the mass of the load, c is the viscous damping coefficient and F_c is the viscous resistance.

Now the velocity change due to the viscous force during an excitation of one period T will be analyzed.

$$v_{t_1} = v_{t_0} - \int_{t_0}^{t_1} \frac{F_c(t)}{m} dt \tag{5.40}$$

$$v_{t_1} = v_{t_0} - 4 \cdot \int_0^{1/4T} cos(\omega_0 t) dt \cdot \frac{v_{t_0} \cdot c}{m} \tag{5.41}$$

$$v_{t_1} = v_{t_0} - \frac{4 \cdot v_{t_0} \cdot c}{m} \cdot \left[\frac{sin(\omega_0 t)}{\omega_0}\right]_0^{1/4T} \tag{5.42}$$

$$v_{t_1} = v_{t_0} - \frac{4 \cdot v_{t_0} \cdot c}{m \cdot \omega_0} \tag{5.43}$$

Now take equation 5.38, substitute in equation 5.37:

$$\omega_0 = \sqrt{\frac{k}{m}} \tag{5.44}$$

Substitute ω_0 in equation 5.43.

$$v_{t_1} = v_{t_0} - \frac{4 \cdot v_{t_0} \cdot c}{\sqrt{m \cdot k}} \tag{5.45}$$

$$\frac{v_{t_1}}{v_{t_0}} = 1 - \frac{4 \cdot c}{\sqrt{m \cdot k}} \tag{5.46}$$

Now rewrite Ψ.

$$\Upsilon = \frac{\Delta U}{U} \tag{5.47}$$

$$\Upsilon = \frac{E_{t0} - E_{t1}}{E_{t0}} \tag{5.48}$$

$$\Upsilon = \frac{0.5m(v_0^2 - v_1^2)}{0.5mv_0^2} \tag{5.49}$$

$$\Upsilon = \frac{(v_0^2 - v_1^2)}{v_0^2} \tag{5.50}$$

$$\Upsilon = 1 - (\frac{v_1}{v_0})^2 \tag{5.51}$$

Where E_{t0} is the energy of the system at t=0. Now substitute equation 5.46 in equation 5.51.

$$\Upsilon = 1 - \left(1 - \frac{4 \cdot c}{\sqrt{m \cdot k}}\right)^2 \tag{5.52}$$

Hence a relation between Ψ and c is obtained. Now the relation is rewritten to obtain an expression for c.

$$\pm\sqrt{1-\Upsilon} = 1 - \frac{4 \cdot c}{\sqrt{m \cdot k}} \tag{5.53}$$

$$c = \frac{\sqrt{m \cdot k}}{4}(1 \pm \sqrt{1-\Upsilon}) \tag{5.54}$$

$\Upsilon = 0$ means that there is no energy discipation. So if $\Upsilon = 0$, c must also be 0. Hence the expression for c is:

$$c = \frac{\sqrt{m \cdot k}}{4}(1 - \sqrt{1-\Upsilon}) \tag{5.55}$$

Υ, m and k are all known hence the viscous damping c with a good order of magnitude can be implemented.

Concluding this section, F_{hoist} is implemented like equation 5.30, with the right order of magnitude of viscous damping coefficient.

CALCULATION OF τ

In Equations 5.24 to 5.27 the orientation of the hoist cable with respect to the body reference frames is calculated (γ and δ). Furthermore the force F_{hoist} which is acting on the tip of the crane is calculated in Equation 5.30. In this subsection the forces and moments are calculated which act on the center of gravity of the vessel and the load ($\vec{\tau}_{load}$ and $\vec{\tau}_{vessel}$).

First the forces X, Y, and Z are calculated doing simple geometric calculations.

$$X = F_{hoist} \cdot sin(\gamma) \cdot cos(\delta) \tag{5.56}$$

$$Y = F_{hoist} \cdot sin(\gamma) \cdot sin(\delta) \tag{5.57}$$

$$Z = F_{hoist} \cdot cos(\gamma) \tag{5.58}$$

Now the moments K, M, and L are calculated which act on the centers of mass.

$$K = b \cdot Z - c \cdot Y \tag{5.59}$$

$$M = a \cdot Z - c \cdot X \tag{5.60}$$

$$L = -b \cdot X + a \cdot Y \tag{5.61}$$

Using these equations vectors $\vec{\tau}_{load}$ and $\vec{\tau}_{vessel}$ are calculated. Hence the interaction between the load and the vessel due to the crane is determined.

5.2.8. NUMERICAL SOLVER

In this section the settings for the numerical solver which is used by Simulink to solve the differential equations are short described and motivated. Simulink is provided with a number of numerical solvers which have their advantages and disadvantages. The task is to choose the best solver for this model. This section is based on the Simulink manual[Mathworks, 2014].

The Imtech Vessel model and DP controller have their own fixed step cycle time. This Imtech model is a real-time computer system hence a fixed step solver is chosen because it is more difficult to map a variable step size to a real-time clock. A drawback

of this choice is that a variable step solver could have shorten the simulation time of the model significantly. A variable-step solver allows this savings because, for a given level of accuracy, the solver can dynamically adjust the step size as necessary and thus reduce the number of steps. Whereas the fixed-step solver must use a single step size throughout the simulation based upon the accuracy requirements. On the one hand, to satisfy these requirements throughout the simulation, the fixed-step solver might require a small step and consequently a computational expensive simulation model is obtained. On the other hand, the Imtech vessel model and DP system is only working in real time simulation speed hence the simulations take a long time anyway.

Furthermore the model is considered to be non-stiff. There is not a standard rule of thumb for what is a stiff and non-stiff system, but generally stiffness can be described as having time constants in a model that vary by several orders of magnitude. As we have 2 inertial bodies with relatively large inertia and they are not differing several order of magnitude, the model is considered to be non-stiff. Explicit solvers are designed for nonstiff problems, hence an explicit solver is chosen. The ode4(Fourth-order-Runge-Kutta) explicit solver is chosen.

In [Mathworks, 2014] a method of choosing the order of accuracy of the fixed step solver is suggested, which is taking the lowest order of accuracy and comparing the results with a variable step solver. If they are the results are equal this is the right order of accuracy, if not a higher order has to be selected. Unfortunately this is not a possibility, as there is being worked with a real time system. So to be sure a small time step of 0.005[s] is set in Matlab Simulink and the Imtech model, which is 20 times smaller than the normal timestep used for the Imtech vessel model. For the Imtech DP Controller the timestep is taken to be 0.025[s] which is 8 times as small as the normal used step size. Experimenting with 10 times larger time step and ode3 leaded to no difference between simulation results, consequently in any case the chosen values are conservative.

5.2.9. VISUALIZATION

Because visualization is a very effective tool for verifying models a 3D visualization is made. Now one can see straight away whether the model is acting as expected or not. Furthermore a good visualization is also useful for qualitative verification tests. For example if there is a force applied, will the vessel accelerate to the right direction, will the vessel find an equilibrium velocity, etc.

The animation of the model is made with the Simulink 3D animation plugin where virtual worlds can be set up in Virtual Reality Modeling Language(VRML). In this virtual world, objects can be placed and with the use of inputs from the Simulink model to the virtual world objects can be translated and rotated. Now the vessel, crane base, crane tip and load are placed in the virtual world and set to behave as in the model. Furthermore also a waterplane is added to the model and some different camera positions are set. In Figures 5.4a, 5.4b and 5.4c the 3D visualization is showed. In the figures the red cone is the bow of the vessel, the gray box the body of the vessel, the green box the crane base, the large yellow ball is the crane tip and the small yellow ball is the COG of the heavy load.

Furthermore an online vessel control panel is implemented. With this control panel the model can be controlled online during a simulation. With this control panel there can be added a force forward and backward, and a yaw moment clockwise and counter clockwise. Furthermore the crane settings can be changed as turning the crane with respect to the crane base, the hoist cable length can be changed and the boom angle can be changed. Figure 5.4d shows the online vessel control panel.

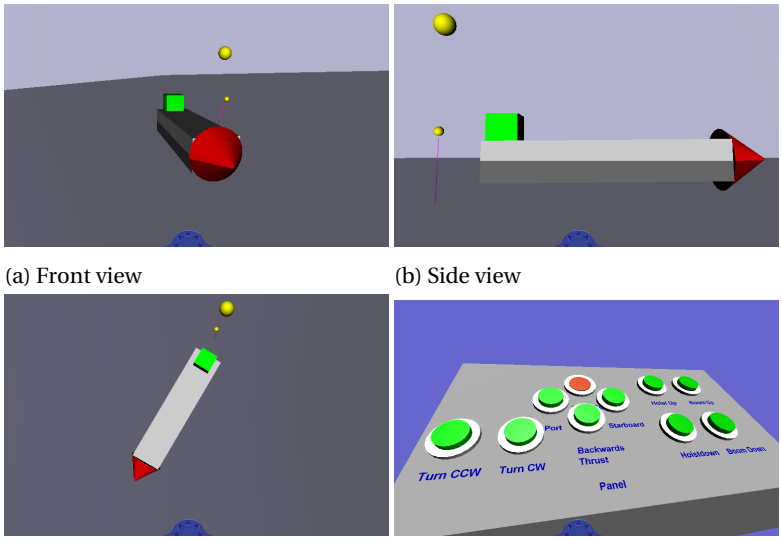

(a) Front view (b) Side view

(c) View from above (d) Online vessel control panel

Figure 5.4: Overview of 3D visualization of simulation model.

5.2.10. VERIFICATION AND VALIDATION

Verification is the process of confirming it is correctly implemented with respect to the conceptual model which is done until now. Furthermore, validation is the process of checking the accuracy of the model's representation of the real system. In this section verification and validation steps are undertaken at the same time.

As already mentioned one of the purposes of making a 3D visualization of the model was to build a tool for verification. Looking at the physical model while running the model is very powerful as strange behavior is recognized immediately. The simulations are done with all kind of different situations simulated. For example without heavy load, with heavy load, free floating in the crane and with a heavy load in fixed position. By observing the behavior of the 3D model is judged that the system has a good face validity.

After that the following simulation tests are done to verify the simulation model even more:

1. **Swinging of heavy load in crane of heavy lift vessel.**
   A simulation of a heavy load of 532[t] in the crane with an initial position outside an equilibrium. Now the heavy load should sway in the crane of the vessel. Also the motion of the heavy load should interact with the motion of the vessel and dampen out in a reasonable time.

2. **Drop of heavy load from small height and emerge to an equilibrium due to damping**
   A simulation of a heavy load of 532[t] will drop from 2[m] height. This is not in line with a real world operation as nobody will intend to drop a weight of 532[t] from 2 meters attached to a crane. However, the simulation is valuable to test the implementation of the internal damping in the cable and snatching of the cable. Furthermore the quantitative values of the roll and pitch of the equilibrium states of the vessel can be compared to hand calculation results.

3. **Full thrust while the cable is attached to a fixed point.**
   In this simulation the vessel's crane is pointed towards starboard. The hoist cable is attached to a fixed point in air such that the hoist cable is pulled taut straight downwards but without initial tension. Now the vessel is ordered to apply full

thrust ahead. The vessel should sail in a circles about the fixing point of the hoist cable. Also this simulation is not in line with a real operation. However natural behavior of the vessel can be inspected in the complete range of over -180 to +180 degrees of heading. This is important, among other reasons, because the transition area between 360 and 0 degrees is sensitive for implementation errors.

4. **Increasing tension in hoist cable while the cable is attached to a fixed point.** In this simulation the crane is pointed towards stern. The fixed attachment point of the cable is pulled downward such that the tension in the cable will grow. Now the pitch of the vessel also increases, the tip of the crane moves to a new equilibrium point which is exactly above the attachment point. This means the vessel center of gravity will be pushed away from the load as one can see in 3.5. Checking this ensures that the crane forces are correctly calculated during pitch angles and translated to the right motion.

The 4 tests are reported and discussed in details in Appendix A. Concluding this section, the model is reacting as expected and the model passes the 4 verification and validation tests.

5.3. DETAILED IMPLEMENTATION OF THE CANDIDATE SOLUTIONS

In Figure 4.1 the schematic representation of the proposed conceptual solution architecture is depicted. Of this solution architecture, the computer simulation implementation of the *Original System* part is discussed in Section 5.2.

The implementation of the *Proposed solution to the mooring stiffness problem* part in the simulation model is depicted in red in Figure 4.1. The way the *Controller API* incorporates the estimated force ($\vec{\eta}_{vessel}$) depends on the chosen solution candidate. The implementation of each solution candidate is described next.

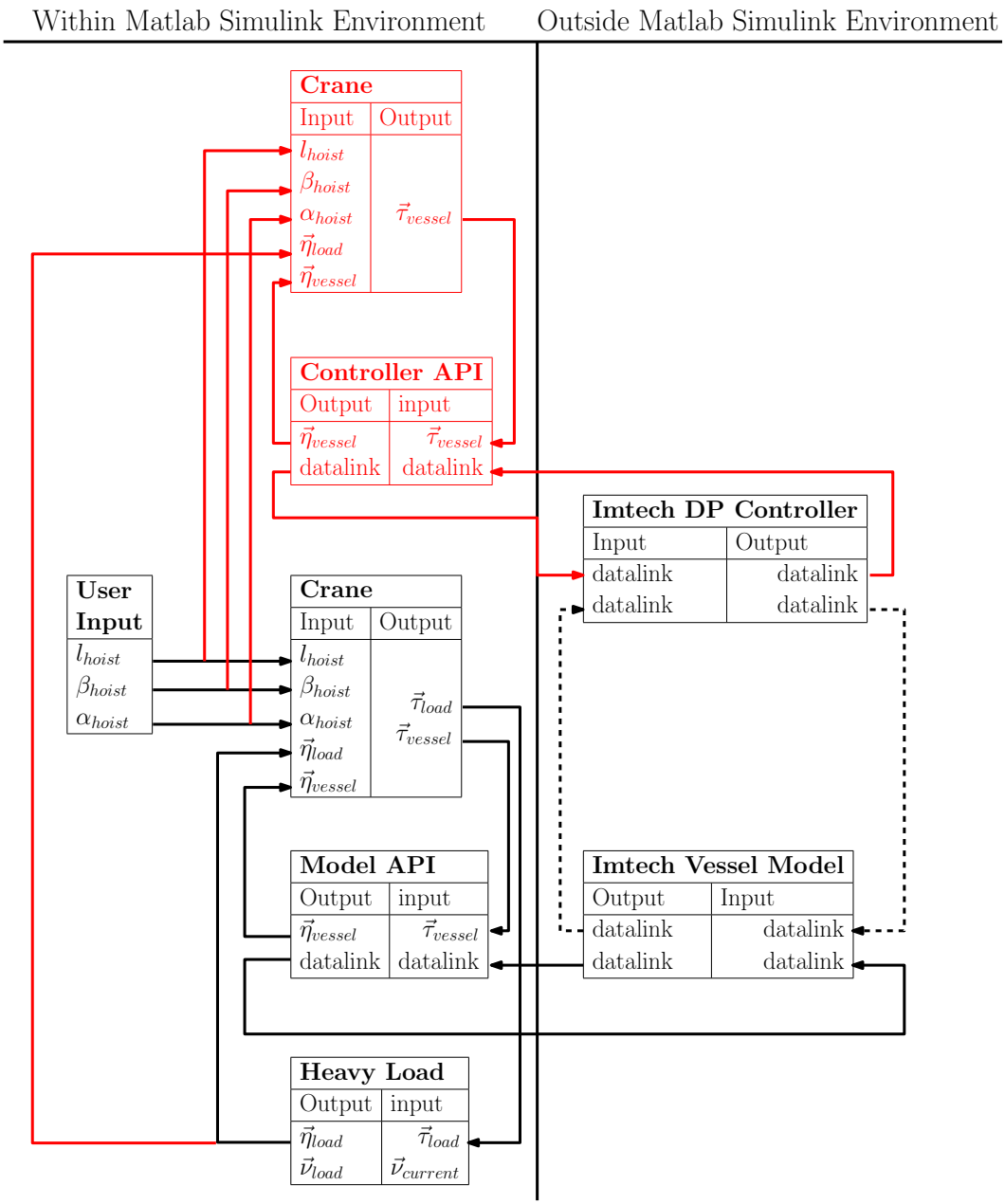

Figure 5.5: Model Layout with the datastream between main model blocks. The Imtech vessel model and DP controller are accessed from Matlab Simulink by Application Programming Interfaces (API)

5.3.1. IMPLEMENTATION OF THE 4 CANDIDATE SOLUTIONS

In Figure 4.2 a high level overview was depicted of the implementation of the solution candidates. Now the implementation of each solution candidate is described.

SOLUTION CANDIDATE 1. FF SOLUTION

The *Feed Forward Solution* candidate, or *FF Solution* candidate in short, is easily implemented. As the Imtech DP Controller has the possibility to feed forward the forces in surge and sway direction and the moment in yaw direction. So the mooring stiffness force is multiplied by the *Feed Forward Gain* and implemented in the DP Controller as Feed Forward. Also the forces and moments in surge, sway, yaw, roll and pitch direction are fed into the Kalman filter.

SOLUTION CANDIDATE 2. KALMAN SOLUTION

The *Mooring Stiffness Force Feed in Kalman Filter Solution* candidate, or *Kalman Solution* candidate in short, is relatively easy implemented. As the Imtech DP controller also has the possibility to feed forces and moments into the Kalman filter. This is implemented in surge, sway, yaw, roll and pitch direction.

SOLUTION CANDIDATE 3. CORRECTED SOLUTION

The *Thrust Capability Corrected Mooring Stiffness Force Feed Forward Solution* candidate, or *Corrected Solution* candidate in short, determines a gain for which part of the mooring stiffness force is fed forward. If the gain is 1 the mooring stiffness force is fed forward completely. And if the gain is 0 the mooring stiffness force is not fed forward. This Feed Forward Gain is also depicted in Figure 4.2. In total 3 gains are calculated, for surge, sway and for yaw.

The gains will be calculated by mapping the 'busyness' of the thrusters to a certain feed forward gain. As described in Appendix B the thruster configuration for the simulated vessel is two main thrusters with rudder, 3 bow and 2 stern thrusters. For surge motion is expected that the main thrusters will limit the feed forward thrust and for sway and yaw mainly the bow and stern thrusters will limit the feed forward thrust. Hence the implementation is simplified by calculating 1 gain for yaw and sway. Also is expected that all bowthrusters obtain approximately the same thruster setpoints from the allocation algorithm. Consequently the bow thrusters can be seen as 1 group of thrusters with the same thruster setpoint(RPM). This is also expected for the stern thrusters. Visual inspection of the behavior of the thrusters during DP enforces this expectation. The following variables are used in this analysis:

Variables	Unity and description
$A_{RPMdelivered}$	Thruster amplitude which is delivered by thrusters [rpm]
A_{RPMmax}	Thruster amplitude which can be maximally delivered by thrusters [rpm]
$G_{FFsurge}$	Feed Forward Gain in Surge direction []
$G_{FFswayyaw}$	Feed Forward Gain in sway and yaw direction []
ψ	A measure for free capability of one thruster []
Ψ	A measure for free capability of a thruster group, (e.g All main thrusters) []
$\overline{\Psi}$	Ψ filtered []
$\psi_{PropellerSB}$	ψ for the starboard side main thruster []
$\psi_{PropellerP}$	ψ for the port side main thruster []
$\psi_{ThrustersBow}$	ψ for the bow thrusters []
$\psi_{ThrustersStern}$	ψ for the stern thrusters []
τ_{Surge}	Time constant of the first order filter of Ψ_{Surge} [s]
$\tau_{SwayYaw}$	Time constant of the first order filter of $\Psi_{SwayYaw}$ [s]

The feed forward gains $G_{FFsurge}$ and $G_{FFswayyaw}$ is calculated as follow.

$$\psi = 1 - \frac{A_{RPMdelivered}}{A_{RPMmax}} \tag{5.62}$$

$$\Psi_{Surge} = min(\psi_{PropellerSB}, \psi_{PropellerP}) \tag{5.63}$$

$$\Psi_{SwayYaw} = min(\psi_{PropellerBow}, \psi_{PropellerStern}) \tag{5.64}$$

It is undesirable if the values for Ψ are oscillating much faster than the thrusters can respond. Consequently the values for Ψ are filtered by a first order lowpass filter. The lowpass filter is defined as:

$$\frac{\overline{\Psi}(s)}{\Psi(s)} = \frac{1}{1+\tau s} \qquad Laplace\ Domain \tag{5.65}$$

$$\tau \frac{d\overline{\Psi}(t)}{dt} + \overline{\Psi}(t) = \Psi(t) \qquad Time\ Domain \tag{5.66}$$

The time constants of the lowpass filter are chosen on $\tau_{Surge} = \tau_{SwayYaw} = 5s$ after some trail and error experimenting with the time constants. Now a steady filtered value for the free capability of a thruster group is obtained. Next a lookup table is used to couple the desired $G_{FFsurge}$ and $G_{FFSwayYaw}$ to $\overline{\Psi}$. The lookup table is defined the same for surge and sway.

$$G_{FFSurge} = G_{FFSwayYaw} = Lookup(\overline{\Psi}) \tag{5.67}$$

$$Lookup(\overline{\Psi}) = 0 \qquad for\ 0 < \overline{\Psi} < 0.25 \tag{5.68}$$

$$Lookup(\overline{\Psi}) = 4\overline{\Psi} - 1 \qquad for\ 0.25 < \overline{\Psi} < 0.5 \tag{5.69}$$

$$Lookup(\overline{\Psi}) = 1 \qquad for\ 0.5 < \overline{\Psi} < 1 \tag{5.70}$$

This lookup table settings will ensure that if the thrust $A_{RPMdelivered}$ is approaching A_{RPMmax}, the thrust feedforward is scaled towards zero. And consequently, the capability of the thrusters is only used for feed forwarding the mooring stiffness forces if it is not endangering the position keeping.

SOLUTION CANDIDATE 4. FILTERED SOLUTION

The idea of the *Filtered Mooring Stiffness force Estimation Feed Forward Solution* candidate, or *Filtered Solution* candidate in short, was to filter the roll and pitch before these states are fed to the crane model. The idea is to filter the roll and pitch by a first order low pass filters like 5.65 and 5.66. An example of the true roll and pitch and the filtered roll and pitch during simulation with normal operational conditions[1] is depicted in Figure 5.6.

The values for τ of the first order filters for roll: 15[s] and pitch: 10[s]. The figure shows for these values of τ that the fast fluctuating part of the roll and pitch motion is filtered but the slower transient part of the roll and pitch motion is maintained.

[1] The normal operational conditions are considered to be during seastate test between stage III and IV referring to Table 5.6 and Figure 5.8.

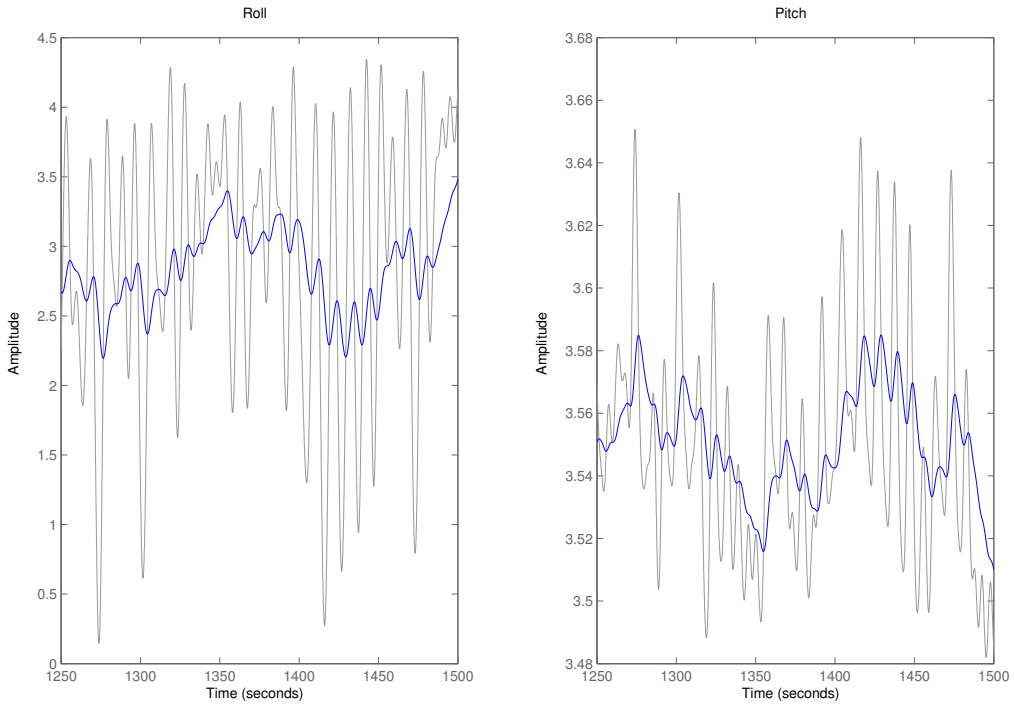

Figure 5.6: Result of the chosen filter values, the blue line is the filtered value of the gray line.

5.3.2. IMPLEMENTATION DP SETPOINT ADAPTION

In Section 4.4.3 the implementation of DP setpoint adaption concept is motivated. The idea is to automatically adapt the DP setpoint, such that when the offset is zero the crane tip is perfectly above the load and no horizontal mooring stiffness forces are present. In this section the implementation of the DP setpoint adaption is discussed.

The idea of this implementation of the DP setpoint adaption is that the setpoint is a function of merely:

- Heading setpoint from DP controller
- The crane user input settings
- The position and orientation of the heavy load ($\vec{\eta}_{load}$)

Hence it is not dependent to any state of the vessel itself. This is a very important aspect of the implementation, as in the hypothetical case the DP setpoint would be function of a state of the vessel it is likely that the DP setpoint adaption will interfere with the DP controller. For example if the true pitch would be used for calculating the DP setpoint. When the setpoint is achieved the pitch is changed and the setpoint is not the perfect setpoint anymore. This would result in a very complicated dynamic system.

The DP setpoint adaption is implemented as is depicted in Figure 5.7. The implementation is an iterative numerical loop. The calculation begins with the following:

- The crane user input settings
- The position and orientation vector of the heavy load $\vec{\eta}_{load}$
- An initial position and roll and pitch of the vessel $\vec{\eta}_{vessel}$
- Heading setpoint from DP controller

Using this data the forces and moments on the vessel τ_{vessel} is calculated by the crane model which is described in Section 5.2.7. Now τ_{vessel} is used to calculate the roll and pitch of the vessel by the linear pitch and roll model which is described by Equation 5.14

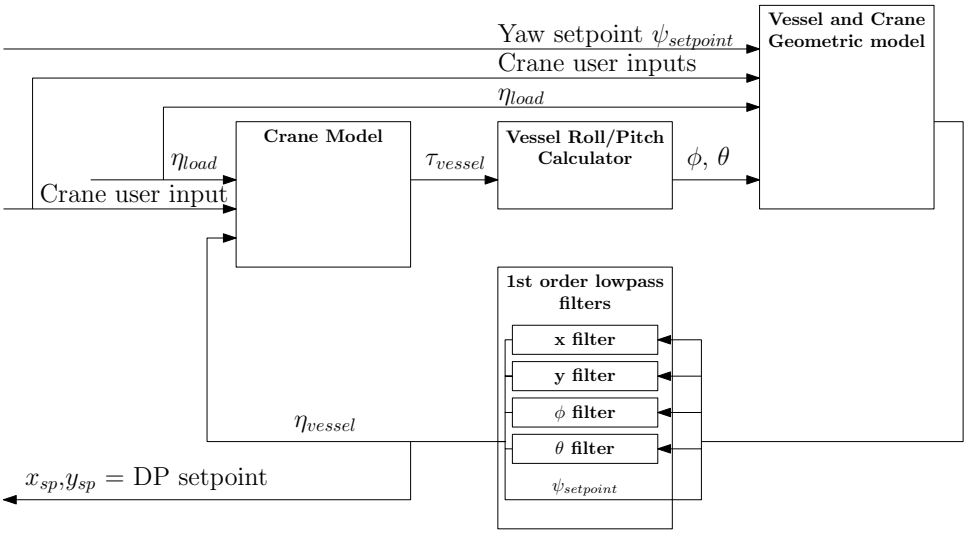

Figure 5.7: Layout of DP setpoint adaption implementation

in Section 5.2.5. Using the calculated roll, pitch and DP heading setpoint the distance between the crane tip and vessel origin is calculated in world coordinates. Now the calculated distance is added to the heavy load world coordinates and afterwards the correct DP setpoint is calculated for the roll and pitch which belong to the inital vessel position. The x and y coordinate, and the roll and pitch are inputted in a first order low pass filter as described by Equations 5.65 and 5.66 with a small time constant of 4 seconds, to achieve a stable numerical loop. Afterwards the filtered x_{sp} and y_{sp} value are the DP setpoint which is inputted in the DP controller. Next the x_{sp}, y_{sp}, roll and pitch together with the heading setpoint is input to the next numerical calculation cycle. The idea is that the DP setpoint converges towards an equilibrium. If the crane settings, heading setpoint, $\vec{\eta}_{load}$ are not changed, the DP setpoint will not change either.

5.4. GENERAL SIMULATION ENVIRONMENT

In this section the general simulation test environment is described which is used during all simulations experiments in this thesis, if not otherwise specified. The reader is reminded that the general values of parameters and settings are described in Appendix B.

In all simulations conducted in Chapter 6 the crane is pointed towards stern (α = 180). The reason for this is already mentioned, the surge movement of the vessel has the lowest damping in comparison to the yaw and sway movement hence only this motion is investigated regarding the instability. As already mentioned in Section 5.1, each implemented solution candidate is tested by two simulation tests (i.e. the baseline test and the seastate test). Now the simulation details are discussed.

BEFORE STARTING THE SIMULATION

The initial locations of the heavy load is exactly below the crane tip of the vessel, with no tension in the hoist cable but the hoist cable is taut.

The heavy load position is rigidly defined by a vector without any dynamics, which means that the hoist cable is attached to a rigid point. This simulates the moored stage during the installation of a topside on a jacket operation. The initial velocity of the vessel is zero.

During the *baseline test* the environmental conditions are no wind, waves and current. As already mentioned during the baseline test a periodic force is applied on the

vessel such that the vessel without any solution should become instable. This periodic force is defined later in 6.1.1, i.e. during presenting the results of phase 1 of the scoring strategy.

During the *seastate test* the vessel model is subjected to environmental forces defined as Seastate 3. This was already implemented in the Imtech vessel model itself. Imtech vessel model uses the Pierson Moskowitz Spectrum. Wind load is defined with 13,0[kn] and wave load is described as 0.9[m] significant height with wave period peak of 7.5[s]. The wave impact is calculated using basic vessel parameters like significant wave height, wave period, heading of waves, average wind speed, beam at the water line, acceleration of gravity, length at the water line and 3 empirical effectiveness factors for yaw roll and pitch. No current is modeled. The wind and waves are coming from the same direction. Assuming the heading of the vessel is 0 degrees (to the north), the wind and waves are coming from 330 degrees(North-West). The wind will deviate +-8 degrees randomly.

The Imtech vessel model and DP system software is started, where after the Simulink simulation is started within 5 seconds automatically. Now the simulation is started.

AFTER STARTING THE SIMULATION

The baseline test and the seastate test are defined in Table 5.6. Note that the Greek numbers coincide with the Greek numbers in figure 5.8. Furthermore note that t_1 is representing a time instance for the Baseline test and t_2 is representing a time instance for the Seastate test.

From	to	description:
$t_1 = 0[s]$ $t_2 = 0[s]$ (I)	$t_1 = 0[s]$ $t_2 = 0[s]$ (I)	Simulink started, no tension hoist cable taut
$t_1 = 2[s]$ $t_2 = 330[s]$ (II)	$t_1 = 40[s]$ $t_2 = 825[s]$ (III)	The position of the heavy load is forced to lower 7 meters with a constant velocity. This will increase the tension in the hoist wire gradually, to 3917[t] to simulate the moored stage with tension in the cable. No ballasting is implemented so a certain pitch is also obtained.
$t_1 = 40[s]$ $t_2 = 825[s]$ (III)	$t_1 = 1800[s]$ $t_2 = 2310[s]$ (IV)	The position of the heavy load is constant again
$t_1 = 1800[s]$ $t_2 = 2310[s]$ (IV)	$t_1 = 1820[s]$ $t_2 = 2706[s]$ (V)	The position of the heavy load is forced to rise 7 meters with a constant velocity to simulate the release of tension, the weight transfer from crane to jacket. Hence transition between moored stage to free floating stage is done here.
$t_1 = 1820[s]$ $t_2 = 2706[s]$ (V)	$t_1 = 2000[s]$ $t_2 = 3300[s]$ (VI)	The position of the heavy load is constant in its begin situation, so free floating stage except the crane is still attached but in principle no tension.

Table 5.6: Description of baseline test and seastate test. t_1 is representing a time instance for the baseline test and t_2 is representing a time instance for the seastate test

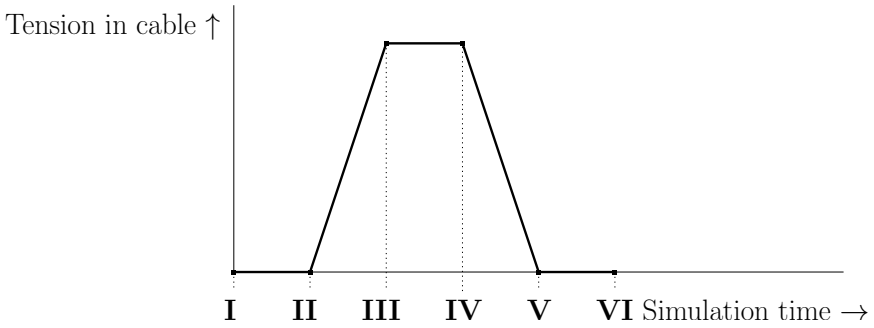

Figure 5.8: Tension VS Simulation Time

One could remark that there is a difference between a real-world topside installation on a jacket and the simulated operation. The difference is that the heavy load is never floating in the air between time instances III and IV. Consequently, the operation during simulation is never in the hoisting DP operation stage.

This way of simulation is chosen because it is less complicated for implementation. Furthermore, it does not have disadvantages because the critical aspects of the topside installation on a jacket regarding the mooring stiffness problem taken into account. I.e. the most critical stage during this operation is when the tension in the cable is the largest, and this is between III and IV. That is also why this period is chosen to take relatively long in the simulations, regarding to a real-world operation. Furthermore the other critical stage is taken into account, which is the transition between moored stage and free floating stage. Consequently when the candidate solutions are performing well in this simulation environment it will solve the problems related to the mooring stiffness problem.

Now the measures for scoring the solution candidates are discussed.

5.5. MEASURES FOR SCORING THE SOLUTION CANDIDATES

The requirements for a conceptual solution are described in Section 4.1. Obviously the performance of the solution candidates can and will be valued on qualitative elements. But to score the solution candidates objectively, scoring measures have to be defined based on the requirements from Section 4.1. With these measures the solution candidates are studied in Chapter 6.

First variables which are used throughout this section are described in the following Table. After that the scoring measures are defined.

Variable	Unity and description
t_{domain}	A period of time, later specified [s]
n	a simulation time step []
$t_{moored,b}$	Time instance of which the moored stage begins [s]
$t_{moored,e}$	Time instance of which the moored stage ends [s]
$t_{freefl,b}$	Time instance of which the free floating stage begins [s]
$t_{freefl,e}$	Time instance of which the free floating stage ends [s]
t_I, t_{II}, t_{III}, t_{IV}, t_V, t_{VI}	Refer to the time instances following to the roman numbers in Table 5.6 and Figure 5.8 [s]
x	Surge position of vessel [m]
$p_{x,DP}$	Position of DP setpoint in surge direction [m]
Δx_{max}	Maximal deviation of the surge position of vessel from setpoint, in a certain time period. [m]
Δx_{mean}	Mean deviation of the surge position of vessel from setpoint, in a certain time period. [m]
u_{mean}	Mean velocity in surge direction [m/s]
I_{mean}	Mean built up current in surge direction [m/s]
Ψ_{mean}	Mean thruster usage in surge direction []
X_{mean}	Mean horizontal force in surge direction [N]

Now some definitions of variables which are used throughout this section are given:

$$t_{moored,b} = 0.5(t_{II} + t_{III}) \tag{5.71}$$

$$t_{moored,e} = 0.5(t_{IV} + t_V) \tag{5.72}$$

$$t_{freefl,b} = t_V \tag{5.73}$$

$$t_{freefl,e} = t_{VI} \tag{5.74}$$

$$\Delta x_{max} = max(|x - p_{x,DP}|) \tag{5.75}$$

$$\Delta x_{mean} = \frac{1}{n \in t_{domain}} \sum_{n \in t_{domain}} |x - p_{x,DP}| \tag{5.76}$$

$$u_{mean} = \frac{1}{n \in t_{domain}} \sum_{n \in t_{domain}} |u| \tag{5.77}$$

$$I_{mean} = \frac{1}{n \in t_{domain}} \sum_{n \in t_{domain}} |I| \tag{5.78}$$

$$\Psi_{mean} = \frac{1}{n \in t_{domain}} \sum_{n \in t_{domain}} \Psi \tag{5.79}$$

$$X_{mean} = \frac{1}{n \in t_{domain}} \sum_{n \in t_{domain}} |X| \tag{5.80}$$

SURGE DEVIATION DURING MOORED STAGE

As already mentioned during the topside heavy lift operation a narrow clearance is to be maintained between the vessel and heavy load. Consequently, the maximal surge deviation is the main measure of valuing the solution candidates. Furthermore the mean offset is also a good measure. The maximal and mean offset is to be as small as possible. The following period of time is defined as the moored stage:

$$t_{moored,begin} < t_{domain} < t_{moored,end}$$

MEASURES:

- The largest deviation in surge direction $\Delta p_{x,max}$ during moored stage
  The less the better. The maximum acceptable value within a operation is 3[m].
- Mean absolute offset in surge direction $\Delta p_{x,mean}$ during moored stage
  The less the better.

SURGE DEVIATION AFTER STAGE TRANSITION FROM MOORED STAGE TO FREE FLOATING STAGE

A part of the mooring stiffness problem is the poor position keeping after stage transition from moored stage to free floating stage. The maximal and mean deviation in the following time period is a measure for the performance with respect to the mooring stiffness problem part after stage transition from moored DP to Free floating DP operational stage.

$$t_{freefl,begin} < t_{domain} < t_{freefl,end}$$

MEASURES:

- The largest deviation in surge direction Δx_{max} during free floating stage
  The less the better.

- Mean absolute offset in surge direction Δx_{mean} during free floating stage
  The less the better.

OSCILLATORY SURGE BEHAVIOR

A part of the mooring stiffness problem is the instable behavior vessel. Oscillatory behavior can be a sign for beginning or almost instable behavior. The Oscillatory behavior can be measured with mean velocity.

MEASURES:

- Mean absolute velocity in surge direction u_{mean}
  The less the better.

THRUSTER USAGE

Low thruster usage is favorable due to a number of reasons. Firstly, if the thruster usage is almost at it's maximum, possibly the position keeping will be in danger. When a small distortion appears, no thrust reserve is present for reacting on this. Furthermore, much thruster usage is in principle not necessary, as the vessel is operating in light weather conditions and the mooring stiffness helps the vessel to stay in position. The last reason is that in principle fuel consumption can be decreased with lower thruster usage.

MEASURES:

- Mean thruster usage reserve Ψ
  When the first priorities are fulfilled, having low thruster usage Ψ is favorable.

ESTIMATED CURRENT DEVIATION

As already mentioned in Section 3.2, because of the nature of the current model buildup technique, all unmodeled long lasting forces are included into the 'current'. Hence the more estimated current which is not due to environmental forces, the worse the current model buildup is applied. Poorly estimated current can lead to poor performance of the DP system after the stage transition from moored to free floating stage. The current used as measure is the current in surge direction.

MEASURES:

- Mean absolute current I_{mean}
  The mean absolute current should be around 0.13[m/s]. As this is the current which is needed to counteract forces of seastate 3. This particular current value is obtained by doing a simulation of the vessel in seastate 3 without crane forces.

HORIZONTAL MOORING STIFFNESS FORCES

Horizontal mooring stiffness forces via the crane induce extra load on equipment. Furthermore these forces influence the position of the vessel. The effect of this influence has to be estimated and estimations always have a (small) error. Hence it is better to prevent the horizontal forces than have to estimate them.

MEASURES:

- Mean absolute horizontal force in surge direction X.
  The lower the better.

6

RESULTS

In Section 5.1 the strategy of scoring the solutions was discussed. A three phase scoring strategy was proposed to score the candidate solutions. In Section 6.1 the results of the conducted scoring strategy are presented. The reader is reminded that a summary of the scoring strategy with schematic overview of the used model configurations is depicted in Table 5.1.

After conducting the 3 phases of the scoring strategy an interesting phenomena is observed, which is the dependence of surge resonance frequency on surge amplitude. This dependence is discussed in Section 6.2. Subsequently, the poor performance of the feed forward candidate solution is explained in Section 6.3. And finally the poor performance of the Filtered solution candidate is discussed in Section 6.4.

To help improve the understanding of this chapter and Chapter 7, the following two dynamic systems are defined here:

1. *the System*
   Which is the heavy lift vessel with a crane in moored stage. In other words, the heavy load is rigidly attached on the jacket as depicted in Figure 3.2b.

2. *the System+DP*
   Which is *the System* of point 1, with the DP system enabled. So the DP system is also applying forces to the heavy lift vessel by means of its thrusters.

6.1. RESULTS OF SCORING STRATEGY

In this section the results of the scoring strategy are presented in 3 phases. First phase 1 is discussed.

6.1.1. PHASE 1: REPRODUCTION MOORING STIFFNESS PROBLEM IN MODEL

In industry practice *the System+DP* have become instable due to mooring stiffness forces, as is described in Section 3.2. First of all it is noted that *the System* itself is a stable system, i.e. the DP system is the cause of the instability. Computer simulation tests have indicated that *the System+DP* does not become instable when *the System+DP* is not actuated. This shows that *the System+DP* requires a disturbance to become instable. It is not trivial to find a disturbance which causes *the System+DP* to become instable. A periodic force with decreasing frequency is used to achieve this task.

The simulations in phase 1 are conducted to reproduce the problem that is to be solved. In other words, to prove that it is possible for *the system+DP* to become instable in the simulated environment. But also to find the conditions of the point of instability, which are used as baseline tests for phase 2 and phase 3.

Experiments show that the point of becoming instable is found within a certain surge amplitude deviation. Two simulation tests are shown in this paragraph. One point right before*the System+DP* becomes instable and one point right after *the System+DP* becomes instable. The true point of becoming instable is expected to be between the two aforementioned points.

SIMULATION SETTINGS

The periodic force with decreasing frequency is derived by trial and error and defined as follows:

$$
\begin{aligned}
&u(1) = 0 && for && 0 < t < 200\\
&u(1) = 62[kN] && for && 200 < t < \tau\\
&u(1) = 0 && for && \tau < t < 2000\\
&u(2) = 25 + u(3) * t && for && 0 < t < \tau\\
&u(2) = 0 && for && \tau < t < 2000\\
&u(3) = 45/\tau && for && 0 < t < 2000
\end{aligned}
$$

$$Fx = u(1) \cdot sin^2\left(2\pi\left(\frac{t}{u(2)} + \frac{2t^2 \cdot u(3)}{u(2)^2}\right)\right)$$

As already mentioned, the latter periodic force is also used in the Baseline Test in phase 2 (Section 6.1.2) and 3 (Section 6.1.3) of the scoring strategy.

The first simulation, of which results are shown in Figure 6.1, is a simulation with a periodic force defined by $\tau = 800[s]$. This is the minimum τ for which *the System+DP* becomes instable.

The second simulation, of which results are shown in Figure 6.2, is a simulation with a periodic force defined by $\tau = 780[s]$. This is the maximum τ for which *the System+DP* is still stable.

SIMULATION RESULTS

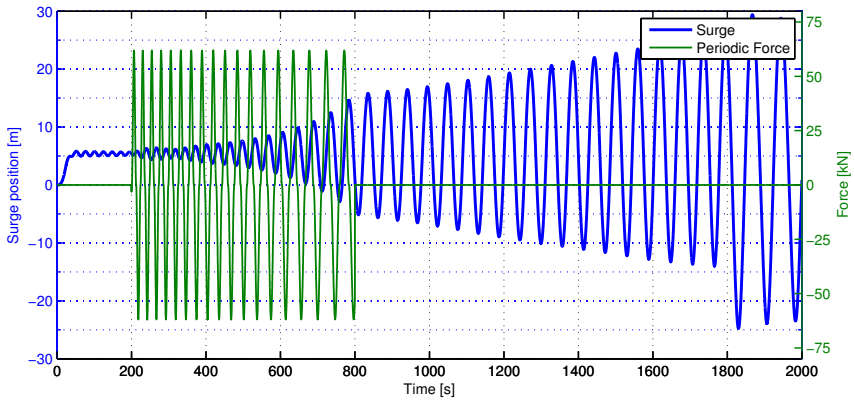

Figure 6.1: Position in surge direction after actuating the vessel with a periodic force from τ = 200[s] to τ = 800[s].

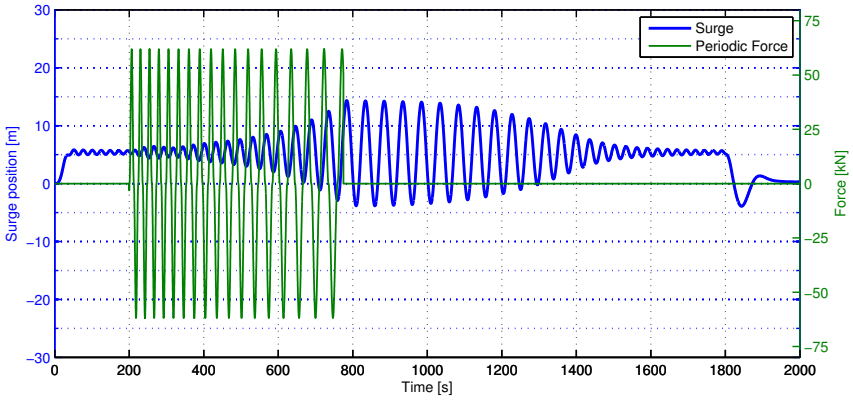

Figure 6.2: Position in surge direction after actuating the vessel with a periodic force from τ = 200[s] to τ = 780[s].

Figure 6.1 shows that the results reproduce the instability of the mooring stiffness problem. The surge amplitude of the vessel when it is close to instability, but not yet instable, is 8.4[m]. Furthermore, the figure shows that the surge amplitude of the vessel of just beyond instability is 10[m]. With the two simulations in this section a range between 8.4[m] and 10[m] of surge amplitude is obtained for which *the System+DP* becomes instable.

Now the baseline test is defined as $\tau = 850[s]$. The choice of $\tau = 850[s]$ instead of $\tau = 800[s]$ is to be sure that *the System+DP* will become instable without any solution candidate.

The figures also show that the surge position is not fluctuating around 0[m] but around 5.6 [m]. This effect is explained earlier in this report. The vessel pitches due to the high tension in the cable following the contour of Figure 5.8. Due to the pitching of the vessel the crane tip will change position with respect to the reference point of the vessel. So the neutral position, i.e. the position which will create no mooring stiffness forces, is no longer 0[m]. This effect was the reason for suggesting the DP Setpoint adaption. In the following phases of the scoring strategy the neutral position of the vessel is calculated. This is named *Neutral Pos* in the graphs. The term *neutral position* is used further on in this report and calculated by the DP Setpoint adaption.

6.1.2. PHASE 2: TESTING 4 CANDIDATE SOLUTIONS, USING MODEL STATES

The goal of this phase is to choose the best performing solution candidate. In this phase the 4 candidates are tested. Apart from this, the case where no solution candidate applied, is tested as a reference. Next, the effect of DP Setpoint adaption is scored by doing tests having DP setpoint turned on and off. In this phase the position and orientation states from the vessel model are used to calculate the mooring stiffness forces on the vessel, instead of the vessel states estimated by the DP Controller. Two tests are performed for each candidate solution. The first test is a baseline test to study whether the solution is stabilizing *the System+DP*. The second test is the Seastate test to study the performance of the candidates in realistic environment.

To quantify the performance of the candidates the following set of measures are used, which are defined and described in detail in Section 5.5:

- The largest deviation in surge direction Δx_{max} during moored stage
- Mean absolute offset in surge direction Δx_{mean} during moored stage
- The largest deviation in surge direction Δx_{max} during free floating stage

- Mean absolute offset in surge direction Δx_{mean} during free floating stage
- Mean absolute velocity in surge direction u_{mean}
- Mean thruster reserve Ψ_{mean}
- Mean absolute current I_{mean}
- Mean absolute horizontal mooring stiffness force in surge direction X_{mean}

SIMULATION SETTINGS

The settings used for the simulation are the settings of the general simulation environment described in Section 5.4. A number of tests have been carried out: The Baseline test, the Seastate test for *the System+DP* with solution candidates 1, 2, 3 and 4 and the Seastate test without a candidate. All tests are done with the DP setpoint adaption switched on and off which brings the total number of simulation tests to 20.

RESULTS

The results of the simulation tests of phase 2 in this section are presented as follows:

- 6 plots of the Baseline test in Figure 6.3
  - 4 plots of the performance with the solution candidates and with DP setpoint adaption.
  - 1 plot without any solution candidate and without DP Setpoint adaption.
  - 1 plot of the estimated current by the DP controller, for the cases with and without solution candidates.
- 1 plot of Baseline test without a solution candidate but with DP setpoint adaption in Figure 6.4. This shows that with DP setpoint adaption, *the System+DP* also becomes instable during the Baseline test.
- 6 plots of the Seastate test in Figure 6.5
  - 4 plots of the four different solution candidates during seastate 3. These plots are with DP setpoint adaption.
  - 1 plot of a simulation without any solution candidate and without DP Setpoint adaption.
  - 1 plot of the estimated current by the DP controller for with and without solution candidates.
- 2 tables of performance measures, measured during the Seastate test.
  - Table 6.1 shows the results of the simulations with DP setpoint adaption.
  - Table 6.2 shows the results of the simulations without DP setpoint adaption.

  The tables are included for two reasons. First of all, to compare the performance of the candidates objectively during a realistic simulation environment of the Seastate test. Secondly, to compare the performance of the candidates between the situation where DP setpoint is adapted and where it is not adapted.

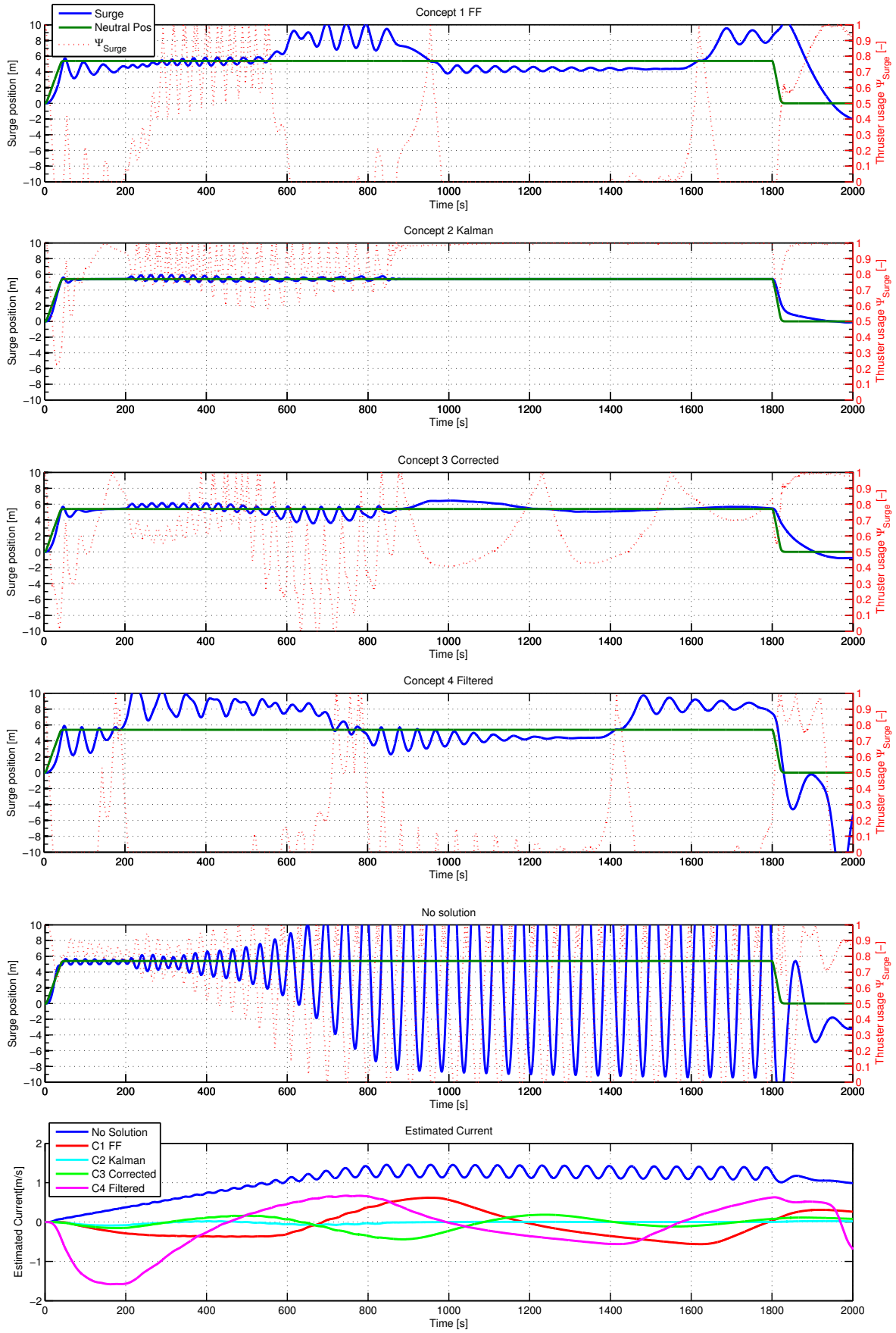

Figure 6.3: Results of the Baseline Test

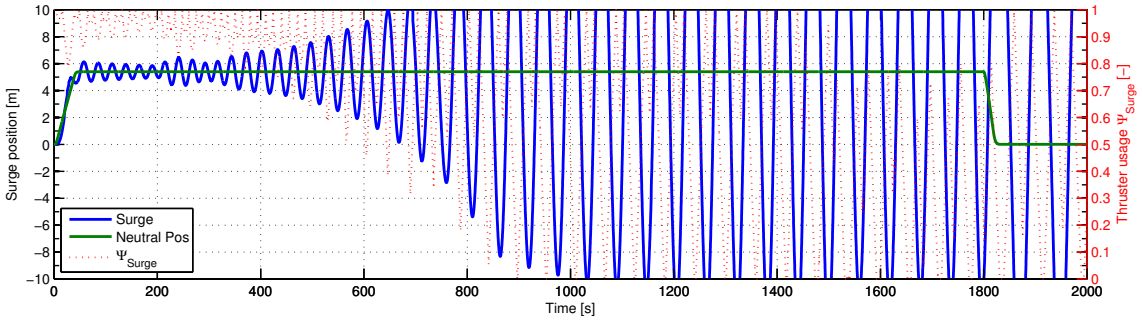

Figure 6.4: Results of the Baseline test without solution and with DP setpoint adaption enabled.

From Figures 6.3 and 6.4 the following can be noted:

First of all, the *the System+DP* becomes instable for the cases without a solution candidate and with and without DP setpoint adaption. This was expected, as described in Section 6.1.1.

From this, one can conclude that the DP Setpoint adaption on its own does not stabalize *the System+DP*.

Secondly one can conclude from Figure 6.3 that all four candidate solutions stabilize *the System+DP*.

Thirdly, when comparing candidates 1 and 4 to candidates 2 and 3, Figure 6.3 shows that the surge position deviation from the neutral position is relatively large, the mean thruster reserve Ψ_{mean} being generally very low and finally the current being poorly estimated. Consequently, the Feed Forward(1) solution candidate and the Filtered(4) solution candidate seem to perform poorly compared to the Kalman(2) and Corrected(3) solution candidates.

Next, when comparing the Kalman(2) to the Corrected(3) solution candidate, the Kalman(2) candidate seem to perform better. The surge position and thruster reserve (Ψ_{surge}) of the Kalman(2) candidate are more steady than the corresponding values of the Corrected(3) candidate solution.

In spite of the previous remarks, the only conclusions drawn from Figures 6.3 and 6.4 are the following: Firstly, all solution candidates (i.e. 1,2,3 and 4) stabilize the System+DP. Secondly in the situation of only DP Setpoint adpation enabled, and no further solution candidate enabled, the *the System+DP* is not stabilized. For this reason, the solution candidate is no longer considered a possible solution. Next the results of the Seastate test are shown.

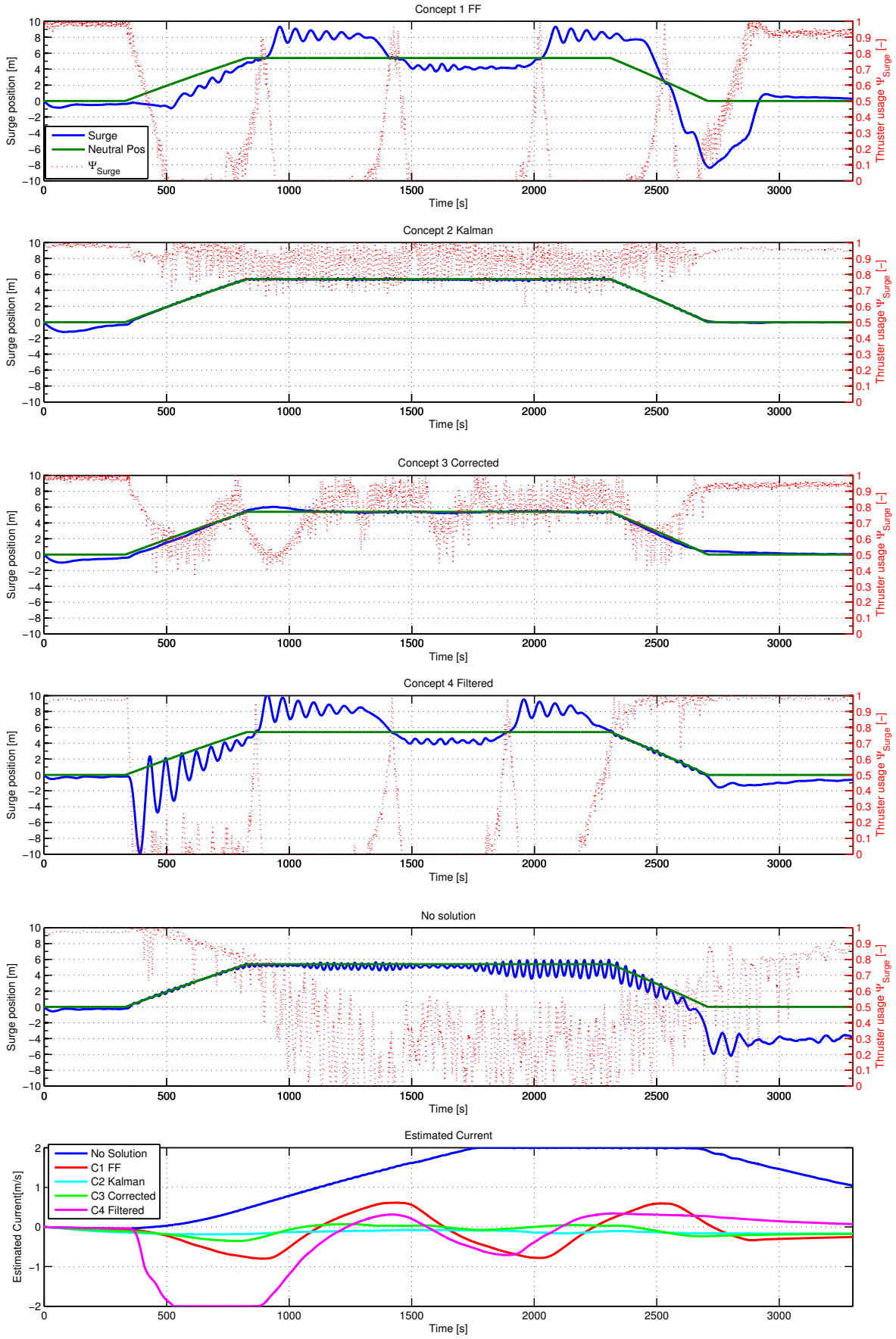

Figure 6.5: Results of the Seastate Test

From Figure 6.5 the following can be noted:

Firstly, the simulation without a solution candidate does not become instable, but the surge position shows relatively high frequency oscillatory behavior especially between t=1500[s] and t=2500[s]. This indicates a high effective spring stiffness as theoretically analyzed in Section 3.2. Furthermore, this Figure shows that the estimate current for the case of no solution is the worst estimated from all solution candidates. This leads to poor performance after the stage transition from moored to the free floating stage, which is shown by the surge error of approximately 4 meters between t=2500[s] and t=3000[s].

Secondly, the Seastate test shows that the Feed Forward(1) candidate and the Filtered(4) candidate seem to perform poorly compared to the Kalman(2) and Corrected(3) candidates. Again the surge position deviation from the neutral position are relatively large for candidate 4 especially during increase of the load. The same is true for candidate 1, especially after stage transition from moored stage to free floating stage. Furthermore the mean thruster reserve Ψ_{mean} is generally very low and the current estimation is poor.

Thirdly, just like during the Baseline test, when comparing the Kalman(2) and the Corrected(3) candidates the Kalman(2) candidate seem to performing best, as the surge is more steady and the thruster reserve is larger and more steady.

Fourthly, one might remark that the surge position offset of the vessel increases to about 1[m] in all candidates during t=0[s] to t=300[s]. This is explained by the fact that from t=0[s] the net force on the vessel is not zero, but the vessel is in neutral position(i.e. the mooring stiffness forces are zero). The estimated current is 0 [m/s] and the environmental forces only begin to act at t=0[s]. Hence the DP system has to find it's steady state and this takes some time.

In spite of the previous remarks, no conclusions are drawn from these plots. Next, the tables with performance measures during the Seastate test are shown.

With DPSPA		Candidate1	Candidate2	Candidate3	Candidate4	No Solution
Δx_{mean} (moored)	[m]	1.88	0.05	0.13	1.66	0.18
Δx_{max} (moored)	[m]	3.93	0.26	0.63	4.77	0.48
Δx_{mean} (free floating)	[m]	2.31	0.03	0.19	0.97	0.15
Δx_{max} (free floating)	[m]	8.40	0.12	0.44	1.60	0.41
u_{mean}	[m/s]	0.030	0.017	0.013	0.043	0.047
Ψ_{mean}	[-]	0.26	0.90	0.80	0.41	0.84
I_{mean}	[m/s]	0.41	0.13	0.12	0.54	0.03
X_{mean}	[kN]	716	27.4	56.9	618	69.8

Table 6.1: The values of measures during the Seastate test with DP Setpoint adaption. ***DPSPA = DP Setpoint Adaption**

Without DPSPA		Candidate1	Candidate2	Candidate3	Candidate4	No Solution
Δx_{mean} (moored)	[m]	1.18	0.32	0.43	1.32	0.45
Δx_{max} (moored)	[m]	3.82	0.74	1.15	4.91	1.91
Δx_{mean} (free floating)	[m]	1.23	0.28	0.25	1.02	4.28
Δx_{max} (free floating)	[m]	7.86	1.18	2.10	1.49	6.19
u_{mean}	[m/s]	0.014	0.008	0.008	0.042	0.068
Ψ_{mean}	[-]	0.24	0.62	0.55	0.36	0.46
I_{mean}	[m/s]	0.75	0.42	0.51	0.82	1.47
X_{mean}	[kN]	521	112	157	486	199

Table 6.2: The values of measures during the Seastate test without DP Setpoint adaption. ***DPSPA = DP Setpoint Adaption**

Considering Table 6.1 and Table 6.2 the following can be noted: In general the Feed Forward(1) and the Filtered(4) candidate solutions seem to perform poorly comparing to the Kalman(2) and Corrected(3) candidate solutions. In the previous plots this was already noted, but a new observation is that the max absolute offset in surge direction Δx_{max} during moored stage of candidate solutions 1 and 4 is above the acceptable limit of 3[m] surge. This means that the Feed Forward(1) and Filtered(4) candidates are rejected. As already mentioned in the introduction of this chapter, the poor performance of the Feed Forward candidate and the Filtered candidate are studied in Sections 6.3 and 6.4 respectively.

Now, only the four cases of solution candidates of candidate 2 and candidate 3 with and without DP setpoint adaption remain. When comparing the candidates with and without DP Setpoint adaption, the DP setpoint adaption improves all measures except for u_{mean}. Furthermore, when comparing candidate 2 to candidate 3 all measures of candidate 2 scored better than candidate 3, except for u_{mean}. The latter can be explained by the lower effective spring stiffness of the Corrected solution candidate(3) with respect to the Kalman solution candidate (2).

Based on this, candidate 2 with DP setpoint adaption is selected as best solution upon the measures. Only for u_{mean} candidate 3 is performing better in terms of measures, but both are stabilizing the system as seen in Figure 6.3. Hence the Kalman solution candidate(2) with DP setpoint adaption is chosen as winning candidate and is tested in phase 3 of the scoring strategy (Section 6.1.3).

6.1.3. PHASE 3: TESTING WINNING CANDIDATE, USING ESTIMATOR STATES

In this phase the winning candidate of phase 2 is tested, which is the Kalman candidate(2) solution. But now in phase 3 the mooring stiffness forces are estimated with the use of the position and orientation states from the DP controller instead of the true states, as can be seen in Table 5.1. Doing this the performance is tested in a more realistic setting as the DP controller does not know the true model states. These tests allow verifying whether or not the winning solution candidate from phase 2 also performs well with estimated positions and orientation states.

SIMULATION SETTINGS

In phase 3 the same tests are performed as in phase 2, but in this phase only the Kalman candidate(2) with DP Setpoint adaption is tested. The simulation settings are according to the general simulation environment described in Section 5.4.

RESULTS

The results in this phase are compared to the results of phase 2 to verify whether the Kalman solution candidate(2) performs well in a more realistic environment. The results are as follows:

Kalman candidate(2)		True vessel states (Phase 2)	Estimated vessel states (Phase 3)
$\Delta p_{x,max}$ (moored)	[m]	0.05	0.05
$\Delta p_{x,mean}$ (moored)	[m]	0.26	0.35
$\Delta p_{x,max}$ (free floating)	[m]	0.03	0.06
$\Delta p_{x,mean}$ (free floating)	[m]	0.12	0.16
u_{mean}	[m/s]	0.017	0.018
Ψ_{mean}	[-]	0.90	0.90
I_{mean}	[m/s]	0.13	0.14
X_{mean}	[kN]	27.4	27.6

Table 6.3: The values of measures during the Seastate test

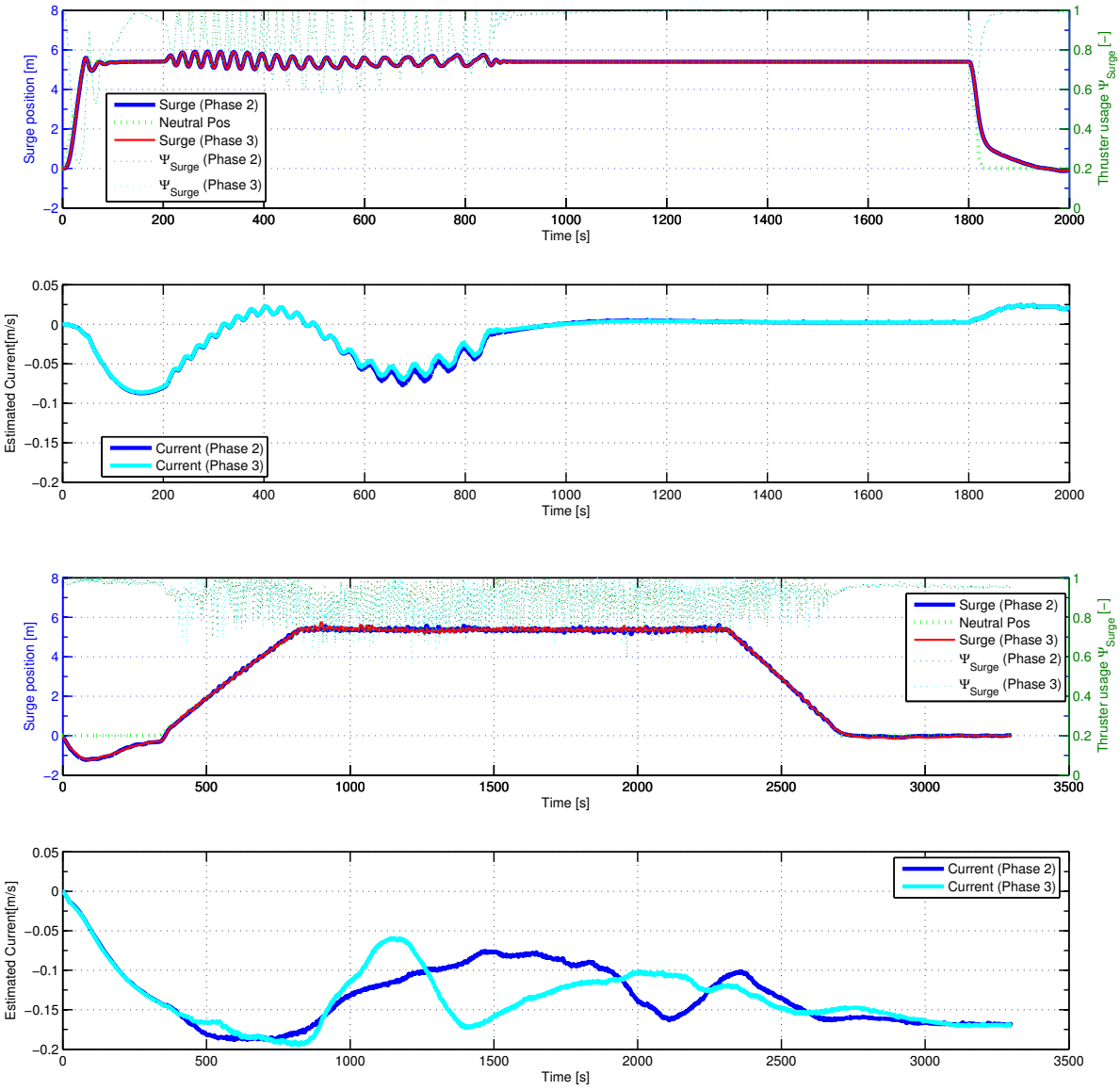

(b) Seastate test

Figure 6.6: Simulation tests with the Kalman solution candidate(2)

The behavior of *the System+DP* during phase 2 and 3 is very similar. This can be seen in the Table with measured datapoints 6.3 and the plots of both the baseline test and the Seastate test Figure 6.6. The current estimation during the Seastate test performs well. The reader should note that the y-axis scale is much smaller than the plots in phase 2. The small differences can be accounted for by stochastic effects of the environmental loads on the vessel. Consequently, hereby is concluded that the winning Kalman candidate(2) is able to achieve approximately the same performance with the use of estimated states by the DP controller, instead of the true model states.

CONCLUSION OF SCORING STRATEGY

Based on this, we conclude that the Kalman solution candidate(2) with DP setpoint adaption is the best performing candidate of all solution candidates, based on the objective measures for scoring solution candidates. The performance of the Kalman solution candidate(2) is also much better than without any solution during the realistic simulation environment. Also the winning Kalman candidate is able to achieve approximately the same performance with the use of estimated states by the DP controller, instead of the true model states.

6.2. SURGE RESONANCE FREQUENCY AS FUNCTION OF SURGE AMPLITUDE

The horizontal stiffness of *the System* was assumed to be constant for small surge deviations in Section 3.2. This was derived from geometrical relationships and the relation was noted in Equation 3.10. With a constant mooring stiffness *the System* becomes a linear second order damped mass spring system. Combining Equation 3.1 with Equation 3.10 and defining the external force in the surge direction as X will lead to the following equation of motion:

$$M\ddot{x} + B\dot{x} + \frac{T}{L}x = X \tag{6.1}$$

The response of the amplitude of oscillation to a periodic force X of the system in Equation 6.1 is shown in Figure 6.7. In this Figure the frequency response is shown for different damping factors. Figure 6.7 shows that *the System* with constant mooring stiffness has 1 resonance frequency. The resonance frequency of the system is given by:

$$\omega_0 = \sqrt{\frac{(T/L)}{M}} \tag{6.2}$$

Equation 6.2 shows that the resonance frequency is independent of the amplitude of the external force X.

If *the System* would be linear the surge oscillation frequency would be constant like described in Equation 6.2. However, simulations show that the frequency of the surge oscillation is not constant but it is a function of the amplitude of the surge oscillation. This observation is the reason for the analysis in this section. The goal of this analysis is to answer the following question: Is the surge resonance frequency of *the System* function of the surge amplitude? If so, how can this be explained?

The question is answered by first observing the behavior of the surge frequency in the computer simulation environment, which is described in Section 6.2.1. Secondly, the relation is analyzed theoretically in Section 6.2.2.

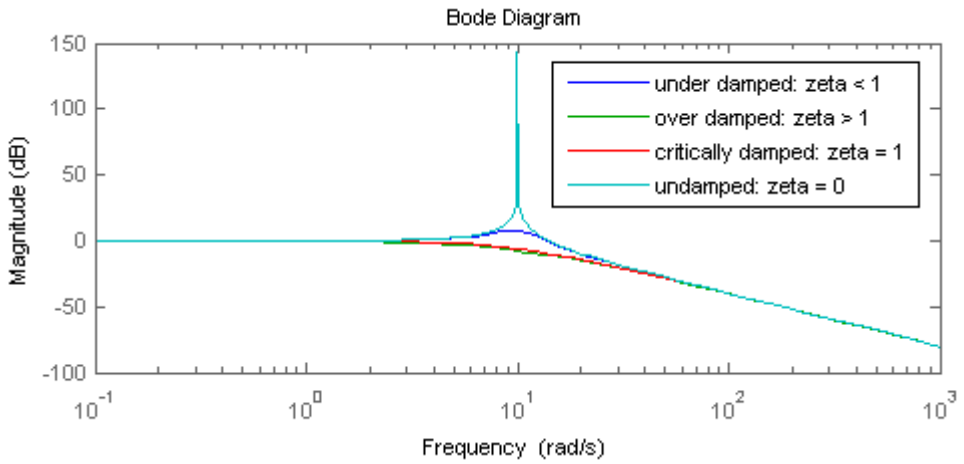

Figure 6.7: Example of the frequency response of a linear second order damped mass spring system

6.2.1. ANALYSIS IN SIMULATION ENVIRONMENT

In this section the following two computer simulation tests are performed:

1. **Frequency response test**
   The goal of this Frequency response test is to study whether *the System* is linear or not. In this test *the System* is subjected to a periodic force with different frequencies such that the resonance frequency will be identified. Subsequently, different amplitudes of the periodic force are used, which are 20.2[kN] and 182[kN]. The results of these tests allow us to conclude whether or not *the System* is linear by observing whether there is a shift in frequency of the resonance peaks.

2. **The Amplitude-Period table test**
   The goal of this Amplitude-Period table test is to obtain a table with numerical values of the resonance frequency belonging to a specific surge amplitude. This table is used in Section 7.1.2.

Next, the simulation settings of the two simulation tests are discussed.

SIMULATION SETTINGS

Unless otherwise specified, the simulation is done according to the general simulation environment of Section 5.4. During both tests the following settings are implemented:

- The DP system is disabled
- No wave, wind and current load on the vessel
- The heading of the vessel is fixed
- The simulation of the mooring stiffness forces is equal to the simulation tests during the scoring strategy in Section 6.1. I.e. according to Table 5.6 and Figure 5.8. But now the time instances I, II, III, IV, V and VI are according to Table 6.4

Time instance	Frequency response test	Amplitude-Period table test
I	t = 0[s]	t = 0[s]
II	t = 275[s]	t = 275[s]
III	t = 550[s]	t = 550[s]
IV	t = 20000[s]	t = 3000[s]
V	t = 20000[s]	t = 3000[s]
VI	t = 20000[s]	t = 3000[s]

Table 6.4: Time instances of frequency response and amplitude-Period table tests according to Figure 5.8

The forces on the vessel are defined in this follow section. For the frequency response test a periodic force is actuating the vessel in surge direction and this force is defined as:

$$X = A \cdot sin^2\left(2\pi \frac{t}{P}\right) \tag{6.3}$$

As mentioned before, the simulations are done for the cases A=20.2[kN] and A=182[kN]. During the frequency response simulation test, the period P is increased in steps. The period P is set to 5[s], 10[s], 20[s], 30[s], 40[s], 50[s], 60[s], 70[s], 80[s] and 90[s] as shown in Figure 6.8.

For the Amplitude-Period table test *the System* is actuated by a large force manually in surge direction around t=600[s] to create large a surge amplitude. Afterwards the vessel is no longer actuated by manual forces. Now *the System* will decay slowly in surge amplitude due to the damping.

RESULTS OF FREQUENCY RESPONSE TEST

Figure 6.8 reveals that *the System* has indeed a single resonance frequency, similar to the linear second order mass spring system. Furthermore, Figure 6.8 shows that the resonance frequency of *the System* during an applied periodic force of 20.2[kN] is the closest to 1/40[Hz], hence a period P of 40[s]. When a periodic force with amplitude of 182[kN] is applied a resonance frequency closest to 1/60[Hz] is obtained. The corresponding surge amplitudes are 4[m] and 23[m], respectively. This concludes that the frequency of the resonance is a function of the amplitude of the vessel surge motion. This allows us to conclude that the surge resonance frequency is indeed function of the surge amplitude.

Next, the results of the Amplitude-Period table test are presented.

RESULTS AMPLITUDE-PERIOD TABLE TEST

A table with numerical values of the resonance frequencies belonging to a certain surge amplitude is obtained in this section. This table is presented in Table 6.5. The data in this table is measured from the plot of *the System*'s behavior during the Amplitude-Period table test, which is depicted in Figure 6.9. The calculation method of the datapoints in the table is as follow:

From the graph of Figure 6.9 two successive data points are selected manually at the two maximums. This part is zoomed in like in Figure 6.10, which acts as an example of determining 1 data point. One data point is selected at the minimum which is between the two successive maximums. The surge of the two maximums are averaged and the surge of the minimum is subtracted. Where after the period time is calculated using the time between the two successive maximums.

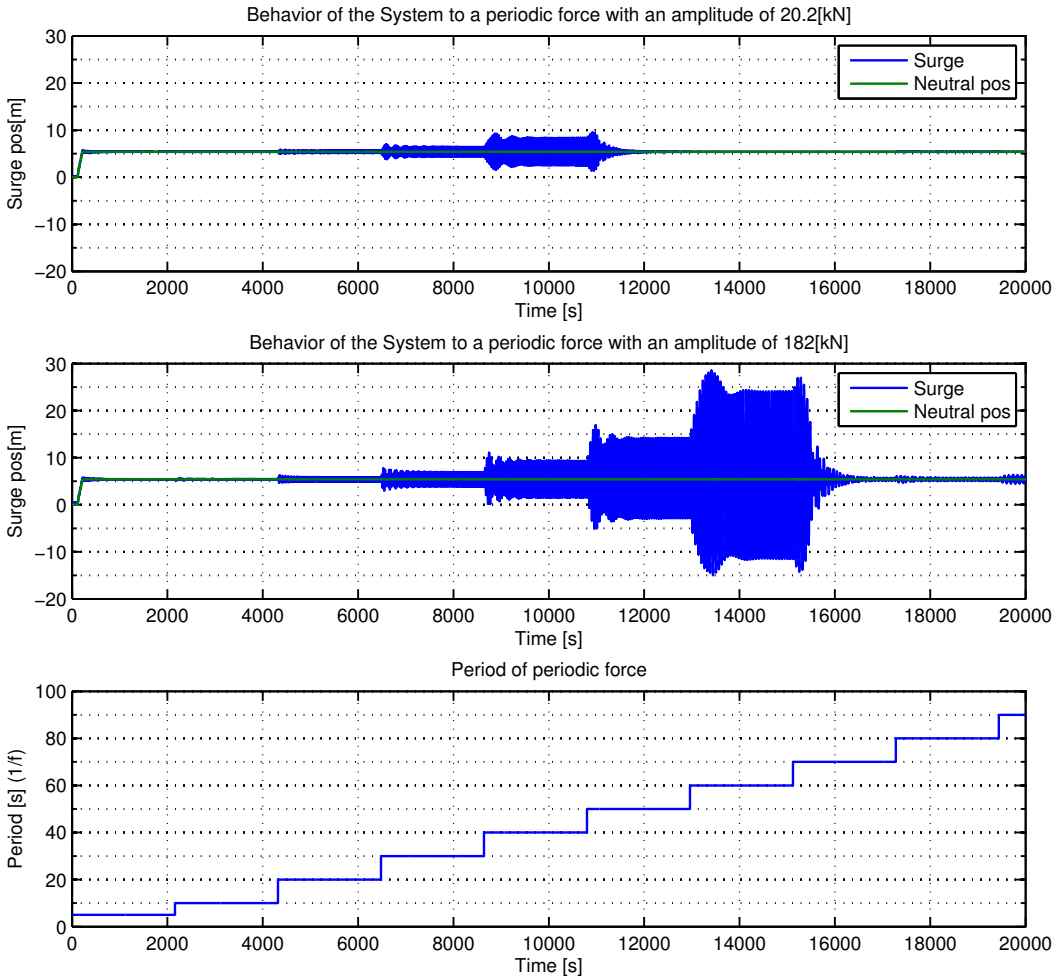

Figure 6.8: Results of the **frequency Response test**.

The values of Figure 6.10 are used for the following calculation example:

Data point	Max	Min	Max
t =	1112	1139	1164
Surge =	13.67	-1.742	12.16

$$A = 0.5(0.5(13.67 + 12.16) - (-1.742))$$
$$A = 7.33[m]$$
$$P = 1164 - 1112$$
$$P = 52[s]$$

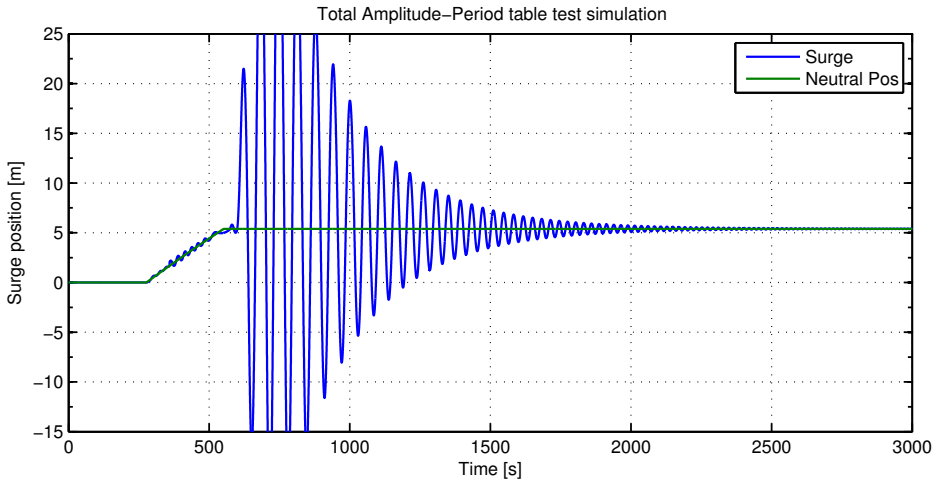

Figure 6.9: **Amplitude-Period table test** total simulation

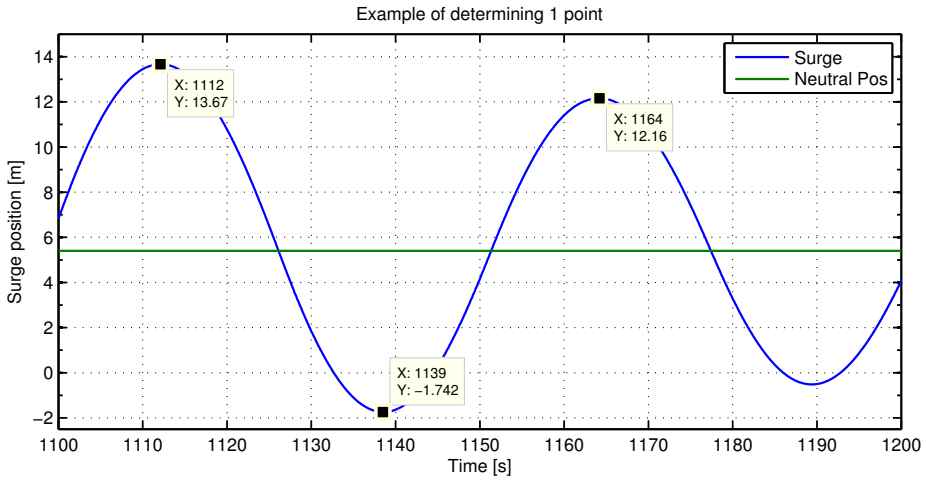

Figure 6.10: An example of determining 1 point for Table 6.5

Surge amplitude [m]	**period of oscillation [s]**
0.030	13
0.069	16
0.114	18
0.199	21
0.514	27
0.943	31
1.727	36
3.061	43
6.045	50
11.15	57
18.03	62
24.11	64

Table 6.5: Surge oscillation period points as a function of surge amplitude measured in the Amplitude-Period table test

Now a theoretical explanation is searched for the non linearity.

6.2.2. THEORETICAL ANALYSIS OF NON LINEARITY OF THE SYSTEM

In Section 6.2.1 is shown that in the simulation environment the oscillation frequency of *the System* is a function of the surge amplitude. Now the question rises: "Why is *the System's* relation between surge deviation and horizontal force non linear, if the cable force is implemented linearly and the angles are small?" The validity of the simulation model is in doubt if no answer is found to this question. A very thorough study is necessary to give the complete answer to the latter question, but in this section a simplistic approach is followed to show that a non linearity between surge deviation and horizontal mooring stiffness force theoretically exists.

The System is a system with different kind of dynamic mechanisms interfering with each other. When the vessel moves horizontally, a mooring stiffness force is induced. This force will pose a moment on the vessel where the vessel rolls or pitches. In this analysis only pitching of the vessel is studied. Suspected is that the change of the mooring stiffness shown in Section 6.2.1, i.e. the non linear relation between surge deviation and horizontal force, is due to coupling of the pitch motion of the vessel with the horizontal forces.

This is examined by finding an expression for the horizontal force (X) as function of the surge position (Δx). By deriving this expression the coupling of the pitch(θ) to the horizontal force(X) is studied. In Figure 6.11a a sketch is depicted of the forces in the tip of the crane and in Figure 6.11b a sketch is depicted of the geometries of the vessel and crane.

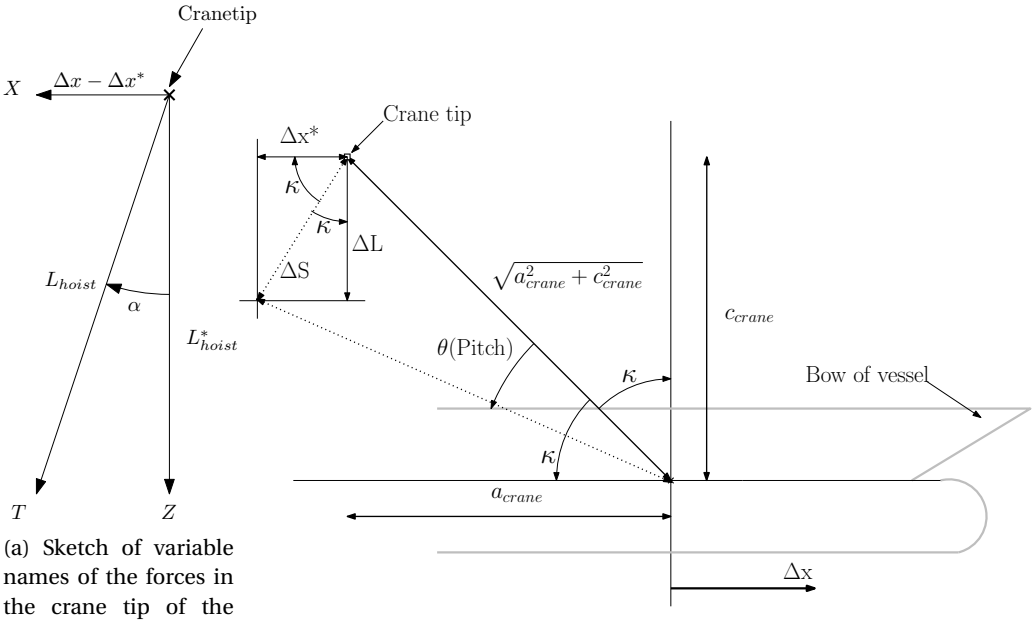

(a) Sketch of variable names of the forces in the crane tip of the heavy lift vessel

(b) Sketch of the variable names of the vessel's geometries

Figure 6.11: Sketch of the used variable names in this analysis

In this analysis the following simplifications are done:

1. α is small
2. $a_{crane} = c_{crane}$
3. $\theta(pitch)$ is small

RELATION BETWEEN X,Z,T AND Δx

First the relation between X, Z, the cable tension T and the surge deviation Δx is examined. Let's consider the forces on the tip of the crane as sketched in Figure 6.11a. Because of simplification 1 the following can be stated:

$$Z = T \tag{6.4}$$
$$L_{hoist} = L^*_{hoist} \tag{6.5}$$
$$X = sin(\alpha)T \tag{6.6}$$
$$\alpha = \frac{X}{T} \tag{6.7}$$
$$\alpha = \frac{\Delta x - \Delta x^*}{L_{hoist}} \tag{6.8}$$

Substituting α with equation 6.7 and 6.8 results in:

$$X = \frac{T \cdot (\Delta x - \Delta x^*)}{L_{hoist}} \tag{6.9}$$

THE CHANGE OF POSITION OF THE CRANE TIP DUE TO PITCHING OF THE VESSEL (θ)

The following relation is valid due to the Simplification 3:

$$sin(\kappa) = sin(45) = \frac{1}{\sqrt{2}} \tag{6.10}$$
$$\Delta x^* = \Delta L \tag{6.11}$$

The following relation is valid due to the simplification 2

$$\Delta S = sin(\theta)\sqrt{a^2_{crane} + c^2_{crane}} \tag{6.12}$$
$$\Delta S = \theta\sqrt{2}a_{crane} \tag{6.13}$$
$$\tag{6.14}$$

Consequently, the distance of the crane tip downward due to pitching of the vessel is:

$$\Delta L = sin(\kappa)\theta\sqrt{2}a_{crane} \tag{6.15}$$
$$\Delta L = \theta a_{crane} \tag{6.16}$$

THE MOMENT EQUATION IN PITCH ROTATION DIRECTION

The moment M, around the y-axis(pitch rotation axis) due to the restoring force by the hydrostatics:

$$M = \rho g \nabla \overline{GM_L}\theta \tag{6.17}$$

And due to the forces X and Z in the tip of the crane:

$$M = a_{crane} \cdot Z - c_{crane} \cdot X \tag{6.18}$$
$$M = a_{crane}(Z - X) \tag{6.19}$$

THE CHANGE OF POSITION OF THE CRANE TIP ΔL, DUE TO OTHER EFFECTS

Let's observe ΔL, the change of crane tip position in downward direction, due to other effects than pitching. ΔL is limited by the crane cable if the hoist cable is pulled taut. During the moored stage a change of ΔL can be due to the following two effects:

1. Strain of cable
   Now let's consider ΔL due to the strain in the hoist cable. With the used simulation parameters from Appendix B, a load of 4000[t] will cause a strain of the cable of 0.19 [m]. Furthermore, the tension in the cable is approximately constant during surge oscillation. Consequently, ΔL due to strain of the cable will be negligible.

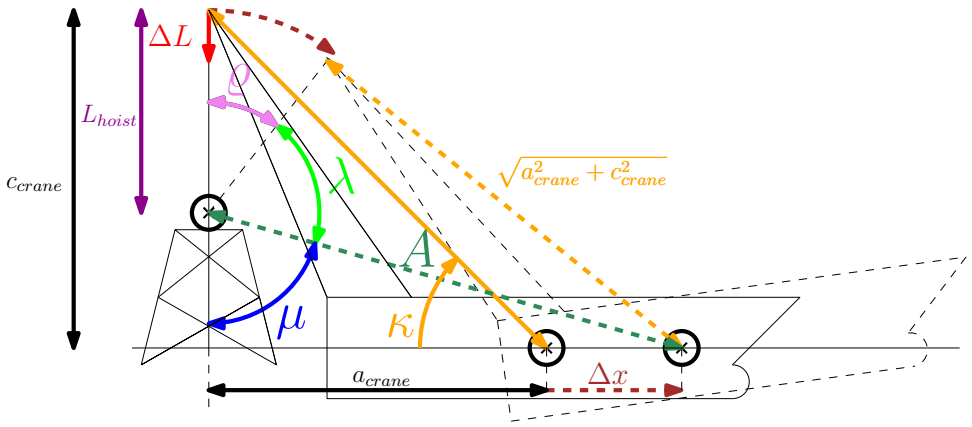

Figure 6.12: Variables for geometric analysis of relation between Δx and ΔL

2. Geometric relation between Δx and ΔL
   The following equation holds due to Assumption 2:

$$\sqrt{a_{crane}^2 + c_{crane}^2} = \sqrt{2}a_{crane} \tag{6.20}$$

Because of Equation 6.10, the following equation holds:

$$A = \sqrt{(\sqrt{2}a_{crane} - L_{hoist})^2 + (\sqrt{2}a_{crane} + \Delta x)^2} \tag{6.21}$$

Furthermore,

$$\mu = tan^{-1}\frac{\sqrt{2}a_{crane} + \Delta x}{\sqrt{2}a_{crane} - L_{hoist}} \tag{6.22}$$

Applying the cosine rule:

$$\lambda = cos^{-1}\frac{-(\sqrt{2}a_{crane})^2 + A^2 + L_{hoist}^2}{2AL_{hoist}} \tag{6.23}$$

Consequently,

$$\rho = 180 - \lambda - \mu \tag{6.24}$$
$$\Delta L = L_{hoist} - cos(\rho)L_{hoist} \tag{6.25}$$

Finally, calculating ΔL by using the the geometric relations between Δx and ΔL lead to a negligible value. I.e. Δx between -10 and 10 meters lead to maximum ΔL of 0.05[m] at -10[m] for the vessel parameters in Appendix B.

With the use of Equations 6.16 and 6.17, a load of 4000[t] and the parameters of Appendix B a value of ΔL of 5.8[m] is obtained. Furthermore, as concluded in points 1 and 2 other effects to ΔL are negligible. Consequently, ΔL is a constant value of 5.8[m].

FINALLY, OBTAINING AN EXPRESSION FOR THE HORIZONTAL FORCE AS FUNCTION OF SURGE AMPLITUDE

Next θ is substituted combining Equation 6.17 and 6.16.

$$M = \frac{\rho g \nabla \overline{GM_L} \Delta L}{a_{crane}} \tag{6.26}$$

An expression is obtained based on Equation 6.19 by substituting M with Equation 6.26, X for Equation 6.9 and Z for Equation 6.4. After rearranging the terms the following equation is obtained:

$$X = \frac{\rho g \nabla \overline{GM_L} \Delta L}{a_{crane}^2 (L_{hoist} - \Delta x - \Delta L)} (\Delta x - \Delta L) \tag{6.27}$$

CONCLUSION

Let's focus on Equation 6.27, this is an expression in the form of:

$$X = \frac{C_1}{C_2 - \Delta x} (\Delta x - C_3) \tag{6.28}$$

Of which $C_1, C_2 and C_3$ are constant values. Consequently, $\frac{C_1}{C_2 - \Delta x}$ is the mooring stiffness which is a function of Δx. Hereby is concluded that the relation between surge deviation and horizontal force is non linear because of coupling of the pitch motion of the vessel with the horizontal forces. With ΔL of 5.8[m] and the parameters of the simulation model as is described in Appendix B, the relation between F_X and Δx is plotted in 6.13.

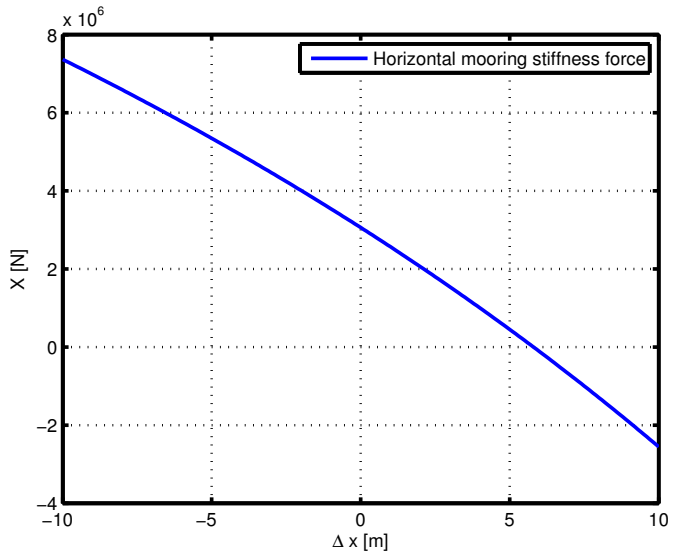

Figure 6.13: Horizontal force as function of surge deviation

6.3. POOR PERFORMANCE OF FF SOLUTION CANDIDATE(1)

The results in Section 6.1.2 show that the Feed Forward(1) solution candidate performs poorly. This is contrary to the results in literature [Waals, 2010], which show promising performance of feed forward of mooring stiffness forces. Where does the difference between literature and simulation results come from?

When inspecting the performance of the Feed Forward candidate(1) in Figure 6.5 one can see that the thruster reserve Ψ_{surge} is very low compared to the well performing Kalman candidate. This means that at least one thruster is applying maximal thrust most of the time. This seems to indicate that the thrusters are the lacking factor of the feed forward solution candidate. The following hypothesis is posed:

> The Feed Forward solution is a good solution in theory, but for realistic heavy lift vessels it does not work, as the mooring stiffness forces feed forward demand can't be achieved by realistic thrusters.

This hypothesis is analyzed by doing the following two simulation tests:

1. **Simplified thruster model test**
   A simple model of the thrusters is used to test whether or not the thrusters can satisfy the demand of the mooring stiffness forces feed forward during normal operating conditions. If this is not the case it can be concluded that the mooring stiffness forces feed forward demand can't be achieved by realistic thrusters.

2. **Conceptual working test**
   This simulation is conducted to test whether the Feed Forward solution performs well conceptually. A Seastate test is conducted with the Feed Forward candidate(1) just like in phase 2 of the scoring strategy, but now with unrealistic high performance thrusters and rudders. If the Feed Forward candidate(1) performs well with the unrealistic thrusters and rudders, it can be concluded that the FF solution candidate is a good solution conceptually.

6.3.1. SIMPLIFIED THRUSTER MODEL TEST

For this test, first a mooring stiffness force profile is to be chosen which represent normal operating conditions. The performance of the Kalman solution candidate(2) is assumed to be adequate. Consequently, the mooring stiffness force profile during a simulation with the Kalman solution should represent the normal operating conditions. This is why the simulation of the vessel during the Seastate test with Kalman solution candidate(2) is chosen which was depicted in Figure 6.5. The mooring stiffness force profile is selected from t= 1600[s] to t=1650[s] because it is in mid simulation so no extraordinary effects are taking place during this time range. The chosen force profile of mooring stiffness forces via the crane is shown in Figure 6.14.

A simple thrust model is created which imitates the Imtech thruster model, and afterwards this thruster model is used to observe whether or not the mooring stiffness force profile can be fed forward by the thrusters. In other words, the model is used to observe whether or not the mooring stiffness force profile can be counteracted by the thrusters. Next, the simple model of the thruster is discussed.

SIMULATION SETTINGS

First the variables are defined and then the thruster model is given.

Variables	Meaning of variable
A_{RPM}	Thruster amplitude[%rpm]
Acc_{RPMmax}	Maximal thruster acceleration in [%rpm/s]
$X_{Thruster}$	Thrust produced by thrusters [kN]
$X_{Thruster,max}$	maximum force by thrusters at 100% rpm [kN]
X_{Crane}	Force on vessel via crane
dt	Time step

The control law for the thrusters in this simple model is to just follow the mooring stiffness force profile. So X_{Crane} is to be followed by $X_{Thruster}$. The limiting factors which contribute to a difference between setpoint and true thrust are due to maximal thruster acceleration[%rpm/s] and the maximal thruster force at 100% rpm [kN].

The thruster control is programmed to feedforward the mooring stiffness forces, so

the thrusters are modeled by the following rules:

$$
\begin{aligned}
&if(X_{Crane} > X_{Thruster}\ AND\ A_{RPM} < 100\%)\\
&A_{RPM} = A_{RPM} + Acc_{RPMmax} \cdot dt\\
&elseif(X_{Crane} > X_{Thruster}\ AND\ A_{RPM} > -100\%)\\
&A_{RPM} = A_{RPM} - Acc_{RPMmax} \cdot dt\\
&end\\
&X_{Thruster} = sign(A_{RPM}) \cdot X_{Thruster,max} \cdot (A_{RPM}/100\%)^2
\end{aligned}
$$

The maximal thruster acceleration is 5[%rpm/s] and the maximum thruster force produced at 100[% rpm] is $X_{Thruster,max} = 466[kN]$. These values are taken from the simulation model, as described in Appendix B. $dt = 0.1$[s]. Furthermore, two extra simulations are performed with a maximal thruster acceleration of 20[%/s] and 50[%/s] to show what the effect would be when the maximal thruster acceleration is increased. The results can be seen in Figure 6.14.

RESULTS

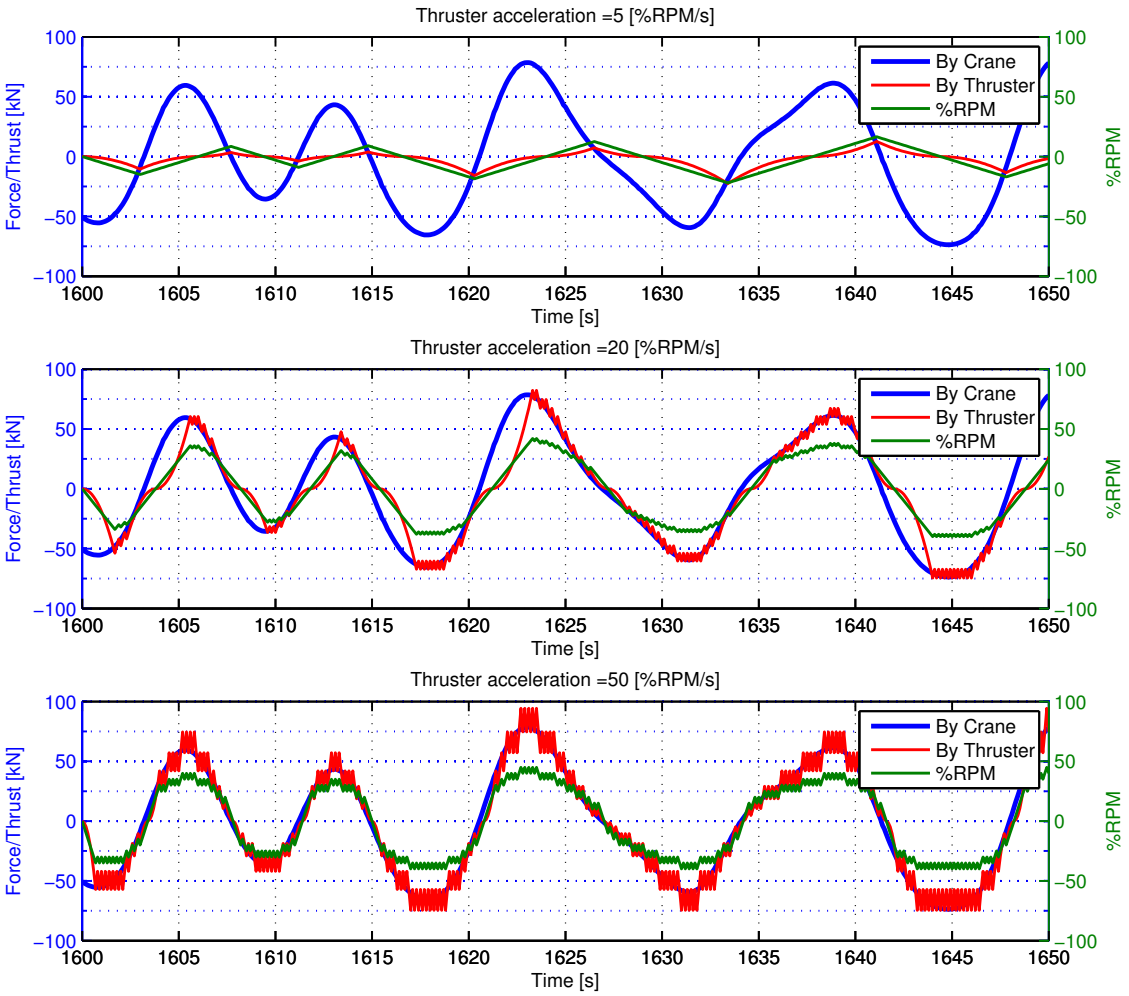

Figure 6.14: Tests with a simplistic thruster model with different thruster acceleration rates.

The figure shows that the performance of the thrusters with a maximal thruster acceleration of 5[%rpm/s] is very poor. The thrusters can't deliver the demand of the mooring stiffness forces feed forward at all. With a maximal thruster acceleration of 20[%rpm/s] the performance is already much better, but with a maximal thruster acceleration of 10 times the original maximal thruster acceleration, $10 \cdot 5[\%/s] = 50[\%/s]$, the thrusters can follow the mooring stiffness forces perfectly.

From this, we conclude that the thrusters indeed can not satisfy the demand of the mooring stiffness forces feed forward during normal operating conditions. The limiting factor is thruster acceleration and not maximal thruster force. Another thing to note is that apparently the maximal thrust of the thrusters is not a limiting factor during this operation.

6.3.2. CONCEPTUAL WORKING TEST

Now to test whether the feed forward solution is conceptually a good solution, a simulation test with Feed Forward solution candidate(1) is conducted but now with unrealistic fast responding thrusters and other actuators. The maximal thruster forces are unchanged.

SIMULATION SETTINGS

In this simulation with unrealistic fast thrusters the simulation settings are according to the Seastate test general simulation environment described in 5.4.

The unrealistic fast responding thrusters and other actuators are implemented as follows. The maximal thrust acceleration of main thrusters, bow thrusters, stern thrusters and finally the maximal rudder rate in degrees per seconds are multiplied by 20. Also any of the controllable pitch propellers limitations are removed. This means that the acceleration of the main actuators of the vessel is twenty times as high.

RESULTS

The results are shown in Figure 6.15 and the values for the scoring measures can be seen in Table 6.6. In this table, the measures of the Feed Forward candidate(1) with unrealistic fast thrusters are compared to the Feed Forward candidate(1) and the Kalman candidate solution from phase 2 of the scoring strategy.

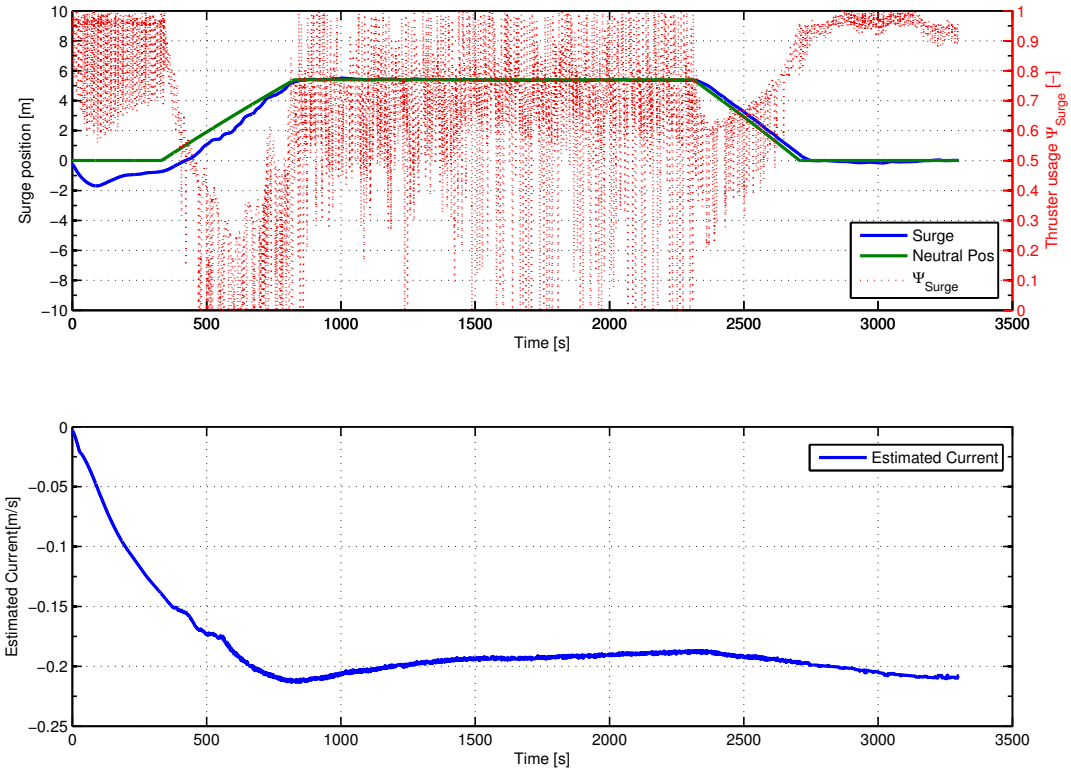

Figure 6.15: FF solution candidate with unrealisticly fast thrusters during Seastate 3 test.

		FF Solution*	FF Solution**	Kalman Solution
$\Delta p_{x,mean}$ (moored)	[m]	0.11	1.88	0.05
$\Delta p_{x,max}$ (moored)	[m]	1.04	3.93	0.26
$\Delta p_{x,mean}$ (free floating)	[m]	0.07	2.31	0.03
$\Delta p_{x,max}$ (free floating)	[m]	0.40	8.40	0.12
u_{mean}	[m/s]	0.004	0.030	0.017
Ψ_{mean}	[-]	0.71	0.26	0.90
I_{mean}	[m/s]	0.20	0.41	0.13
X_{mean}	[kN]	48.4	716	27.4

Table 6.6: The values of measures for scoring solution candidates. *=With unrealistic fast actuators, **=Normal actuators, values from Section 6.1.2.

The Feed forward candidate(1) with unrealistically fast thrusters show acceptable performance in general. The figure shows that the performance is the worst when the current is not still estimated well, however, after the current is estimated precisely the surge is quite steady. The current stabilizes around 0.2 [m/s] which is correct. Although the performance of the feed forward candidate is good, the Kalman solution candidate(2) performs better in all measures except for the measure u_{mean}. In this simulation u_{mean} is the lowest of all simulations. This is explained by the fact that feedforwarding of the mooring stiffness forces will decrease the effective spring stiffness as was explained in Section 4.3.

CONCLUSION

The theory from the paper [Waals, 2010] of feedforwarding the mooring stiffness forces is the basis of the Feed Forward candidate(1). This candidate showed poor performance in phase 2 of the scoring strategy. This section proved that the thrusters can't follow the fast fluctuating mooring stiffness force profile during normal operating conditions. This is because the maximal thruster acceleration is too low. When the maximal thruster acceleration is a factor 10 higher the thrusters can follow the mooring stiffness force profile adequately.

The aforementioned is used to try to prove the conceptual functioning of the Feed Forward candidate. For this reason, the maximal thrust acceleration of all thrusters and the maximal rudder rate are multiplied by twenty. With this the candidate solution with unrealistic fast actuators show adequate performance, but generally not better than the Kalman solution candidate(2). With this, we conclude that the solution is a good solution in theory but not in reality because the thrusters have to be much faster than is realistic.

With this, the hypothesis at the beginning of this section is proven to be correct.

6.4. POOR PERFORMANCE OF FILTERED SOLUTION CANDIDATE(4)

The results in Section 6.1.2 show that the Filtered candidate solution(4) performs poorly. In this section, is of the reason for this poor performance is analyzed.

To analyze the poor performance in Section 6.1.2, the behavior during the Seastate test in phase 2 of the scoring strategy is studied. The true horizontal force in surge direction and the Filtered horizontal force in surge direction are plotted in Figure 6.16. The time range is between t=200[s] and t=1200[s].

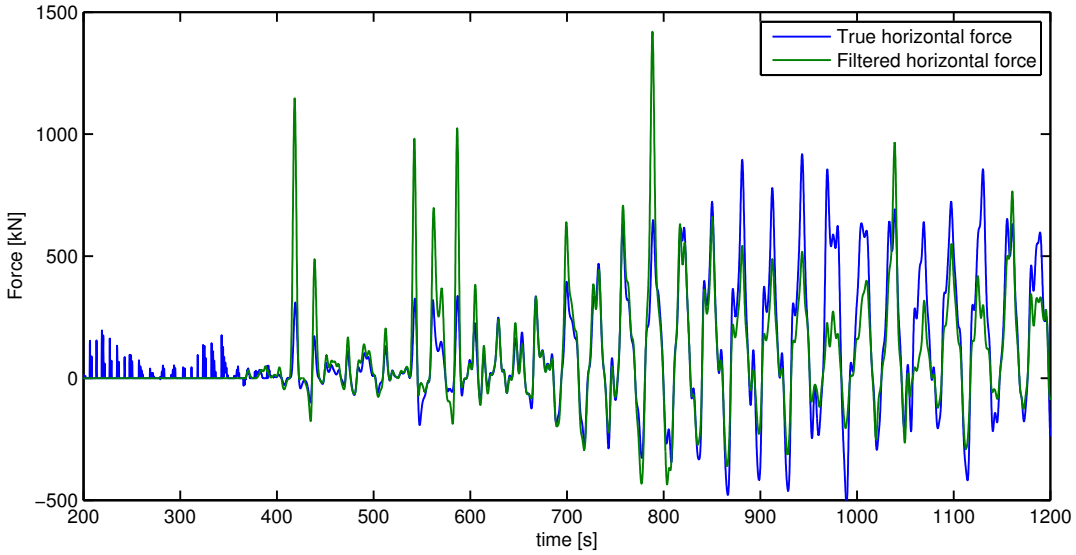

Figure 6.16: True versus filtered horizontal force in surge direction

The idea of the Filtered solution candidate(4) is that the fast fluctuating part of the mooring stiffness force is periodic due to roll and pitch motion of the vessel. It is not necessary to counteract this periodic part of the force by the thrusters directly because the net force is zero. So the periodic part of the force must be filtered out to prevent the thrusters from being overloaded. The idea is to do this cleverly by not filtering the final estimated force because this would introduce a delay to the estimation of the mooring stiffness forces. But by filtering the roll and pitch states by a low pass filter before these states are used for estimating the mooring stiffness forces. So the horizontal x and y

positions are not filtered before calculating the mooring stiffness forces. This should result in less lag introduced by filtering in the estimation of the mooring stiffness forces.

Figure 6.16 shows that the filtered solution candidate(4) does not succeed in filtering the fast fluctuating part and obtaining a slower transient behavior. On the contrary, the filtered force is sometimes even larger than the true force, especially between time instances t=400[s] and t=800[s]. Section 6.2 describes that the mooring stiffness decreases when the surge oscillation amplitude increases. The relaxation of the mooring stiffness is theoretically explained and attributed to pitch and surge interaction. The filtered forces can even be larger because due to filtering of the pitching the relaxation of the mooring stiffness. Therefore the solution candidate is effectively not working hence this candidate is not further studied.

In the next chapter the results in this chapter are further discussed.

7

Discussion, Conclusion and Recommendations

As already mentioned in the previous chapter, to help improve the understanding of Chapter 6 and this Chapter, the following two dynamic systems are defined here:

1. *the System*
   Which is the heavy lift vessel with a crane in moored stage. In other words, the heavy load is rigidly attached on the jacket as depicted in Figure 3.2b.

2. *the System+DP*
   Which is *the System* of point 1, with the DP system enabled. So the DP system is also applying forces to the heavy lift vessel by means of its thrusters.

In section 7.1.1 the validity of the results is discussed by pointing out possible flaws in the study and results are criticized.

Using this information a further analysis of the stability of the System+DP is done in section 7.1.2, answering the following two questions:

- Can the instable point of the mooring stiffness problem which is found in section 6.1.1) theoretically and quantitatively be estimated?
- Is the Kalman solution candidate(2) always stabilizing the system+DP which is modeled?

With all results, theory and analyses there is discussed whether the goal is achieved of solving the mooring stiffness problem. Which the answer is, yes and no. This elaboration of the results lead to recommendations to further studies in section 7.2. After that conclusions are wrapped up in section 7.3.

7.1. Discussion

7.1.1. Limitations of the methods

The following limitations and remarks have to be discussed:

- As already mentioned, the Imtech DP controller is implemented in vessels all over the world and therefore it can be assumed it is very well developed. The Imtech vessel model however, is only used for in-house testing and developing the Imtech DP controller. Although the model is verified with the use of scale model tests, it is not guaranteed that the model is meeting reality. Also the Imtech model has been a 'gray box' for the author of this thesis, as the author has been aware of the

general working of the model but not the exact details. Possibly the hydrodynamic model is not very accurate, especially for maneuvering. Furthermore thruster-hull interaction and changes in hydrodynamic damping are probably not included.

It had to be remarked in this section that the author have been relying on the correctness of the vessel model, without checking every detail. However, this is not considered as a problem because the qualitative results in this study are not relying on an accurate vessel model. If the hydrodynamic damping would be, lets say, twice as much in real life. The general qualitative conclusions are still valid. Probably some numerical values obtained in this study are different but the relations are still the same. Furthermore the main reason for making a simulation model was to compare the the solution candidates. The candidates are compared using the same model and consequently the results will be still valid if the vessel model is not correct.

- As explained in Section 2.3, the Imtech DP controller is outfitted with a model of the vessel. This model is used, among other things, to calculate the thruster settings belonging to a certain control action. Due to an error a deviation in the modeled thrusters existed, between the DP controller and the vessel model. This deviation between the thruster models existed during all simulations in this report, except in the simulation in Section 6.3.2 where this difference is removed. The only difference was that the thrusters in the vessel model produce 1.27 times as much thrust(i.e. Force in Newton) than was assumed by the DP controller model. The difference in the models became apparent when the conceptual working of the *FF solution* candidate was tested with unrealistic fast thrusters, in Section 6.3.2. With the difference in the models the performance was poor, and without the difference in the models the performance was adequate as described in Section 6.3.2.

  Although this was because of an error in the settings in the DP software, it is not changing any of the conclusions of this study. Furthermore in real life also differences between the true vessel and a model exist. So the difference in the thruster models can be realistic and can be used to note something about the robustness of the controller to modeling errors.

  The first note on robustness is that the Kalman Solution conceptual solution is showing good performance with this difference in thruster models. The second note is that the Kalman solution candidate(2) is more robust against modeling errors than the Feed Forward solution candidate with unrealistic fast thrusters as described in Section 6.3.2.

- Let's consider the *Feed Forward Gain* which is depicted in Figure 4.2. The *Feed Forward Gain* gain is used for decreasing the mooring stiffness force feed forward in the Corrected solution candidate(3). Until now is assumed that for the Feed Forward solution candidate(1) and the Filtered solution candidate(4) a *Feed Forward Gain* of 1 is used(i.e. the mooring stiffness forces are 100% fed forward). But during simulations the performance of candidates 1 and 4 was very poor, therefore is chosen to try and increase the performance. Consequently, the *Feed Forward Gain* is decreased to 0.64 for candidates 1 and 4 (i.e. only 64% of the mooring stiffness is fed forward). It was expected with this new *Feed Forward Gain* the performance would increase because the thrusters can better follow the reduced feed forward control law.

  To summarize the latter paragraph, in all simulation tests regarding the solution candidates 1 and 4 in this report the *Feed Forward Gain* of 0.64 is used. Except in the simulation in Section 6.3.2 of which a *Feed Forward Gain* of 1 is used.

  In Sections 6.3 and 6.4 is studied why the candidate solutions 1 and 4 performed poorly. With this knowledge can be concluded that decreasing the *Feed Forward*

Gain did not contribute to the poor performance hence the lowering of the feed forward gain does not change any of the conclusions in this thesis.

7.1.2. STABILITY ANALYSIS OF THE SIMULATION MODEL *with vs without* KALMAN SOLUTION

This section will discuss the results presented in Chapter 6. In the results of Section 6.1.1 it was shown that there is a certain surge amplitude for which *the System+DP* becomes instable. For the heavy lifting industry it could be interesting to know when this instability is commenced. Furthermore *the System+DP* with the Kalman solution candidate(2) initiated showed good and stable performance. Here it is interesting to know whether the Kalman solution candidate(2) is guaranteeing stability. For example to make a better choice whether the Kalman solution is worth to be further developed. Therefore an analysis is conduced in this section on stability of the of *the System+DP* for two cases, i.e. with and without the Kalman solution candidate(2). The goal of this section is to answer the following questions:

- Can the surge amplitude for which *the System+DP* becomes instable, which is obtained in Section 6.1.1, be theoretically determined? If so, for what surge amplitude does *the System+DP* become instable in theory?
- Can it be guaranteed that the Kalman solution candidate(2) is stabilizing *the System+DP*?

The analysis will be done for the heavy lift vessel which is modeled in this report. So the results of the analysis in this section are valid for only this vessel. But this analysis gives more results, as a qualitative analysis method for answering this questions for other heavy lift vessels is obtained. Furthermore it was already elaborated in general why the Kalman solution should increase the performance in Section 4.4.2. But after the analysis more qualitative insights are obtained.

THE DP SYSTEM FEEDBACK LOOP

Prior to the stability analysis a small recapitulation and an overview of the nomenclature of the DP system is presented (See Figure 7.1). As already explained the Kalman filter ob-

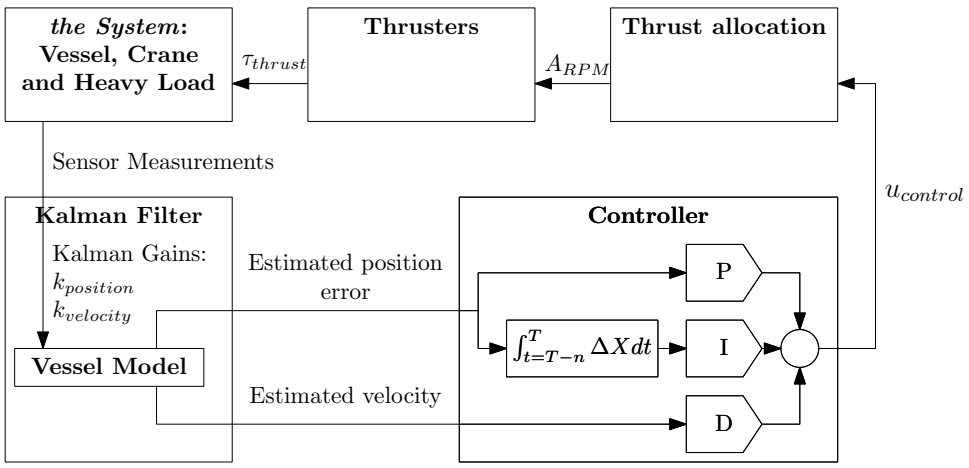

Figure 7.1: Feedback loop of DP system

tains sensor information and uses this, together with a model of the vessel, to determine the motion of the vessel. The Kalman gains are used to choose whether to give more emphasis to sensor information or to model information, depending on which information is the most trustworthy. The PID controller obtains velocity and position information

from the Kalman filter and determines the control action by summing the calculated proportional, integral and derivative parts. After that the control action ($u_{control}$) is sent to the thrust allocation. The allocation will calculate the amplitude in RPM (A_{RPM}) to be delivered by the thrusters. The thrusters will apply the requested thrust force(τ_{thrust}). The vessel will accelerate due to this thrust force where after the motion is sensed by the sensors. And finally, being back to the sensor information again, the feedback control loop is closed.

STABILITY CRITERION

Now the criterion of stability for *the System+DP* is discussed which is used in the stability analysis. This criterion is based on the fact that *the System+DP* is stable by all means when the net energy (i.e. Kinetic and potential) is zero or negative. Please follow the following thought experiment.
In this thought experiment the energy to or from *the System+DP* is observed to obtain the stability criterion. First two simplifications are made:

1. *The System+DP* only motion is the oscillating in the frequency of its own oscillation frequency.
2. There is no force adding/subtracting energy to/from *the System+DP*, other than the thrusters. Hence the damping of the System+DP by viscous damping is neglected.

Now some variables are defined which are used in this analysis.

Variables	Unity and description
A_{RPM}	Thruster amplitude[%rpm]
$X_{Thruster}$	Thrust produced by thruster [kN]
P	Power to the system [W]
u	Velocity in surge direction [m/s]
Δx	Surge position offset [m]
Φ	lead or lag period [s]
ϕ	lead or lag factor [°]

In this thought experiment the thrust is quadratic dependent on the surge deviation Δx as is described in Equation 7.1. The thrust reacts only to the surge position offset as if only the proportional part of the controller is activated. A lead or lag in the thrust w.r.t. the surge deviation is introduced if $\Phi \neq 0$.

$$X_{Thruster}(t-\Phi) \propto -\Delta x^2(t) \tag{7.1}$$

The instantaneous power to or from the system due to the thrusters is defined as:

$$P(t) = u(t) \cdot X_{Thruster}(t-\Phi) \tag{7.2}$$

In control theory periodic motion is analyzed in degrees of phase, of which 360 ° is one period. When is spoken about 30 degrees phaselag, is meant a lag of 30/360 of one period in seconds.

Now, in this thought experiment the net power to or from the system is analyzed in the following situations:

- The thrust is leading nor lagging w.r.t. the surge deviation ($\phi = 0°$)
- The thrust is lagging w.r.t. the surge deviation ($\phi = -30°$)
- The thrust is leading w.r.t. the surge deviation ($\phi = 30°$)

To analyze the net power the instantaneous power is plotted as function of time in Figure 7.2. Also the other variables are ΔX, u ,$X_{Thruster}$ are plotted to observe the relationships of equations 7.1 and 7.2

After observing Figure 7.2 it becomes clear what happens to the net power to *the System*. With a phase of 0 degrees the power to the system is equal to the power from the

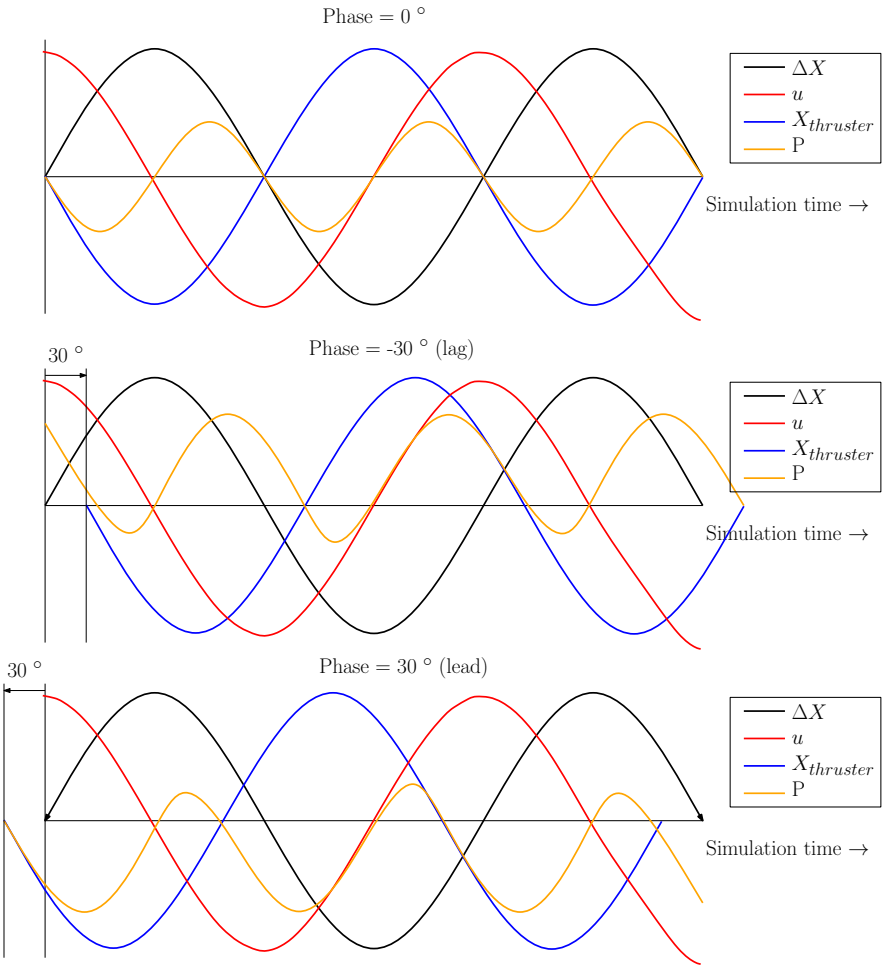

Figure 7.2: Power to or from system comparison with 30° phase lead, 0° phase lag and 30° phase lag between thruster force and position offset.

system, hence the net energy in the system will be constant. When the phase is negative (lag) the average power to the system is larger than the power from the system, so a increase in energy of the system will be the fact. For a positive phase (lead) the other way around.

The second simplification can not be made in real life. So *the System+DP* is not instable by definition if the phase of the open loop from sensor measurements to $X_{thruster}$ is negative. As there is also dissipation for example by hydrodynamic damping. Furthermore, this analysis is only valid for a phase $\phi > -180°$ and $\phi < 180°$.

Now the thought experiment is concluded and the stability criterion is obtained. If the phase of the open loop from sensor measurements to $X_{thruster}$ is positive, the net energy to the system by the thrusters is negative, so *the System+DP* is stable. If the phase is negative, the net energy to the system by the thrusters is positive. Consequently *the System+DP* is possibly instable.

STABILITY ANALYSIS

Now with the stability criterion in mind a stability analysis is done for *the System+DP*, by analyzing the lead or lag of all components of the DP System. The following components are observed:

1. Sensor
2. Kalman Filter

3. Controller
4. Thrust allocation
5. Thrusters

According this numbering, a detailed discussion is following of the phase lead or lag of each component.

1. The sensors are assumed to produce no phase delay. As the update rates are orders higher than the period of *the System+DP*.

2. The phaselag by the Kalman filter is obtained experimentally. For doing so a plot of the true vessel position and velocity from the model and estimated position and velocity from the Kalman filter is obtained.

SIMULATION SETTINGS

For obtaining the phase delay no new simulation test is conducted, but the simulation results from phase 1 of the scoring strategy is used. The results of the test to find the maximal surge amplitude while *the System+DP* is stable is used. (Section 6.1.1 Figure 6.2). For the results of this test a small subsection of the total simulation time is taken, of t=900[s] to t=1000[s]. In this time range *the System+DP* is near instability and therefore this is an interesting point to observed for stability.

RESULTS

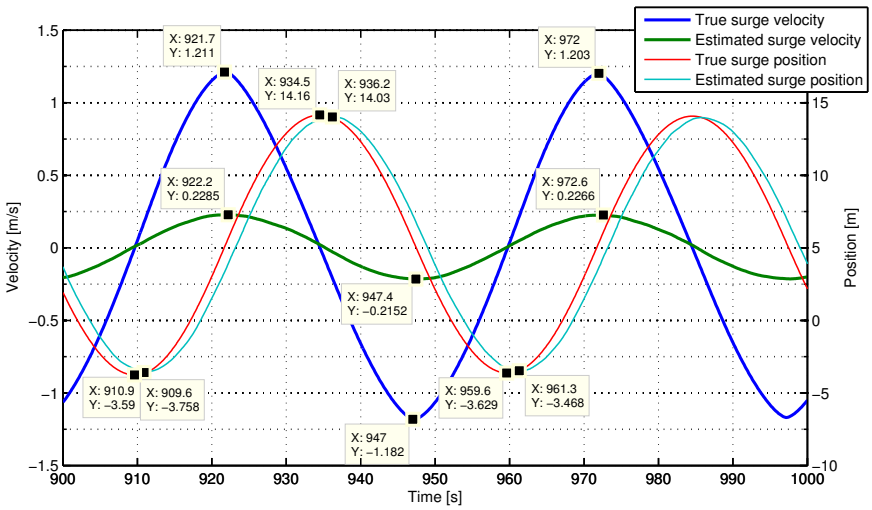

Figure 7.3: Plot of estimated states and true states, for determining the phase lag of the Kalman filter.

In this analysis the following variables are used:

Variables	Unity and description
u_{model}	True surge velocity [m/s]
u_{Kalman}	Estimated surge velocity by the Kalman filter [m/s]
$surge_{model}$	True surge position [m]
$surge_{Kalman}$	Estimated surge position by the Kalman filter [m]

With the data from Figure 7.3 the following terms are calculated:

- Difference in amplitude of u_{model} and u_{kalman}
  $\frac{u_{model}}{u_{kalman}} = \frac{(1.211)-(-1.182)}{(0.229)-(-0.2152)} = 5.39$

- Difference in amplitude of $surge_{model}$ and $surge_{kalman}$
  $\frac{surge_{model}}{surge_{kalman}} = \frac{(14.03)-(-3.468)}{(14.16)-(-3.63)} = 1.017$
- Period
  $T = 972 - 921.7 = 50.7[s]$
- Phaselag between u_{model} and u_{Kalman}
  $\frac{922.2-921.7}{50.7} \cdot 360° = 3.6°$
- Phaselag between $surge_{model}$ and $surge_{kalman}$ $\frac{936.2-934.5}{50.7} \cdot 360° = 12.07°$

In summary, without the Kalman solution candidate(2) the position estimation by the DP system is quite similar to the position of the vessel ($surge_{model} = surge_{kalman}$), but the estimated velocity amplitude by the Kalman filter is 1/5.4 of the true velocity. Furthermore without solution the position and velocity phase lag is estimated to be 4 and 13 degrees. This will be simplified from now as a lag of 10 degrees for both the position and velocity.

With the Kalman solution candidate(2) is assumed that the there is no difference in amplitude and no lag between the surge and velocity of the vessel.

3. The phaselead by the controller is obtained numerically using data from simulation tests. The PID controller was described in Section 3.2 Equation 3.5, as follow:

$$F_P = p\Delta x$$
$$F_I = I\int_{t=T-n}^{T} \Delta x dt$$
$$F_D = D\frac{dx}{dt}$$
$$F_{DP} = F_P + F_I + F_D$$

The proportional control action does not affect the phase. The integral action is assumed to be low such that it becomes only important in a frequency range outside the scope of this analysis. The derivative action is producing phase lead between 0 and 90 degrees.

Figure 7.1 shows that the position and velocity have separate Kalman gain factors. Consequently $u_{kalman} \neq \frac{dsurge_{kalman}}{dt}$ or in other words u_{kalman} and $surge_{kalman}$ are decoupled. In Figure 7.3 can be seen that the amplitude of the estimated velocity is 1/5.4 of the true vessel velocity. Practically this makes the derivative action of the controller 1/5.4th as large as it would have been with true vessel velocity. As already mentioned, with the Kalman solution candidate(2) the differences between estimated and true velocity are assumed to be negligible.

To determine the effect to the phase by the controller a frequency response phase plot of the PID controller is produced for two cases:

(a) For the case with Kalman solution candidate(2), because the velocity estimation is assumed to be perfect the original D-action is used.

(b) For the case without Kalman solution candidate(2), because the velocity estimation is assumed to be 1/5.4th of the true velocity, the effective D-action is also 1/5.4th of the original D-action.

SETTINGS

Variables	Value	Meaning of variable
I	0 [-]	Integral gain
D_{WS}	17.16	Derivative action (from Imtech DP Controller)
D_{WOS}	17.16/5.4	Derivative action without solution

Table 7.1: Settings for frequency response phase plot

RESULTS

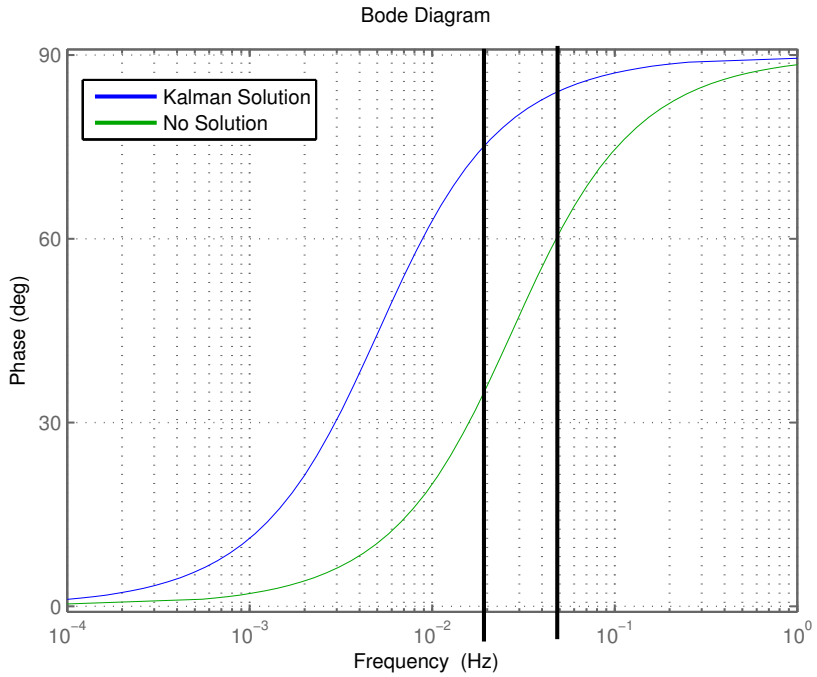

Figure 7.4: Frequency response phase plot. The boundaries of the working area of the controller are illustrated by the two black lines.

The working area of the controller is generally in between a oscillation period of T = 20[s] to T = 50[s] as can be seen in Table 6.5. In Figure 7.4 the following two points are determined.

Period[s]	Frequency [1/s]	Phase lead WOS [deg]	Phase lead WS [deg]	Difference WS-WOS [deg]
20	0.05	61.1	84.2	23.1
50	0.02	36.0	75.7	39.7

Table 7.2: Calculated phaselead with and without solution at working area of controller. (WS=With solution WOS=Without Solution)

Due to the poorly estimated velocity by the Kalman Filter, the effective D-action in the case of no solution is 1/5.4th of the original D-action. The result is a different phase lead by the controller. Within the working area of an oscillation period of 20[s] to 50[s], the increase in phaselead when the solution is implemented is between 23.1 to 39.7 [degrees].

4. Assumed is that no phase lag is in the thrust allocation.

5. The thruster lag is analyzed by doing a simplified analysis of the thrusters. A thruster phase lag is introduced when the thrusters can't achieve the requested control action. Now an expression is found for when this is the case.

   In this section is assumed that the oscillating surge motion of*the System+DP* is a neat sinusoidal motion. Suppose *the System+DP* is in oscillation with such an

amplitude that the thrusters oscillate from -100 [%rpm] to +100 [%rpm]. In one period oscillation thrusters have to accelerate and decelerate from 0 to -100 to +100 to 0 [% rpm], which is 4 times 100 [%rpm] acceleration and deceleration. In the Imtech vessel model the thrusters have a constant maximum thruster acceleration of 5 [% rpm/s]. Now one can calculate the minimum time which is needed for the thrusters to be able to accelerate to the maximum and minimum requested thruster RPM in time:

$$4 \cdot \frac{100[\%RPM]}{5[\%rpm/s]} = 80[s] \tag{7.3}$$

Now the situation sketched above is generalized to further analyze the phase lag by the thrusters:

Variables	Unity and description
$A_{RPMrequested}$	Thruster amplitude requested by controller[% rpm]
$A_{RPMdelivered}$	Thruster amplitude which is delivered by thrusters[% rpm]
P	Period time in [s]
Acc_{RPMmax}	Maximal thruster acceleration in [% rpm/s]
Δx	Position error of the vessel in [m]
$\phi_{Thrusters}$	Phase lag due to thrusters [degrees]
p*	Proportional gain of controller [% rpm/m], to be mathematically correct this proportional gain is different from the proportional gain described in Section 3.2 Equation 3.5 because the thruster capabilities are already included in this proportional term p*

The thrusters can't follow the control demand and a phase lag is introduced if the minimum time which is needed for the thrusters to follow one oscillation. So if equation 7.4 holds, equation 7.5 holds.

$$4 \cdot \frac{A_{RPMrequested}}{Acc_{RPMmax}} > P \tag{7.4}$$

$$A_{RPMrequested} \neq A_{RPMdelivered} \tag{7.5}$$

When Equation 7.4 holds, the thrusters will try to equal the $A_{RPMdelivered}$ and $A_{RPMdelivered}$ as soon as possible. When the period P is far less than the minimum time which is needed for the thrusters to follow one oscillation, the thrusters $A_{RPMdelivered}$ will behave like a sawtooth as an impression can be seen in Figure 7.5.

Now an expression for the phaselag due to the thrusters is obtained, as illustrated in Figure 7.5.

The thruster amplitude $A_{RPMrequested}$ is defined as:

$$A_{RPMrequested} = \Delta x \cdot p^* \qquad |A_{RPMrequested}| \leq 100\% \tag{7.6}$$

The relation in equation 7.6 is from the Imtech model. The thruster amplitude which can be maximally delivered by thrusters during oscillation with period P is defined by:

$$A_{RPMdelivered} = \frac{P \cdot Acc_{RPMmax}}{4} \tag{7.7}$$

Now the phase due to the thrusters can be calculated as follow:

$$\phi_{Thrusters} = -cos^{-1} \frac{A_{RPMdelivered}}{A_{RPMrequested}} \tag{7.8}$$

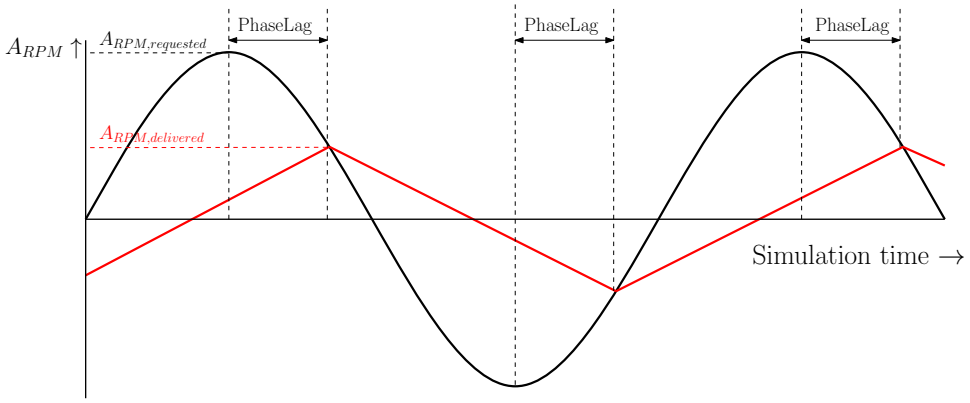

Figure 7.5: Impression of requested thruster amplitude versus delivered thruster amplitude.

To conclude the analysis of the thrusters, when the surge amplitude Δx is increasing the following two mechanisms are working simultaneously regarding the thruster phase lag:

(a) The period P is increases when Δx increases, which can be observed in Table 6.5. Consequently the thrusters have more time to follow the control demand which decreases the phase lag.

(b) Two is that the thruster amplitude $A_{RPMrequested}$ becomes larger hence this increases the phase lag.

To clarify the analysis of stability a calculation example is worked out in the following section.

CALCULATION EXAMPLE

Now a calculation example is worked out for the case without the Kalman solution candidate(2) and with parameters which are realistic and also used in the simulations. These values are:

Variables	Value	Unity and description
p*	11.47	Proportional gain [%rpm/m]
Acc_{RPMmax}	5	maximum thruster acceleration in [% rpm/s]

The example is worked out for the point of the lowest surge amplitude for which the controller will request 100% thrust RPM. Subsequently, equation 7.6 is substituted with $A_{RPMrequested} = 100\%$:

$$\Delta x = \frac{100[\%RPM]}{p^*} = 8.72[m] \tag{7.9}$$

From Table 6.5 can can be obtained that the surge amplitude of equation 7.9 corresponds with a period T ≈ 53[s]. According to the numbering used in the stability analysis in the previous section, the following values of ϕ are obtained:

1. Sensor
   $\phi_{sensor} \approx 0$
2. Kalman filter
   $\phi_{Kalman} \approx$ -10 °.
3. The phase lead by the controller can be obtained from Table 7.2.
   $\phi_{controller} \approx 36.0°$.
4. Thrust allocation
   $\phi_{thrustallocation} \approx 0$

5. The phase lag by the thrusters is obtained by filling in equations 7.7 and 7.8:

$$A_{RPMdelivered} = 50[s] \cdot 5[\%/s]/4 = 62.5[\%RPM]$$
$$\phi_{Thruster} = -cos^{-1}(\frac{1-(100[\%RPM]-62.5[\%RPM])}{100[\%RPM]}) = -51.3[^\circ]$$

$\phi_{thrusters} \approx -51.3$

Now to calculate the total phase lag all phase leads and lags which are described in points 1 to 5 have to be summed. See 7.3 for the overview of all components of this calculation example.

	Phase ϕ [°]
Sensor	0
Estimator/Kalman filter	-10
Controller	49.8
Allocation/power	0
Thrusters	-51.3
Total	-11.5

Table 7.3: Phase of each component in calculation example

From Table 7.3 is concluded that the total phase is negative. Consequently, this situation does not comply the stability criterion. Practically this means that the thrusters are increasing the energy of *the System+DP*. If the energy input by the thrust is higher than the energy dissipation the theoretical point of 8.72[m] will be instable. Interesting is that the theoretical found 8.72[m] is also between the stable and instable point of 8.4[m] and 10[m] which is found practically in chapter 6.1.1.

Next the found relations are all combined and graphically presented.

GRAPH OF PHASE MANIPULATION OF ALL COMPONENTS

Now with the obtained relations a graph is produced which show the total phase of the total chain of components for two cases, i.e. with and without Kalman solution candidate(2). This graph represents the theoretical phase lag between sensor to thrusters calculated with the formulas in this section and the surge amplitude and surge oscillation period relation of Table 6.5.

Now a summary of the method of determining the plot in Figure 7.6 is given.

- The analysis will be done for a surge amplitude Δx of 0[m] to 15[m].
- The relation between surge oscillation Δx and oscillation period is given in 6.5 and interpolated linearly. The interpolation of period of oscillation is also plotted in Figure 7.6.
- The thruster delay is calculated following Equations 7.6, 7.7 and 7.8.
- The phaselag of the controller calculated by interpolating and extrapolating Table 7.2 linearly.
- Furthermore with the Kalman solution candidate(2) is assumed to be 0 degrees phase lag, and without the Kalman solution candidate(2) a phase lag of 10 degrees.

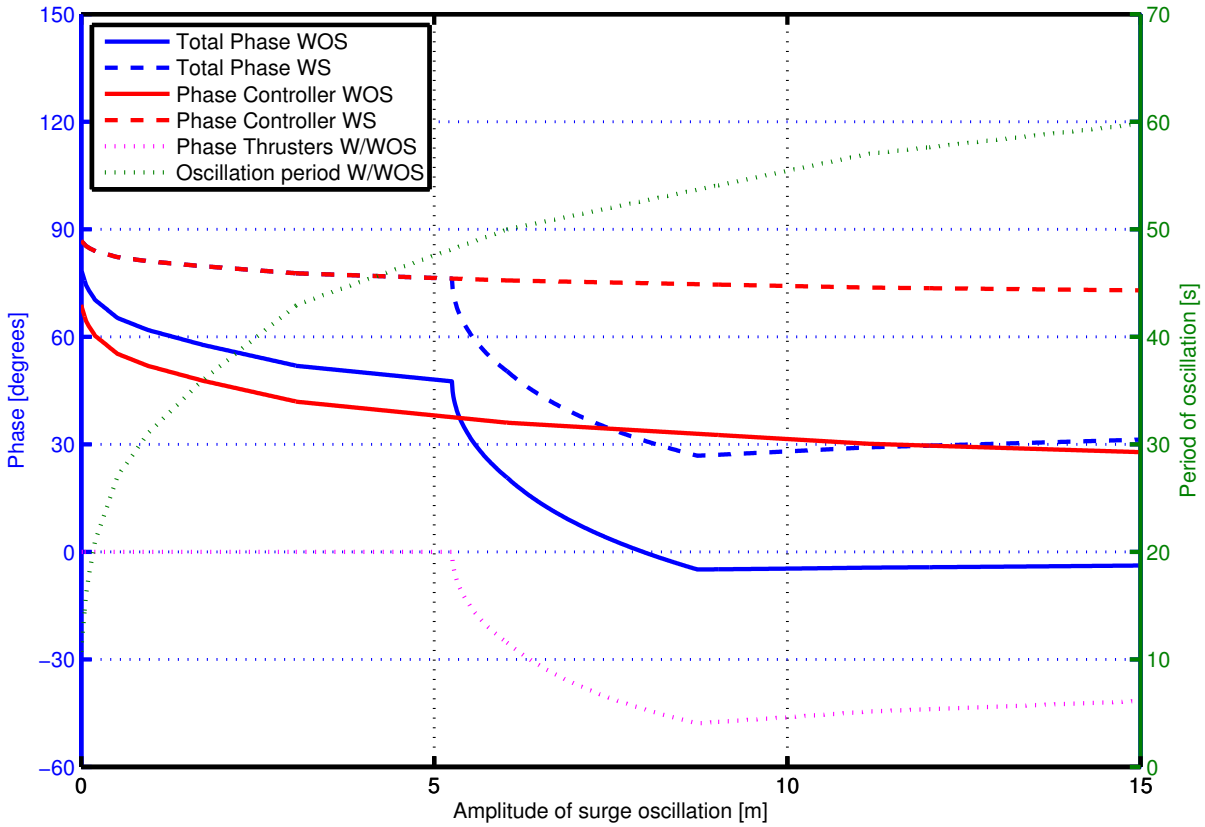

Figure 7.6: Phase manipulation of all components of DP system, WS = With Solution, WOS = WithOut Solution

The observations of this graph are:

- With and without Kalman solution candidate(2), The total phase is decreasing with surge oscillation amplitude.
- With and without Kalman solution candidate(2), The phase due to the controller decreases when ΔX increases.
- With and without Kalman solution candidate(2), From $\Delta X = 5.25$[m] the thrusters begin to introduce a phaselag.
- Without Kalman solution candidate(2), From $\Delta X = 7.95$ [m] the phase is less than 0 °.
- With Kalman solution candidate(2), the minimum phase of 26.81 ° is achieved at $\Delta X = 8.74$[m]. Consequently, the phase is never less than 0 °.

CONCLUSION

Instability of *the System+DP* during oscillating motion sets in if the energy (i.e. combined kinetic and potential energy) in *the System+DP* is increasing. In other words if the net power to *the System+DP* is larger than the net power from the system due to resistance. The DP system will add power to *the System+DP* if the phase of the total chain of components, containing the sensors, estimator, controller, thrust allocation and thrusters, is lower than 0 °. Consequently, if the phase of the total chain is higher than 0 ° *the System+DP* is guaranteed to be stable, within the simplifications throughout this analysis. That is why the phase manipulation of every component in the chain of components is analyzed.

Now Question 7.1.2 which was posed in the introduction of this section is answered. The question was whether the surge amplitude for which *the System+DP* becomes instable can be theoretically determined. From Section 6.1.1 is known that one point exists where *the System+DP* is becoming instable and this is between 8.4[m] and 10[m] surge oscillation amplitude. In the analysis in this section the possibility of becoming instable is theoretically proven to be at a surge oscillation amplitude of 7.95[m] or more. Below this is not possible to get instable. Whether *the System+DP* becomes instable above this amplitude is dependent on the amount of energy which is added to the system by the DP system and retracted from the system by frictional forces of *the System+DP*. This is not further analyzed. So the instable point of the mooring stiffness problem is theoretically proven to be at 7.95[m] surge amplitude or larger.

Now Question 7.1.2 which was posed in the introduction is answered. The question was whether it be guaranteed that the Kalman solution candidate(2) is stabilizing *the System+DP*? With the Kalman solution candidate(2) disabled, the amplitude of the velocity estimation is 1/5.4th of the true velocity. With the Kalman solution candidate(2) enabled is assumed that the velocity is correctly estimated. Because the damping of the controller is linearly dependent on the velocity also the derivative control action of the controller is 1/5.4th in the case of the solution candidate disabled. Less derivative control action lead to less phase lead by the controller. With the Kalman solution candidate(2) enabled *the system+DP* is proven to be stable due to the increase of phase lead due to the Kalman solution candidate(2). The minmal phase lead is proven to be 26.81° or more, consequently it can be guaranteed that the Kalman solution candidate(2) is stabilizing *the System+DP*.

But the answers to the questions are only valid for:

- This modeled vessel with its parameters and its variables.
- The simulation model environment described in Section 5.4.

So whenever one wants to know the answers to these questions, the analysis should be done for the specific vessel with its specific operation and load conditions.

Furthermore the current model buildup of was not taken into account in this analysis. Now some qualitative notes on this subject are made on this subject. Due to an average thrust to ahead or astern the thrusters will earlier be limited by the maximum thruster rpm to one side, and later to the other side. Furthermore, the thrust force is a function of the propeller revolutions squared (i.e. $(X_{Thruster} \propto A^2_{RPM})$) but the maximal thruster acceleration (i.e. Acc_{RPMmax}) is constant. Consequently, due to an average thrust to ahead or astern the net absolute thrust is higher. The consequence is that it is probably that possible instabilities are earlier reached because the addition of energy to *the System+DP* is larger. The result is that the poorly built up current model will increase the chance on instability and this is not taken into account in the analysis in this section. Fortunately with the Kalman solution and DP setpoint adaption the current model is not wrongly estimated and consequently the effect of the current model on this analysis is minimized.

The insights which are gained in this section can be useful for future DP system design. See the recommendations in Section 7.2.

7.2. RECOMMENDATIONS

In this section recommendations are posed for future research. As concluded in Chapter 6 the Kalman solution candidate(2) has good performance. Consequently, the first recommendation is to further develop the Kalman solution candidate(2) to a practical solution. The recommendations for this practical solution is given in Section 7.2.1. Furthermore, an extension to the implementation of the Kalman solution candidate(2) is suggested in Section 7.2.2. A load position estimator is suggested to extend the solution

to all arbitrary heavy lift operations. And finally, aside of the Kalman solution candidate some other recommendations are given in Section 7.2.3.

7.2.1. RECOMMENDATIONS FOR PRACTICAL SOLUTION

- The candidate solutions are tested in a model with the layout as in Figure 5.5. The solution is using an exact copy of the crane model from the heavy lift crane vessel model for the force estimation. Consequently, the model in the solution is exactly the same as the model in the heavy lift vessel model. In practice a perfect model of the used crane is not possible. It is likely that small differences in certain parameters can lead to a large error in the force estimation, so it is probable that the system is not robust to errors in model parameters. For a practical solution it must researched what the influence of errors in the crane model. In other words, one must study what the robustness is to parameter errors. The next items are recommended to study whether it can make the practical solution more robust.
  - An online parameter estimation of the crane model to decrease modeling errors.
  - Perhaps the model can be made less sensitive to modeling errors.
  - Incorporate the hoist tension sensor into the solution.
- It would be great if a solution helps the DP operators to recognize dangerous situations as early as possible. For example, because the horizontal forces are estimated they can be visualized to the DP operator for extra operational information.

7.2.2. HEAVY LOAD POSITION ESTIMATOR

In this section an extension to the solution Kalman solution candidate(2) is proposed. The addition is a heavy load position estimator, such that the forces and moments on the vessel can also be estimated in other situations than during the moored stage. In Figure 7.7 a schematic representation of this idea is shown.

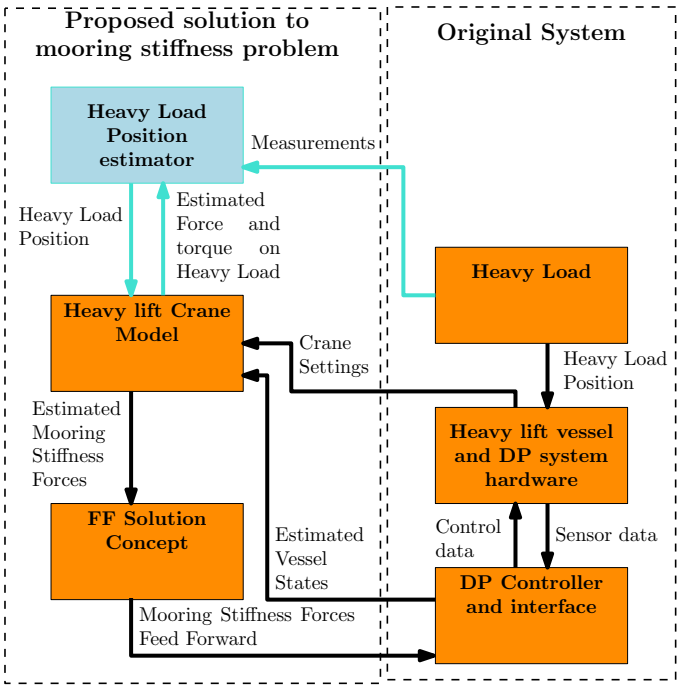

Figure 7.7: Schematic representation of proposed solution with heavy load position estimator.

In best case the solution to the mooring stiffness is generic. Besides the mooring stiffness forces during a topside installation, which is already discussed thoroughly in Section 3.2, there are other typical situations which can induce extra unknown forces via the crane of the heavy lifting vessel. One of the typical situations is when the heavy load is floating in the air. The heavy load can show swaying motion, which induces a certain periodic force on the vessel. Another typical situation is when the intended platform is a floating structure. When a heavy load is hoisted on a floating structure the floating structure will lower in the water. Furthermore if the center of mass of the load is not above the center of buoyancy the floating intended platform will also show roll motion which have influance on the mooring stiffness force. If the Kalman solution candidate is used for this type of operations too, the change of heavy load position should be incorporated into the solution to the mooring stiffness problem. Consequently, a position estimator for the heavy load is added to the solution.

Now the key to success is to estimate the position and orientation of the load relative to the vessel with as much precision as possible, but with an acceptable delay. So all the available information should be used as much as possible to estimate the load. Multiple ways of measuring must be used in order to achieve a high fault tolerance against sensor failures. But also information about dynamic behavior of the load can be used.

7.2.3. GENERAL RECOMMENDATIONS FOR DP

- As mentioned in Section 4.3, finding a new control method which can better cope with the mooring stiffness problem is scientifically very interesting. So it is recommended to examine other control methods.

- In Section 7.1.2 the thrusters appear to add a significant amount of phase lag to the total chain of components of the DP system. It is recommended to study a method to reduce the phase lag of the thrusters which is depicted in Figure 7.5. During oscillation one knows in prior that the control question can't be achieved by the thrusters, so after the peak of the control action the thrusters should decelerate again, instead of the situation in Figure 7.5. In [Klugt, 1987, Section 5.2.2] an identical problem is described for a slightly different application (i.e. Rudder Roll Stabilization). In [Klugt, 1987, Section 5.3] a technique to cope with this problem is proposed, which is called Automatic Gain Control(AGC). A visual representation of the result of using AGC is depicted in Figure 7.8.

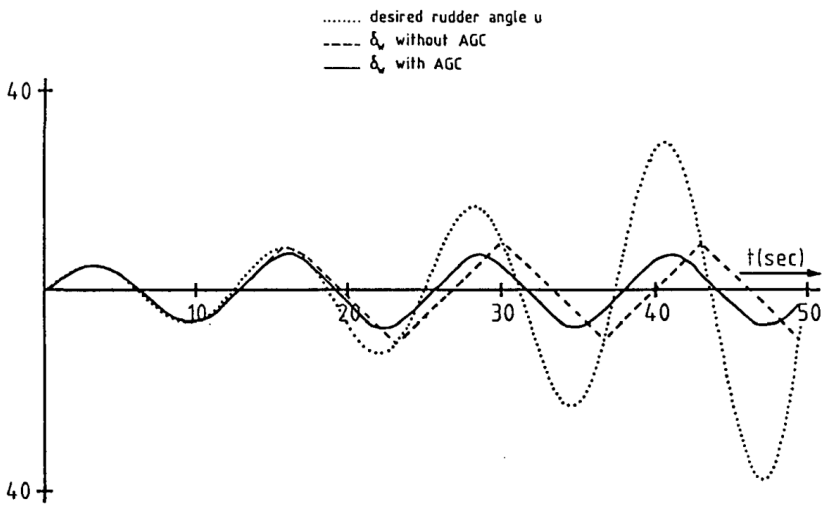

Figure 7.8: With and without Automatic Gain Control(AGC) [Klugt, 1987, Figure 5.6]

- It is recommended to enhance the theoretical analysis of stability from Section 7.1.2. The analysis is done with data from the simulation model. It is recommended to develop a method in such a way that it can be made independent from data from the simulation model.

7.3. CONCLUSION

After the topside is placed on the jacket but before the weight transfer is finished, the system resembles mooring characteristics. Because of the resulting mooring stiffness the heavy lift vessel resembles a damped mass-spring system, which is a different dynamic system than for which the DP controller is tuned for. Consequently, this can result in poor and even instable behavior of the DP system. The ultimate consequence may inflict great (economic) damage, human injury or even loss of lives. This problem is named the mooring stiffness problem.

A conceptual solution to this problem is successfully found in this thesis. In this thesis, 4 different candidate solutions are created based on the idea of the paper [Waals, 2010]. In this paper a method of feeding these forces to the original PID based DP controller is proposed. Furthermore an addition to the 4 candidate solutions is suggested, denoted *DP setpoint adaption*. The idea is that this addition calculates the optimal DP setpoints for the operation and automatically feed it to the DP controller. The addition can be part of the solution but is separate from the candidate solutions. To test the four candidate solutions and the DP setpoint adaption a computer simulation model of a heavy lift vessel installing a topside is developed. This simulation model is based on the Imtech Marine company DP and vessel model which is extended with a heavy lifting crane. Next the results this study are discussed.

WITHOUT SOLUTION

In the simulation environment the mooring stiffness problem is successfully reproduced by applying a certain oscillatory force. After reproducing the problem it could be fully analyzed of which the results are discussed next.

Because of the mooring stiffness forces the effective stiffness of the vessel-topside combination increases significantly. The consequence is that the surge oscillation frequency of the vessel-topside combination is increased. This has the following consequences:

- The control demand is fluctuating more often but the acceleration and deceleration rates of the thrusters are equal. Therefore, the thrusters can't achieve the control demand hence a lag between requested thrust and achieved thrust is obtained.
- The states are estimated poorly because the increase in effective stiffness is not modeled in the Kalman filter. Especially the velocity is estimated poorly.
- Because the damping by the DP system is a function of the estimated velocity, the damping is decreased. Consequently the effective damping is decreased.
- The estimation of the slowly varying environmental load on the vessel (i.e. current model buildup) is worse.

The consequence is that the DP system may show poor and even instable performance. It was shown by simulations that if a certain surge oscillation amplitude threshold is passed due to excitation by external forces, the vessel with DP starts to increase oscillation amplitude by its own. In other words the DP system becomes instable when a surge oscillation amplitude threshold is passed. In this report a theoretical method of determining whether this threshold exists is proposed. If this threshold exists the method can theoretically determine the lower boundary of this surge oscillation amplitude threshold. For the heavy lift vessel in the simulation model the theoretical threshold of instability is determined, which matches the practically obtained value from simulation.

For now, the theoretical method is still relying on data from the simulation. It is recommended to expand the method to use it for stability analysis without a simulation model.

WITH CANDIDATE SOLUTION

Now the most important results of the candidate solutions are discussed.

1. FEED FORWARD SOLUTION

The idea of this candidate solution is to estimate the horizontal mooring stiffness forces and subsequently feed forward these by the vessel's own actuators. As a result the horizontal forces are eliminated whereby the DP controller is not disturbed by the mooring stiffness forces. This idea is described in the paper [Waals, 2010] and performed very well on scale model tests. The good results from this paper are successfully reproduced in this study with unrealistic fast thrusters and rudders.

With the realistic thruster and rudder settings of the simulation model however, this solution candidate is performing very poorly. The cause of this poor performance is theoretically analyzed. The problem is that the thrusters can't follow the demand of the feed forward control law because of too low acceleration and deceleration rates of the thrusters. Consequently, it is concluded that the Feed Forward solution candidate is theoretically a good solution, however practically it is not feasible.

2. KALMAN SOLUTION

The second candidate solution just feeds the estimated forces to the Kalman filter. This candidate solution is performing very good. Due to Kalman solution the state estimation is improved and consequently the damping of the DP system is larger. Furthermore the estimation of the slowly varying environment loads (i.e. current model) is better. This candidate solution is not guaranteeing DP stability under all conditions. However, to determine the stability, with or without the Kalman solution candidate, an theoretical analysis is developed.

3. CORRECTED SOLUTION

The performance of the corrected solution candidate is concluded to be acceptable. However, the Kalman solution candidate is performing better.

4. FILTERED SOLUTION

The idea of the filtered solution candidate is to smartly filter the fast fluctuating part of the mooring stiffness forces resulting in a more steady feed forward thrust demand. However the performance was very poor. The filtering is performed by filtering the roll and pitch of the vessel before the mooring stiffness forces are calculated. In this study is shown theoretically and by means of simulations, that because of pitching of the vessel the mooring stiffness is relaxed. Consequently, this candidate solution is concluded to be not working well because the relaxation of the mooring stiffness is filtered when the pitch motion of the vessel is filtered.

DP SETPOINT ADAPTION

In this study is concluded that the DP setpoint adaption increases the performance.

It is concluded that the proposed Kalman solution candidate is the best performing conceptual solution for solving the mooring stiffness problem. Consequently, the Kalman conceptual solution is recommended to be developed into an industrial solution. DP setpoint adaption can be a valuable addition to the solution.

For the development of the Kalman conceptual solution is recommended to take extra measures to increase the robustness against differences between the heavy lift vessel model and the true heavy lift vessel.

A

VERIFICATION DETAILS

In Section 5.2.10 the model verification and validation tests are discussed briefly. In this appendix chapter the tests are presented and discussed in detail. If nothing else specified, the parameters which are used during the simulations are as described in appendix chapter B. Furthermore, it can be very helpful to keep Figure 5.3 in mind while studying this chapter.

A.1. SWINGING OF HEAVY LOAD IN CRANE OF HEAVY LIFT VESSEL.

This simulation is a simulation of a heavy load of 532[t] in the crane with an initial position outside an equilibrium. Now the heavy load should sway in the crane of the vessel. Also the motion of the heavy load should interact with the motion of the vessel and dampen slowly.

In this test the crane angle w.r.t. the vertical (xz-)plane α is 90 degrees, so the crane is pointed towards port side. The weight of the heavy load is 532[t]. The initial position of the load is chosen such that the hoist cable makes an angle of 45 degrees w.r.t. the z axis and will sway along the length direction of the vessel. I.e. $\delta_{vessel} = 0^\circ$ and $\gamma_{vessel} = 45^\circ$. Surge of the heavy load is defined as motion in the surge direction of the vessel. Sway of the heavy load is defined as motion in the sway direction of the vessel.

In Figure A.1 the results of the simulation test are depicted. One can see the damped swaying motion of the heavy load. The pendulum motion of the heavy load make the vessel go back and forth in surge direction which can be seen by comparing the maximal values of the height of the heavy load with the surge position of the vessel. Furthermore can be seen that the motion of the vessel induced by the heavy load is realistic as the surge of the vessel is opposite to the surge of the heavy load. Also the positive roll is as expected because the crane is pointed towards port side. So this section is concluded by noting that no strange behavior is observed.

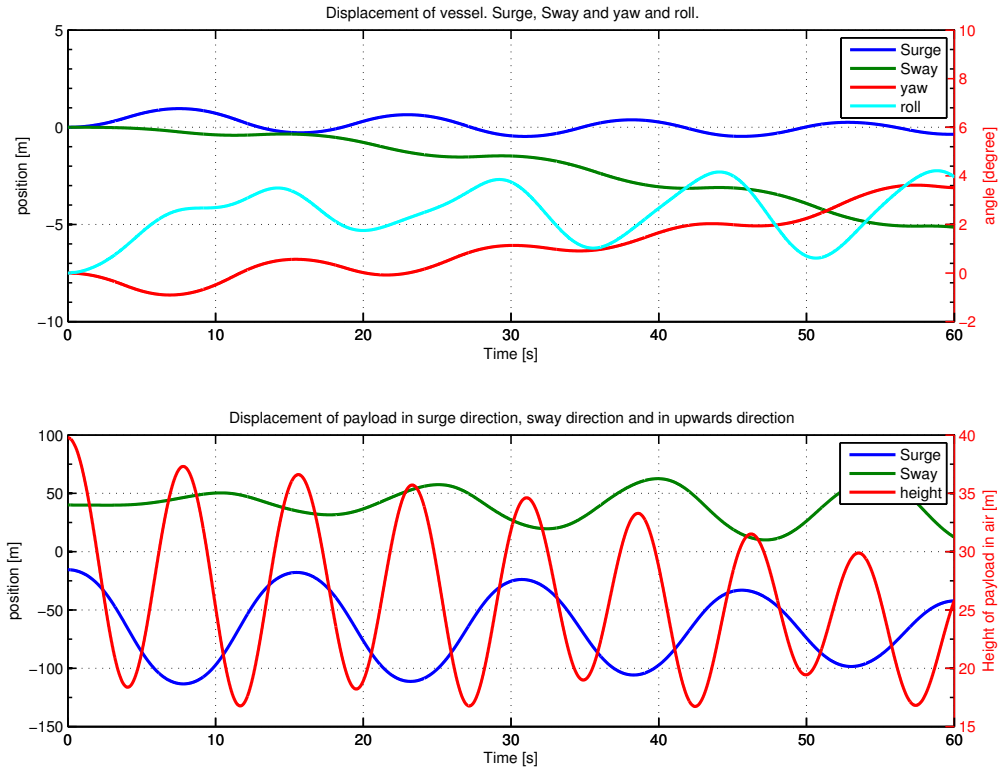

Figure A.1: Results of verification test "Swinging of heavy load in crane of heavy lift vessel"

A.2. HEAVY LOAD WILL DROP FROM SMALL HEIGHT AND EMERGE TO EQUILIBRIUM.

This simulation is a simulation of a heavy load of 532[t] which drops from 2[m] altitude. This is not in line with a real operation as nobody will intend to drop a weight of 532[t] from 2 meters attached to a crane. However, the simulation is valuable to test the implementation of the internal damping in the cable and snatching of the cable. Furthermore the quantitative values of the roll and pitch of the equilibrium states of the vessel can be compared to manual calculation results.

In this test the crane angle w.r.t. the vertical (xz-)plane α is 90 degrees, so the crane is pointed towards port side. The weight of the heavy load is 532[t]. The initial position of the load is set in order that the heavy load is below the crane tip (i.e. the horizontal X and Y coordinates of heavy load and crane tip are equal to each other, and the load will drop 2[m] altitude before pulling the hoist cable taut.

In Figure A.1 the results are depicted of the simulation test. Z is the force on the vessel in body coordinates and it is almost the same as the tension in the cable. It can be observed that the load bouncing in the crane, stabilizing at the end in 5.3e6[N]. This is in line with the weight of the heavy load which is 532[t]. The internal damping and the fact that the cable can only exert pulling force are modeled correctly. The equilibrium of the roll and pitch are respectively around 3.7 degrees and 0.29 degrees, which are also correct values as the following calculations will show.

According to equation 5.14 the restoring moments due to roll and pitch are:

$$K = \rho g \nabla \overline{GM_T} \phi \tag{A.1}$$

$$M = \rho g \nabla \overline{GM_L} \theta \tag{A.2}$$

The force due to the heavy load is in steady state always completely parallel to the z-axis in NED coordinate due to gravitational acceleration. Hence

$$K = cos(\phi) b_{crane} Z + sin(\phi) a_{crane} Z \tag{A.3}$$

$$K = b_{crane} Z + \phi a_{crane} Z, for\ \phi \approx 0 \tag{A.4}$$

$$M = cos(\theta) a_{crane} Z + sin(\theta) b_{crane} Z \tag{A.5}$$

$$M = a_{crane} Z + \theta b_{crane} Z, for\ \theta \approx 0 \tag{A.6}$$

Substituting K and M, solving for ϕ and θ, results:

$$\phi = 3.66^\circ \tag{A.7}$$

$$\theta = 0.289^\circ \tag{A.8}$$

Which is in line with the results of Figure A.2.

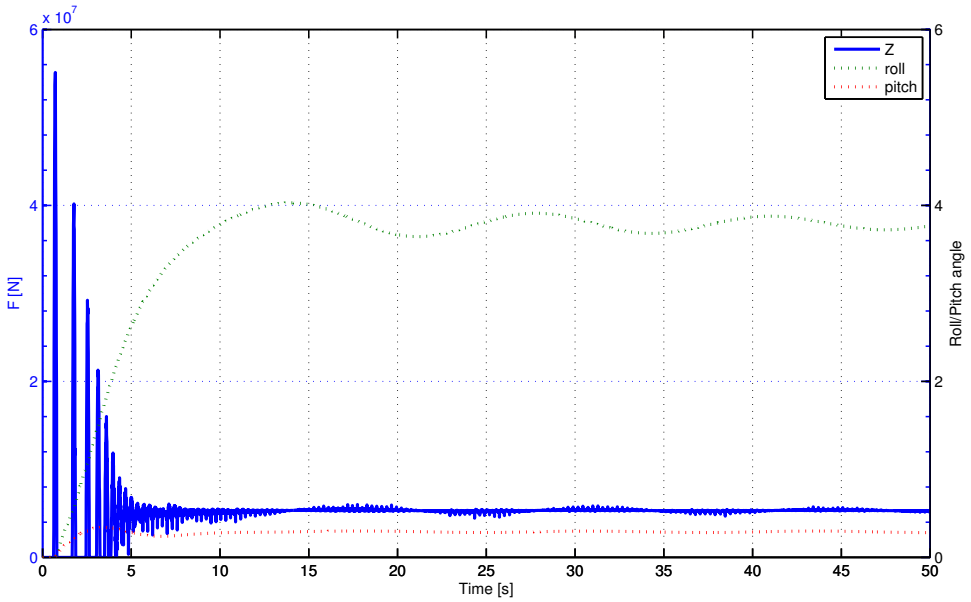

Figure A.2: Results of verification test "heavy load will drop from small height and emerge to equilibrium"

A.3. FULL THRUST WHILE THE CABLE IS ATTACHED TO A FIXED POINT.

In this simulation the crane angle w.r.t. the vertical (xz-)plane α is 90 degrees. The hoist-cable is attached to a fixed point in air such that the hoist cable is pulled taut downwards and but without tension initially. Now the vessel is ordered to apply full thrust ahead. So the vessel will sail circles around the fixing point of the hoist cable. Also this simulation is not in line with a real operation, but the behavior of the vessel can be inspected in the complete range of over -180 to +180 degrees of heading.

Observe the graphs in Figure A.3. In the graphs one can see after starting the simulation forward acceleration, building tension in the hoist cable and after that the vessel is pulled backwards by the crane and the vessel is starting to roll and accelerate in yaw direction. After this a constant velocity is achieved. In the complete range of over -180 to +180 no unnatural behavior is observed.

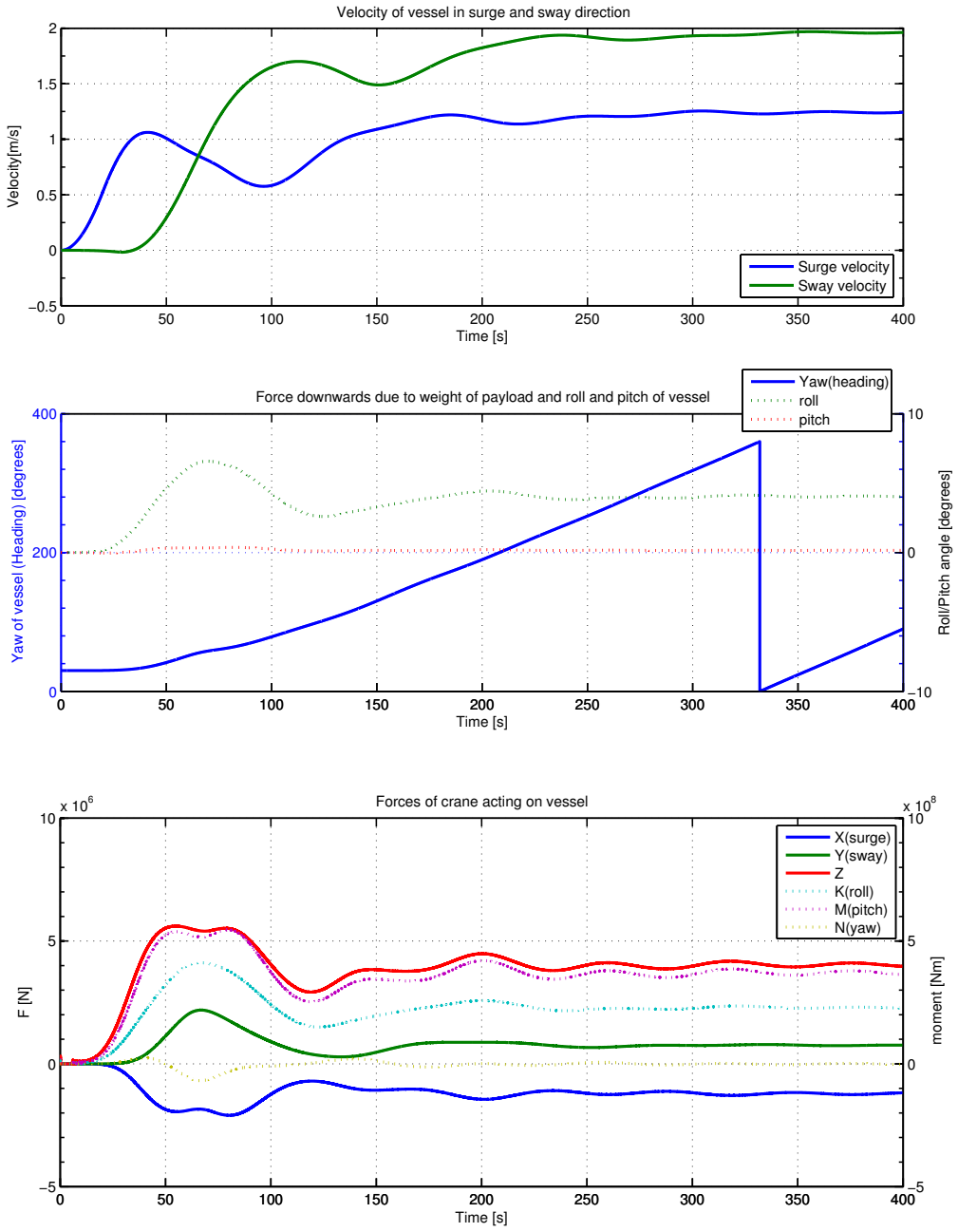

Figure A.3: Results of verification test "Heavy load will drop from small height and emerge to equilibrium"

A.4. INCREASING TENSION IN HOIST CABLE WHILE THE CABLE IS ATTACHED TO A FIXED POINT.

In this simulation the crane is pointed towards stern. The fixed attachment point of the cable is pulled downward such that the tension in the cable will grow. Now the pitch of the vessel also increases and the tip of the crane moves to a new equilibrium point which is exactly above the attachment point. Consequently, the vessel center of gravity will be pushed away from the load as is already depicted in 3.5. Doing this test ensures that the crane forces are correctly calculated during pitching of the vessel and translated to the right motions.

In Figure A.4 the results are depicted of the simulation test. The surge and pitch are both positive which is as expected. The pitch is 3.7 degrees of which its correctness is already verified in A.2. The surge equilibrium point in this simulation is approximately 5.5[m] which will verified with manual calculations.

In Figure A.5 a sketch of the side of the vessel is presented and used to clarify this manual calculations.

$$a_{crane} = -X_{crane} + cos(\beta_{hoist}) L_{crane} \tag{A.9}$$
$$c_{crane} = -Z_{crane} + sin(\beta_{hoist}) L_{crane} \tag{A.10}$$
$$\Delta S \approx sin(\theta) \sqrt{a_{crane}^2 + c_{crane}^2} \tag{A.11}$$

In the case of the used parameters in this simulation:

$$a_{crane} = 105[m] \tag{A.12}$$
$$c_{crane} = 89[m] \tag{A.13}$$
$$atan(c_{crane} / a_{crane}) = 40.3^\circ \tag{A.14}$$
$$\theta \approx 0 \tag{A.15}$$
$$\Delta S = \theta \sqrt{a_{crane}^2 + c_{crane}^2} \tag{A.16}$$
$$\tag{A.17}$$

Hence the value of surge is:

$$surge = sin(40.3^\circ) \Delta S \tag{A.18}$$
$$surge = 5.6[m] \tag{A.19}$$

This is in line with the simulation results.

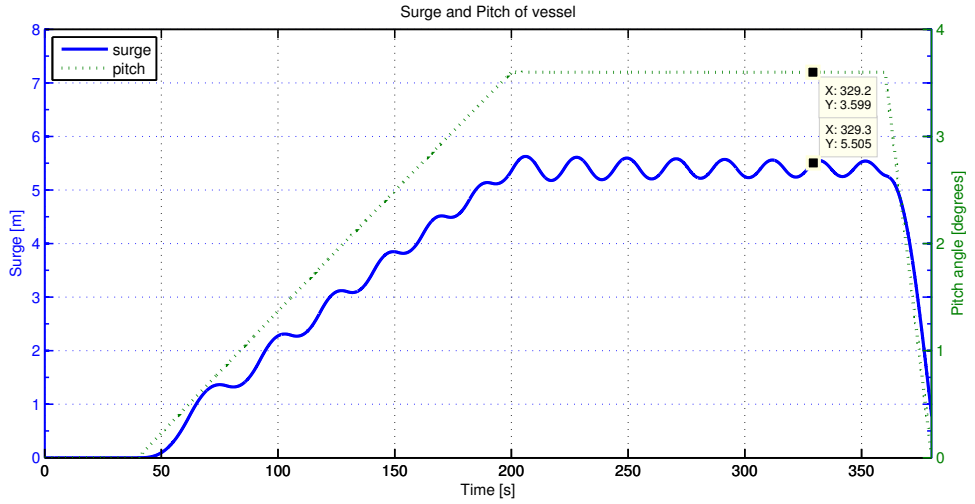

Figure A.4: Results of verification test "Increasing tension in hoist cable while the cable is attached to a fixed point"

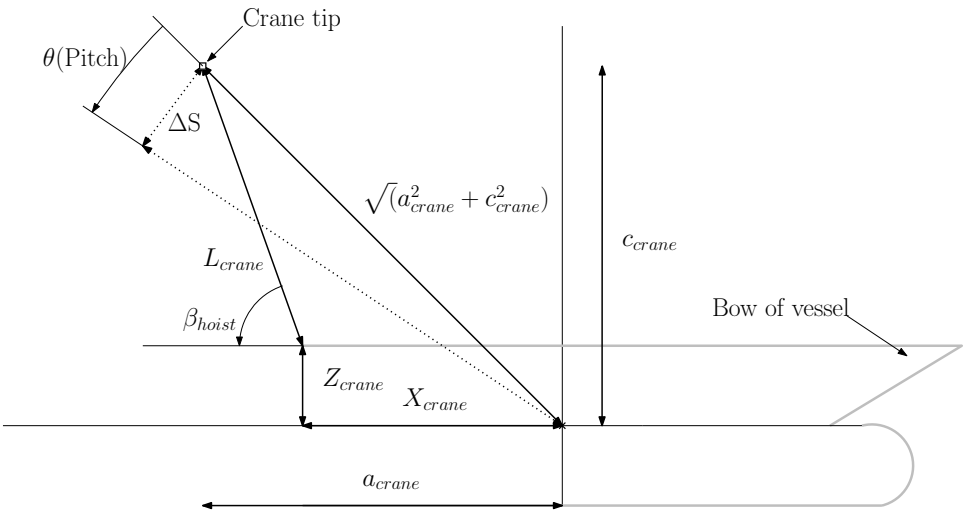

Figure A.5: Sketch of starboard side of Vessel

B

PARAMETERS USED IN SIMULATION

In this thesis many results are presented. If nothing else specified the following parameters are used in simulations and manual calculations.

VESSEL PARAMETERS

The vessel parameters are based on a vessel which is built in real life and outfitted with a DP system of Imtech.

Main vessel parameters	
Length between perpendiculars, L_{PP}	147.60 [m]
Breadth of vessel at waterline, B_{WL}	25.40 [m]
Draught, T	7.50[m]
Displacement ∇	16038 [m^3]
Block coefficient	0.761
Centre of buoyancy (from AP), CB	76.50 [m]
Number of tunnel thrusters stern	2
Maximal thrust of tunnel thrusters stern (together)	20 [kN]
Location of tunnel thrusters stern w.r.t. midship	-63.6, -66.6 [m]
Number of tunnel thrusters bow	3
Maximal thrust of tunnel thrusters bow (together)	156 [kN]
Location of tunnel thrusters bow w.r.t. midship	65.8, 69.3, 72.8 [m]
Number of main thrusters	2
Maximal thrust ahead of main thrusters (together)	1294 [kN]
Maximal thrust backwards of main thrusters (together)	466 [kN]
Location of main thrusters w.r.t. midship	-70.8 [m]
Distance between main thrusters	11.6 [m]
Bow and stern thrusters acceleration	7 [%/s]
Main thrusters acceleration	5 [%/s]
$\overline{GM}_T$	10.83 [m]
$\overline{GM}_L$	389.8 [m]

Table B.1: Main vessel parameters which are used in simulations.

As for the metacentric heights, these are estimated based on breadth, draught, displacement under the assumptions:

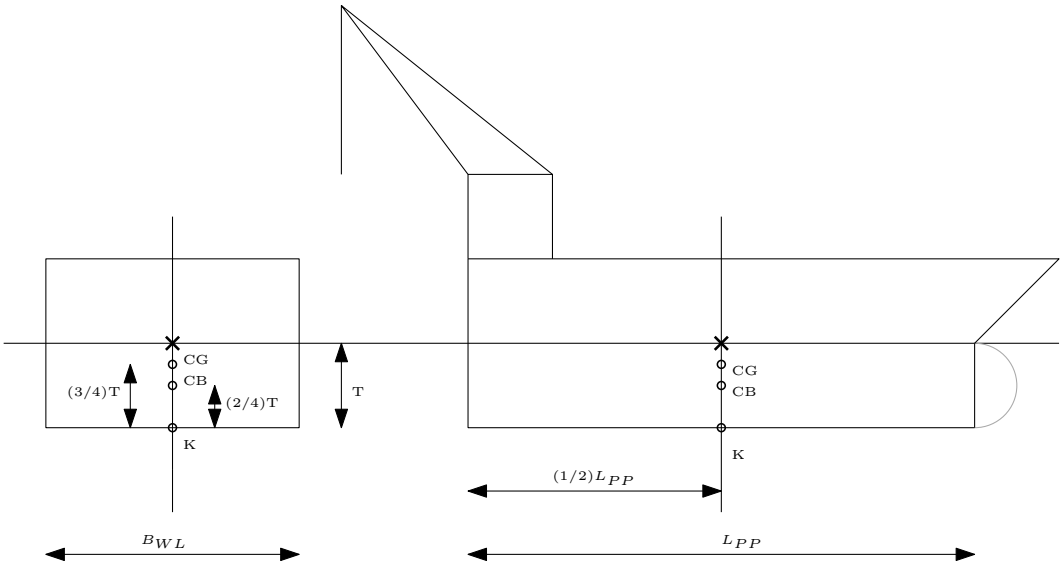

Figure B.1: Sketch of vessel's parameters of which can be used to calculate metacentric height

- The vessel is simplified as a box with dimensions $L_{PP} \cdot B_{WL}$
- Centre of buoyancy (CB) is exactly midship in length and breadth, with a height of 1/2T from K
- Centre of gravity (CG) is exactly midship in length and breadth, with a height of 3/4T from K

Now the metacentric heights are calculated in equations B.1 to B.5. Then the metacentric heights are calculated. See also the sketch of the vessel's parameters of which can be used to calculate the metacentric height in Figure B.1.

$$I_T = \frac{1}{12} B_{WL}^3 L_{PP} \tag{B.1}$$

$$I_L = \frac{1}{12} B_{WL} L_{PP}^3 \tag{B.2}$$

$$\overline{CB\,CG} = \overline{K\,CG} - \overline{K\,CB} \tag{B.3}$$

$$\overline{GM}_T = \frac{I_T}{\nabla} - \overline{CB\,CG} \tag{B.4}$$

$$\overline{GM}_L = \frac{I_L}{\nabla} - \overline{CB\,CG} \tag{B.5}$$

CRANE PARAMETERS AND SETTINGS

The following crane parameters and settings are used for configuring the crane model block.

Crane parameters and settings	
A_{cable}	0.0982 [m^2]
E_{cable}	$120 * 10^9$ [Pa]
L_{crane}	80 [m]
x_{crane}	-65 [m]
y_{crane}	0 [m]
z_{crane}	-20 [m]
α_{hoist}	180 [°]
β_{hoist}	60 [°]
l_{hoist}	70[m]
Ψ_{cable}	0.17[]

Table B.2: Crane parameters and settings

Now the choice of some parameters are discussed. It is assumed that a helical wire rope strand hoist cable is used, with 50 cables of 50 [mm] diameter steel cables.

$$A_{cable} = 50 \cdot 0.025^2 * \pi \tag{B.6}$$

It is assumed that the steel used in the cable has an elasticity modulus of 200 [Gpa]. But due to the layering of the wires the effectiveness of the elasticity modulus is assumed to be 0.7.

$$E_{cable} = 0.7 \cdot 200[GPa] \tag{B.7}$$

The derivation of Ψ_{cable} is done in section 5.2.7.

Heavy load parameters

The following parameters are used for configuring the Heavy load block.

heavy load parameters	
a_{load}	0 [m]
b_{load}	0 [m]
c_{load}	0 [m]
M_RB_{load}	See B.8

Table B.3: heavy load parameters

The heavy load is assumed to be a hollow sphere of 272 tonnes with a radius of 43 [m]. This load has the following mass matrix.

$$M\_RB_{load} = \begin{pmatrix} 0.027 & 0 & 0 & 0 & 0 & 0 \\ 0 & 0.027 & 0 & 0 & 0 & 0 \\ 0 & 0 & 0.027 & 0 & 0 & 0 \\ 0 & 0 & 0 & 35 & 0 & 0 \\ 0 & 0 & 0 & 0 & 35 & 0 \\ 0 & 0 & 0 & 0 & 0 & 35 \end{pmatrix} * 10^7 \tag{B.8}$$

Remember that the heavy load is only used for the verification and validation tests of Appendices A.1 and A.2.

Simulation Parameters

The following simulation parameters are used.

Simulation Parameters	
Sample time Imtech model and Simulink	0.005[s]
Sample time Imtech DP Controller	0.025[s]
Solver	Fixed step 4th-order Runge-Kutta

The simulation parameters are discussed in Section 5.2.8.

C

DEFINITIONS OF NOTATIONS

DOF		Forces and moments			Linear and angular velocities			Position and Euler angles		
1	motions in the x direction (surge)	X	$\vec{f}_b$	$\vec{\tau}$	u	$\vec{v}_b$	$\vec{\nu}$	x	$\vec{p}_n$	$\vec{\eta}$
2	motions in the y direction (sway)	Y			v			y		
3	motions in the z direction (heave)	Z			w			z		
4	rotation about the x axis (roll)	K	$\vec{m}_b$		p	$\vec{\omega}_b$		ϕ	$\vec{\omega}_n$	
5	rotation about the y axis (pitch)	M			q			θ		
6	rotation about the z axis (yaw)	N			r			ψ		

Table C.1: The notation of position, velocity and forces and moments for marine vessels [Fossen, 2011, p. 16]

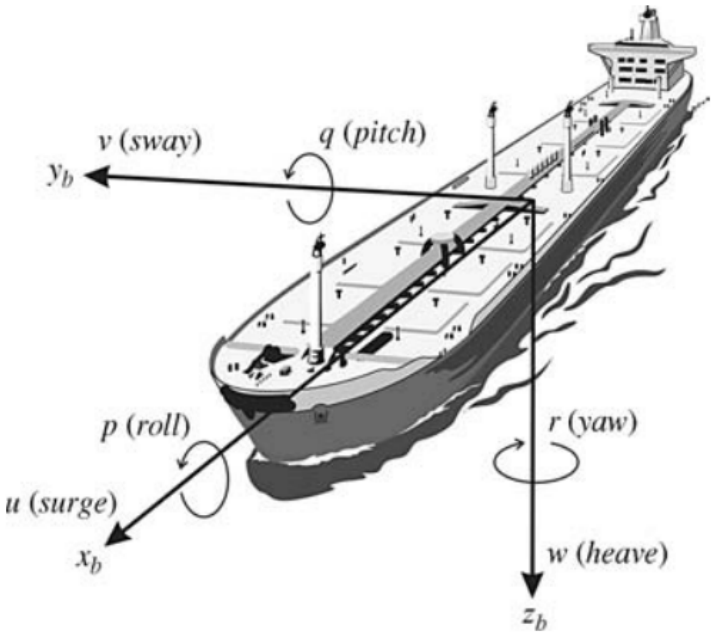

Figure C.1: The 6 DOF velocities u,v,w,p,q,r in the body-fixed reference frame $\{b\} = (x_b, y_b, z_b)$

BIBLIOGRAPHY

Brosilow, C. & Joseph, B. (2002). *Techniques of model-based control*. Prentice Hall PTR.

Deloitte, C. (2011, November). Website blog about north sea offshore decommissioning report. Retrieved from http://www.psg.deloitte.com/ResourcesOilGasReports%20NorthSeaDecommissioning_20111130.asp

Dockwise, C. (2014, February 2). Dockwise vanguard [photograph]. Retrieved from http://gcaptain.com/wp-content/uploads/2013/05/IMG_3071.jpg

El Amam, E. (2013, June). Dynamic positiioning, lecture control systems [powerpoint slides]: Retrieved from tu delft blackboard website course code oe4606. Retrieved from blackboard.tudelft.nl

Fossen, T. I. (2011). *Handbook of marine craft hydrodynamics and motion control*. Wiley.

Fossen, T. I. & Perez, T. (2014, April 25). Marine system symulator(mss). Retrieved from http://www.marinecontrol.org/

HMC, C. (n.d.). History of hmc. Retrieved from http://hmc.heerema.com/content/about/history/

HMC, C. (2002). Imca seminar paper: heavy lifting on dp, and the role of simulators.

HMC, C. (2014, July 18). The thialf heavy lifting vessel. Retrieved from http://hmc.heerema.com/content/fleet/thialf/

HMC, C. (2015, January 15). Heerema thialf [photograph]. Retrieved from http://www.ttalents.com/heerema-installs-offshore-wind-platform/#prettyPhoto/0/

Kaminski, M. (2012a, October). Introduction to offshore engineering, lecture 1 [powerpoint slides]: Retrieved from tu delft blackboard website coarse code oe4606. Retrieved from blackboard.tudelft.nl

Kaminski, M. (2012b, October). Introduction to offshore engineering, lecture 13 [powerpoint slides]: Retrieved from tu delft blackboard website coarse code oe4606. Retrieved from blackboard.tudelft.nl

Klugt, P. v. d. (1987). *Rudder roll stabilization* (Doctoral dissertation, TU Delft).

Mathworks, C. (2014). Matlab simulink manual 2014. Retrieved June 20, 2014, from http://www.mathworks.nl/help/simulink/ug/choosing-a-solver.html

Raoof, M. & Davies, T. J. (2006). Simple determination of the maximum axial and torsional energy dissipation in large diameter spiral strands. *Computers & Structures*, *84*(10-11), 676–689. doi:http://dx.doi.org/10.1016/j.compstruc.2005.11.005

Rock, M. & Parsons, L. (2010, October). *Offshore wind energy fact sheet*.

SHL, C. (2014, July 18). The oleg strashnov heavy lifting vessel data sheet. Retrieved from http://www.subsea7.com/content/dam/subsea7/documents/whatwedo/fleet/rigidpipelay/Oleg_Strashnov.pdf

Thornton, W. (2000). Current trends and future technologies for decommissioning of offshore platforms. In *Otc 12020*.

Unknown. (2014, February 2). Offshore wind farm [photograph]. Retrieved from http://greendiary.com/wp-content/uploads/2013/06/

Waals, O. (2010). On the use of main hoist tension measurement for feed forward in dp systems during offshore installations. In *29th international conference on ocean, offshore and arctic engineering*: *Vol. 1*. (pp. 393–400). doi:10.1115/OMAE2010-20607. eprint: 978-0-7918-3873-0

Wit, C. d. (2009, July 1). *Optimal thrust allocation methods for dynamic positiioning of ships* (Master's thesis, Delft University of Technology).